A USER PROGRAMMABLE BATTERY CHARGING SYSTEM

A Thesis

by

JUDY MARIAN AMANOR-BOADU

Submitted to the Office of Graduate Studies of
Texas A&M University
in partial fulfillment of the requirements for the degree of

MASTER OF SCIENCE

Approved by:

Chair of Committee,	Edgar Sanchez-Sinencio
Co-Chair of Committee,	Sam Palermo
Committee Members	Weiping Shi
	Hank Walker
Head of Department,	Chanan Singh

May 2013

Major Subject: Electrical Engineering

ABSTRACT

Rechargeable batteries are found in almost every battery powered application. Be it portable, stationary or motive applications, these batteries go hand in hand with battery charging systems. With energy harvesting being targeted in this day and age, high energy density and longer lasting batteries with efficient charging systems are being developed by companies and original equipment manufacturers. Whatever the application may be, rechargeable batteries, which deliver power to a load or system, have to be replenished or recharged once their energy is depleted. Battery charging systems must perform this replenishment by using very fast and efficient methods to extend battery life and to increase periods between charges. In this regard, they have to be versatile, efficient and user programmable to increase their applications in numerous battery powered systems. This is to reduce the cost of using different battery chargers for different types of battery powered applications and also to provide the convenience of rare battery replacement and extend the periods between charges.

This thesis proposes a user programmable charging system that can charge a Lithium ion battery from three different input sources, i.e. a wall outlet, a universal serial bus (USB) and an energy harvesting system. The proposed charging system consists of three main building blocks, i.e. a pulse charger, a step down DC to DC converter and a switching network system, to extend the number of applications it can be used for. The switching network system is to allow charging of a battery via an energy harvesting system, while the step down converter is used to provide an initial supply voltage to kick start the

energy harvesting system. The pulse charger enables the battery to be charged from a wall outlet or a USB network. It can also be reconfigured to charge a Nickel Metal Hydride battery. The final design is implemented on an IBM 0.18μm process. Experimental results verify the concept of the proposed charging system. The pulse charger is able to be reconfigured as a trickle charger and a constant current charger to charge a Li-ion battery and a Nickel Metal Hydride battery, respectively. The step down converter has a maximum efficiency of 90% at an input voltage of 3V and the charging of the battery via an energy harvesting system is also verified.

ACKNOWLEDGEMENTS

I would like to thank my committee chair and advisor, Dr. Sanchez-Sinencio for his support, advice and guidance throughout my research study. I like to acknowledge my committee members, Dr. Palermo, Dr. Shi and Dr. Walker, for serving on my defense committee. I also express my gratitude to Dr. Zenon Medina-Cetina for taking time off his busy schedule to substitute for one of my committee members on the day of my defense.

I would also like to express thanks to Dake Tuli and Benjamin Sarpong of Texas Instruments for their support during my years at Texas A & M University. I also extend my gratitude to MOSIS *(*Metal Oxide Semiconductor Implementation Service*)* who provided a means to fabricate my design through their educational program. Thanks also goes to my friends, research colleagues and the department faculty and staff for making my time at Texas A&M University a great experience.

Finally, my gratitude goes to my parents and brother for their encouragement, patience, love and support.

NOMENCLATURE

AC	Alternating current
DC	Direct current
PMOS	P-type metal-oxide-semiconductor
NMOS	N-type metal-oxide-semiconductor

TABLE OF CONTENTS

Page

ABSTRACT ii

ACKNOWLEDGEMENTS iv

NOMENCLATURE v

TABLE OF CONTENTS vi

LIST OF FIGURES viii

LIST OF TABLES xiii

1. INTRODUCTION 1

1.1 Thesis organization 7

2. ENERGY STORAGE AND ENERGY HARVESTING 9

2.1 Energy storage devices 9
2.2 Applications of batteries 10
2.2.1 Portable applications 11
2.2.2 Stationary applications 11
2.2.3 Motive applications 12
2.3 The battery 12
2.3.1 Some commonly used battery terms 14
2.3.2 Battery classifications 17
2.3.3 Major types of battery chemistry 18
2.4 Battery chargers 23
2.4.1 Types of battery charging modes 24
2.4.2 Li-ion battery chargers 28
2.4.3 Li-ion battery charger design considerations 34
2.5 Energy harvesting 36
2.5.1 Solar energy harvesting 37
2.5.2 Thermal energy harvesting 38
2.5.3 Vibration energy harvesting 39
2.6 The battery and the supercapacitor 40
2.7 Overview of charging system 42
2.7.1 Description of charging system block diagram 43
2.7.2 Description of charging system flow process 45

3. PULSE CHARGER 47

3.1 Previous works 47
3.2 Conceptual idea of proposed pulse charger 56
3.2.1 Flow chart of proposed pulse charger 58
3.2.2 Description of block diagram 60
3.3 Circuit level implementation 61
3.3.1 Design of basic building blocks 62
3.3.2 Design of trickle charging phase 79
3.3.3 Design of fast charging phase 84
3.3.4 Protection schemes 87
3.4 The pulse charger 98
3.4.1 Transformation of pulse charger to trickle charger 103
3.4.2 Transformation of pulse charger to constant current charger 104

4. STEP DOWN DC-DC CONVERTER AND SWITCHING NETWORK SYSTEM 107

4.1 Step down DC-DC converter 108
4.1.1 Switched capacitor converter 110
4.2 Switching network system 120
4.2.1 Implementation of the switching network system 121

5. EXPERIMENTAL RESULTS 129

5.1 Proposed pulse charger 130
5.2 Switched capacitor converter 134
5.3 Switching network system 137
5.4 Comparison with previous works 140

6. CONCLUSIONS 143

REFERENCES 144

LIST OF FIGURES

Page

Figure 1 A typical battery charging system. 3

Figure 2 Proposed user programmable battery charging system. 6

Figure 3 Major applications of batteries. 10

Figure 4 Chemical and electrical symbols of an electric cell. 13

Figure 5 Battery feeding current (I) into a load. 14

Figure 6 Dependence of cycle life on DOD. 16

Figure 7 Comparison of battery chemistries in terms of energy density and weight. 23

Figure 8 Conceptual view detailing the main functions of a battery charger. 24

Figure 9 Trickle charge profile. 25

Figure 10 Constant voltage charge profile. 26

Figure 11 Constant current charge profile. 27

Figure 12 Pulse charge profile. 28

Figure 13 A typical charge and discharge profile of a Li-ion battery. 29

Figure 14 Charging profile of a Li-ion battery. 30

Figure 15 Linear and switch mode charger concept. 32

Figure 16 Pulse charger concept. 34

Figure 17 Conventional capacitor versus supercapacitor. 41

Figure 18 Charging system with DC-DC converter and switching network. 43

Figure 19 Flow chart showing the operation of the battery charging system. 46

Figure 20 Proposed block diagram of phase locked battery charger. 48

Figure 21 Implementation of VFPCS. 50

Figure 22 Block diagram of DVVPCS. 51

Figure 23 LTC4052. 52

Figure 24 LTC1730. 53

Figure 25 MAX1879. 54

Figure 26 Conceptual block diagram of proposed pulse charger. 57

Figure 27 Pulse charger flow chart. 58

Figure 28 Block level diagram of pulse charger. 61

Figure 29 Regenerative comparator showing hysteresis. 63

Figure 30 Open loop comparator. 63

Figure 31 Advantage of hysteresis window. 65

Figure 32 Transistor level diagram of comparator. 66

Figure 33 Plot of various transistor parameters versus inversion level. 69

Figure 34 Gain and phase plot of amplifier stage in comparator. 71

Figure 35 Hysteresis of comparator. 72

Figure 36 Hysteresis window of designed comparator. 75

Figure 37 Conceptual idea of DCG. 77

Figure 38 Positive edge triggered flip flop operation. 78

Figure 39 Duty cycle generator. 78

Figure 40 Waveforms of duty cycle generator. 79

Figure 41 Trickle charging phase block diagram. 81

Figure 42 Trickle current, ITC, versus resistance, RTC. 82

Figure 43 Trickle charging phase operation signals. 83

Figure 44 Fast charging phase block diagram. 86

Figure 45 Fast charging phase operating signals. 87

Figure 46 Safe operating region of circuit and battery. 88

Figure 47 Overcurrent protection circuit. 89

Figure 48 Error amplifier, C2, with boosted output impedance. 91

Figure 49 Temperature sense circuit. 93

Figure 50 Output signal of temperature sense circuit. 95

Figure 51 Conceptual idea of overvoltage protection. 97

Figure 52 Overvoltage protection and termination. 97

Figure 53 Detailed block diagram of pulse charger. 99

Figure 54 Pulse charger in normal operation connection diagram. 101

Figure 55 Battery charging using pulse charger. 101

Figure 56 Waveforms showing operation of pulse charger. 102

Figure 57 Operation of pulse charger as trickle charger. 104

Figure 58 Operation of pulse charger as constant current charger. 105

Figure 59 Linear regulator (LDO) and switch inductor converter (buck). 109

Figure 60 Switched capacitor converter. 111

Figure 61 Operation of switched capacitor converter during different clock phases. 112

Figure 62 Transistor level implementation of switched capacitor converter. 116

Figure 63 Operation of switched capacitor converter with V_{batt}=3V at no load. 117

Figure 64 Converter's output voltage variation with load current. 118

Figure 65 Converter output variation with varying battery voltage. 119

Figure 66 Efficiency of switched capacitor converter at 3V input. 120

Figure 67 Flow chart showing conceptual idea of switching network system. 122

Figure 68 Conceptual block diagram of switching network system. 123

Figure 69 Clocked comparator. 123

Figure 70 Operation of clocked comparator. 125

Figure 71 Transistor level implementation of switching network system. 126

Figure 72 Operation of switching network system. 128

Figure 73 Micrograph of user programmable battery charging system IC. 129

Figure 74 Pictorial representation of experimental setup. 130

Figure 75 Test bench to verify operation of proposed pulse charger. 131

Figure 76 Test result verifying operation of proposed pulse charger in normal mode. 132

Figure 77 Trickle mode charging of Li-ion cell using reconfigured pulse charger. 133

Figure 78 Constant current charging using reconfigured pulse charger. 134

Figure 79 Schematic of switched capacitor test bench. 135

Figure 80 Control signal for clock phases and output voltage ripple of converter. 135

Figure 81 Converter's output with a 3V input and increased output capacitance. 136

Figure 82 Output voltage variation versus input voltage variation. 136

Figure 83 Efficiency of converter. 137

Figure 84 Schematic of switching network system test bench. 138

Figure 85 Operation of switching network for supercapacitor and battery < 3V. 139

Figure 86 Operating signals of switching network system. 140

LIST OF TABLES

Page

Table 1 Different battery chemistries 19

Table 2 Comparison of types of Li-ion battery charger 34

Table 3 Design parameters depending on multi cell or single cell applications 36

Table 4 Energy sources and their estimated harvested power 40

Table 5 Comparison of previous works 55

Table 6 Specifications of pulse charger 61

Table 7 Comparator first stage transistor dimensions 70

Table 8 CMOS Schmitt trigger transistor dimensions 74

Table 9 Trickle currents and corresponding resistor values 82

Table 10 Transistor dimensions of C2 92

Table 11 Pulse charger pin descriptions and maximum ratings 100

Table 12 Specifications of the EHS 107

Table 13 Comparison of different step down converters 110

Table 14 Clocked comparator transistor dimensions 125

Table 15 Comparison of proposed charger with previous works 141

1. INTRODUCTION

Most systems, from automobiles to smart phones, are powered by energy storage devices. Energy storage device usage ranges from emergency power to portable devices, which provide the convenience of movement without the impediment of wires. Energy storage devices, such as batteries, have proved to be an important factor in the increase and release of smart and high performance battery powered devices on the market today. With smart computing and portable electronic devices blooming in the global market, consumers are pushing for extended battery power usage and longer lasting batteries to prevent frequent charging and replacement. Companies and original equipment manufacturers (OEM) are therefore investing in smart battery chargers and battery management systems (BMS) and are also looking for new and more efficient ways to make consumers happy in that regard. Battery chargers and BMS continue to be very important in battery powered systems since once the energy is depleted from the battery, it has to be replenished for continuous use, and therefore the market for chargers and BMS will continue to grow as long as there is an increase in demand for rechargeable batteries. According to a recent report by Global Industry Analysts Inc. (GIA), the global consumer batteries market is going to reach $55.4 billion by 2017 [1] and this is being fueled by the rising popularity of portable electronic devices such as smart phones and tablets.

In this day and age, where the world is moving towards green, renewable and sustainable energy, energy storage devices are needed in the area of energy harvesting. Renewable

energy, which is environmentally friendly, can effectively be stored without any environmental hazards for a time frame ranging from a few seconds to several months and reused almost immediately. Renewable energy does not provide a steady stream of power and hence, energy storage is needed for uninterrupted service. Whether macro energy harvesting to feed into the grid or micro energy harvesting for portable applications, the next fifty or more years is going see a lot of investment in renewable energy, and there is therefore going to be a demand for better harvesting techniques and energy storage devices. The advancement of smart power management systems will help support the development of new energy storage technologies. Macro or micro energy harvesting systems will definitely include a charger to replenish any energy lost from the storage device.

Whatever the system may be, from energy harvesting to electric vehicles, battery powered devices go hand in hand with battery chargers and BMS. There is a need to therefore design efficient, smart and intelligent battery chargers for such systems. These chargers should incorporate safety mechanisms to ensure safety of the consumer and also prevent harm to the battery and prolong its life. The state, remaining capacity and life cycle of a battery depends on the quality of charger used to charge it and therefore, the selection of the appropriate battery charger for a specific battery is of great importance when it comes to OEMs. This is to ensure that the life cycle of the battery is extended to prevent frequent replacement.

A typical battery charging system for portable applications is shown in Fig. 1, which takes power from an input source and replaces the energy depleted from the battery. Traditionally, batteries are recharged from a wall adapter. With recent improvements in technology, batteries can be recharged from a Universal Serial Bus (USB) or from an energy harvesting system.

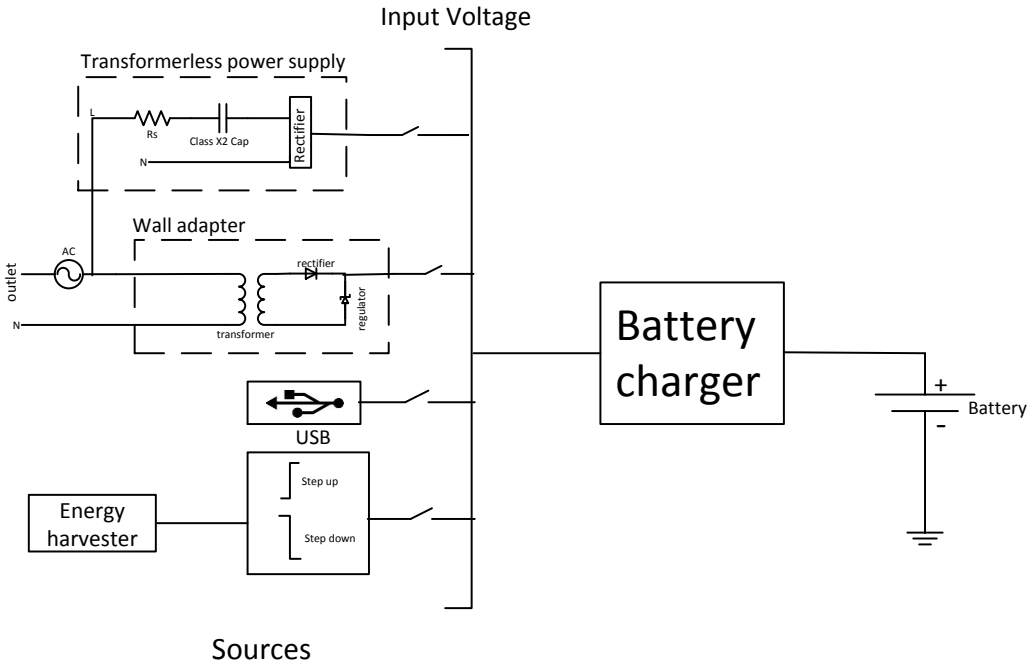

Figure 1 A typical battery charging system.

From a wall outlet, i.e. AC mains, a device known as a wall adapter is used to provide the right input voltage for the battery charger. The standard voltage obtained from the wall outlet is 110Vrms and cannot be directly used to charge a battery. This voltage is stepped down using a transformer, rectified and regulated to achieve a good input

voltage ideal for the charging system. Another method to step down the mains voltage is by using a reactance, which does not only drop the mains voltage but also limits the inrush line current. This method is known as transformerless power supply [2]. It uses a resistor and class X2 capacitor, which could have a voltage rating in the order of kilovolts [3], to drop the mains voltage to smaller voltage which is then rectified for use in portable applications. Though the transformerless power supply consumes much less space and is cheaper than step down transformers, it is not used often because of their non-isolation properties from the mains, which could lead to potential safety concerns.

The input voltage to the charger can also be provided by connecting it to a USB network. The USB network consists of a USB socket and a USB cable [4]. The socket consists of four pins and the cable is constructed using four 20 or 28 American wire gauge (AWG) wires [5]. The USB socket pins include two inner pins for data transfer and two outer pins for power supply. These two outer pins provide the charging voltage and current to the battery charger. Likewise, the USB cable has two wires for power supply and two wires for data transfer. The construction of the standard USB network provides a clean and good voltage for a charging system in portable battery powered applications. The USB outputs a voltage ranging from 4.75V to 5V, allowing a maximum charging current of 0.5A [6].

Using an energy harvester source requires some type of step up or step down circuit depending on the available power the harvester is able to produce. The step up or step down circuit is needed to be able to achieve the right input voltage for the charging system. Energy harvesters, such as solar cells, can output a high or low voltage

depending on the environmental conditions. In cases where the harvester produces a high voltage, which cannot be applied directly to the charging system, a step down circuit, such as a buck converter, is used to reduce the voltage to an ideal value. When the harvester output voltage is low, such as the output power derived from radio frequency emissions, a step up circuit, such as a boost converter or a charge pump, is needed to up-convert the voltage to a value which is suitable to charge the battery. In some cases, the boost or buck converter incorporates the battery charger.

Many battery charging systems use the wall outlet, USB or a combination of the two as input sources. Energy harvesting systems incorporating chargers make use of only energy harvesters as their input sources. Many battery chargers do not use a combination of the three input sources. Also, they do not provide flexibility to users to change the configuration of the chargers to meet a specific need, i.e. to charge different types of batteries. In this thesis, the charging system designed seeks to combine all three inputs, depending on which one is available. It also provides the user with options to change the configuration of the charger to meet a specific need, i.e. the charger can be reconfigured from its original design to behave like another type of charger. This can be a pulse charger, a constant current charger or a trickle charger. This is done to increase the number of applications which can use this system. The benefits of combining different input sources is to extend battery power usage and enable charging under different conditions, such as in applications where a wall outlet is not available, or to make use of available green energy. It can therefore be used in a multi-purpose environment. In order to do this, additional blocks are designed to support the battery charger: a step down DC

to DC converter to serve as a power supply for an energy harvesting system (EHS), and a switching network system to enable the charging of the battery from all available input sources. The conceptual idea for this proposed battery charging system is illustrated in Fig. 2.

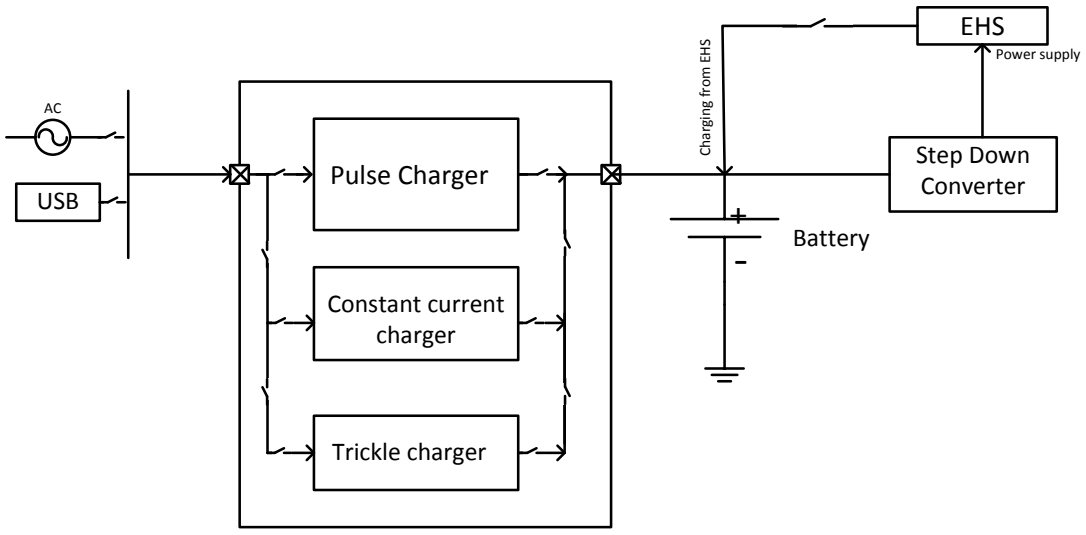

Figure 2 Proposed user programmable battery charging system.

When it comes to the load, the charging system designed is used to charge a battery powering a sensor, preferably a humidity sensor. The system seeks to combine two energy storage elements, i.e. battery and a supercapacitor, to meet the demands of the load, i.e. sensor. A supercapacitor is utilized for short term peak power demand and a battery for constant power demand. The main idea is to increase the life cycle of the battery and to ensure longer periods between charges.

1.1 Thesis organization

The main objective of this thesis is to design a battery charging system capable of supporting USB, AC-DC and energy harvesting applications. The charging system will consist of a battery charger, a step down DC-DC converter and a switching network system to extend the number of input voltage sources that can be used. The main challenge in designing such systems is ensuring the battery charge method is ideal for whatever type of battery used, and then ensuring that the charge profile includes measures to prevent any potential harm to a user and extending the life cycle of the battery. A charging system incorporating safety measures and good charging profile is designed in this thesis.

Section 2 first introduces energy storage elements and energy harvesting, delving into the different types of batteries, charge methods, battery chargers and energy harvesters. It then provides an overview of the entire charging system to be designed.

Section 3 begins by discussing previous works in literature, and then a detailed design procedure of the proposed charger. The conceptual idea and a description of the block diagram are given. Transistor level design of each block is discussed in more detail and then the section concludes with schematic simulation results to prove the design follows the ideal charge profile of the battery used and the safety mechanisms employed in the design work.

Section 4 introduces the two additional blocks, i.e. the step down DC to DC converter and the switching network system. Different types of step down DC to DC converters

are described and the reason behind why a particular topology is chosen over others is given. The design procedure of the converter is discussed and the simulation results to prove the designed circuit works at various load conditions is presented. The detailed process flow of how the switching network work is presented and the transistor level implementation introduced. The section concludes with simulation results which prove that the proposed switching network system enables charging of the battery from an energy harvesting system.

Section 5 takes a look at experimental results showing how the designed system will work under real life conditions. Comparison is made with previous works reported in literature.

In section 6, conclusions are drawn from the results obtained and proposed improvements are discussed.

2. ENERGY STORAGE AND ENERGY HARVESTING

Most systems are powered by energy storage devices and most times these devices need to be recharged to prevent the inconvenience of constant replacement and additional cost. Likewise, energy harvesting goes hand in hand with energy storage and that implies the use of energy storage devices such as batteries and supercapacitors. This section looks at the different applications that make use of batteries, the battery, different battery chemistries, battery charging and an introduction to energy harvesting. The section will conclude with an overview of the entire charging system which includes the charger, switching network system and step down DC to DC converter designed in this thesis.

2.1 Energy storage devices

Energy storage is basically the storage of energy in a device for later use. The uses of this stored energy can be for emergency purposes, portable applications or for reliability reasons. There are many forms of energy storage such as mechanical, thermal, chemical and electrical [7]-[10]. For this thesis, electrical and electrochemical forms of energy storage will be examined. Some major examples of energy storage devices of this form are fuel cells, batteries and capacitors [10]. Fuel cells are generally not for portable applications [11]. They generate electricity through an oxidation or reduction process involving hydrogen and oxygen. A battery converts its internal stored chemical energy into electrical energy while a capacitor stores energy in its electric field [12]. Batteries and capacitors will be the main focus in this thesis.

2.2 Applications of batteries

The usage of energy storage devices, such as batteries, can be found everywhere, from smart phones to smart grids [10], [13]-[15]. In this regard, battery usage can be categorized into three major applications [15]-[17]: portable, stationary and motive. Fig. 3 illustrates a summary of the major battery powered applications.

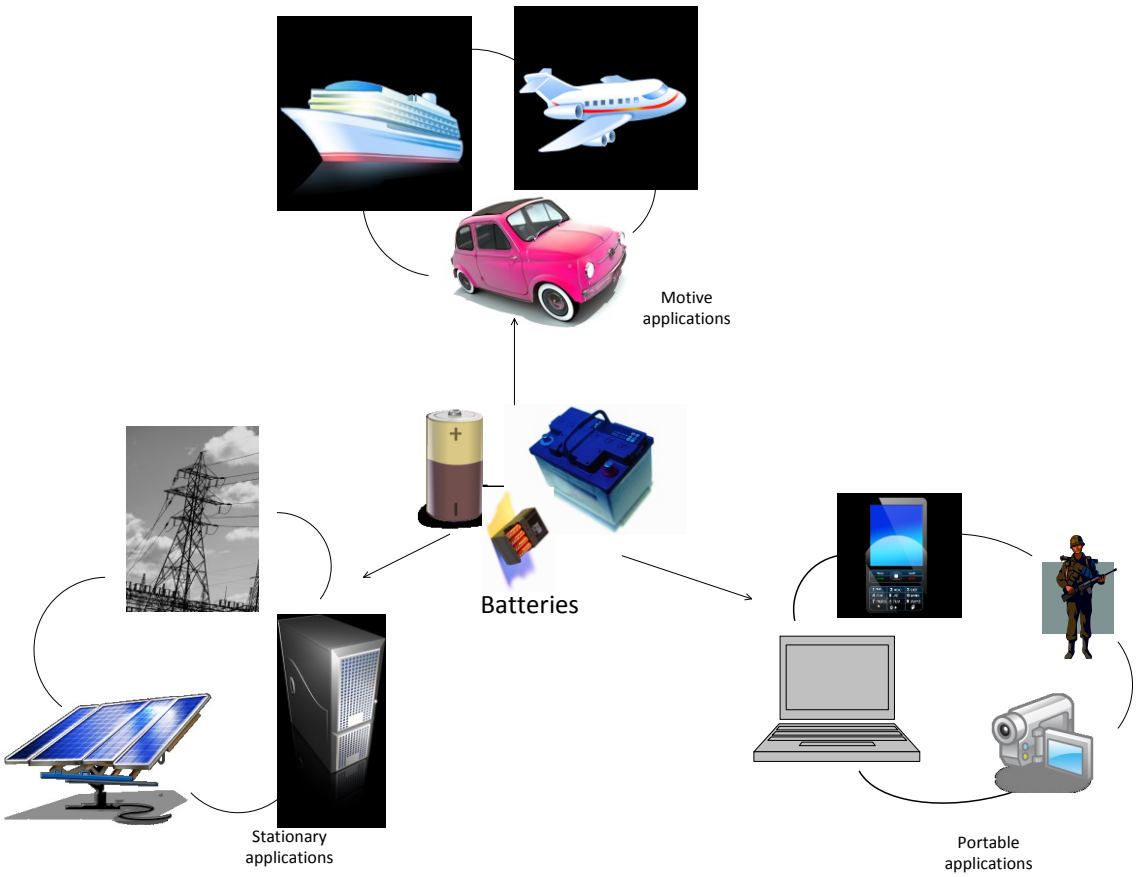

Figure 3 Major applications of batteries.

2.2.1 Portable applications

Portable applications include smart phones, Global Positioning System (GPS), computers, digital cameras and Personal Digital Assistant (PDA). These applications are fuelling the increase in the global market demand for consumer batteries. The medical industry is another area where batteries are used often. This industry is making vast advances in the area of using efficient and long lasting batteries in wearable medical devices and portable medical equipment. For portable applications in the military [18], the ground soldier ensemble is a typical example where the soldier has a wearable computer, wireless transceivers, a head mounted display and a thermal weapon scope, which all contain batteries. These enable the soldier to have decreased reaction time and increased awareness during combat.

2.2.2 Stationary applications

These include standby power plants, which make use of maintenance free batteries, to power electrical and electronic appliances in case of a power outage. With more and more people moving towards cloud computing, there is a need for data storage servers to have uninterruptible power supply to prevent any loss of data. This implies the need for backup power supplied by batteries in case of a major power outage. The smart grid is also an emerging area in the use of batteries for stationary applications [9]. Renewable energy does not constantly provide a steady stream of power, so grid storage batteries are needed to provide uninterruptible power to consumers. The smart grid maintains and controls the electrical grid to ensure that it is balanced and reliable when connected to

energy harvesters. The smart grid includes energy storage, smart meters and efficient distributed generation.

2.2.3 Motive applications

The electric vehicle is one major area in this type of application. Car manufacturers are investing a lot in longer lasting and efficient batteries for electric vehicles as the world moves towards green energy [19]-[20]. Electric vehicles are not only limited to cars but include electric motorcycles, boats and airplanes. Marine transport [21]-[22] is also another major area that makes use of batteries for on board lighting and motor start-up. The usage of batteries in unmanned underwater vehicles (UUV), unmanned aerial vehicles (UAV) and unmanned ground vehicles (UGV) [23] enables the military to undertake dangerous missions without putting military personnel in danger.

2.3 The battery

Having reviewed some applications involving the use of batteries, the battery as an energy storage device has to be defined. A battery is a collection of two or more electric cells, which stores energy for later use. An electric cell is a device, which converts a chemical reaction into electrical energy. A typical electric cell contains a cathode (negative side), an anode (positive side) and the electrolyte. This is illustrated in Fig. 4.

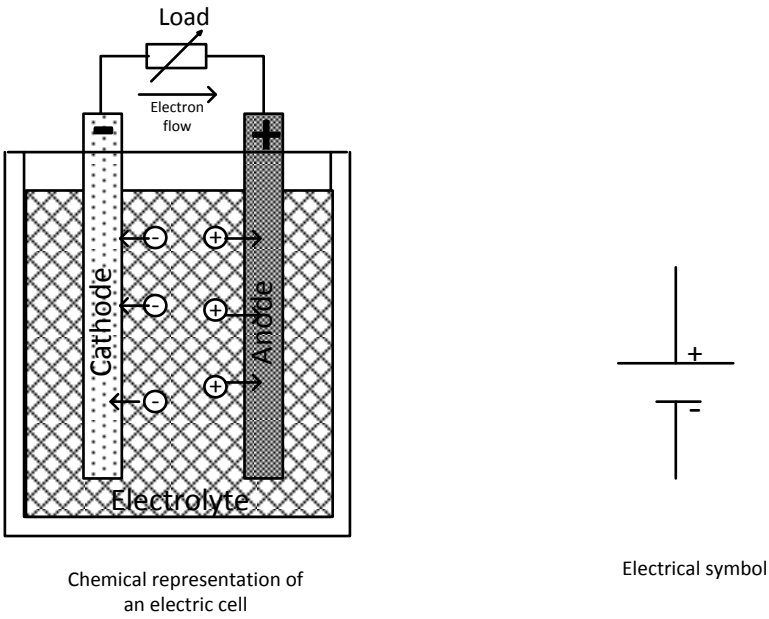

Figure 4 Chemical and electrical symbols of an electric cell.

When a load completes a connection between the anode and the cathode of a battery as shown in Fig. 4, electrons are produced at the anode due to a chemical reaction between the anode material and the electrolyte. These electrons are then absorbed via a similar chemical reaction at the cathode. This process of electron flow is known as electricity.

A battery can be simply modeled as a voltage source in series with a resistance as seen in Fig. 5. The resistance is due to the resistivity of electrodes and electrolyte [24]. The resistance causes an internal voltage drop when the battery is delivering power to a load, which causes the current and voltage available to the load to be reduced. Battery internal resistance can increase due to aging or discharge. The values of the internal resistance vary from milliohms to a few ohms. A battery with a high internal resistance has a lower output current capability, while a battery with a lower internal resistance ensures that a

high current can be delivered when needed [25]. The relationship between the effective battery voltage, V_B, the ideal battery voltage and the internal resistance, r is shown in equation 1.

$$V_B = V_b - Ir \quad (1)$$

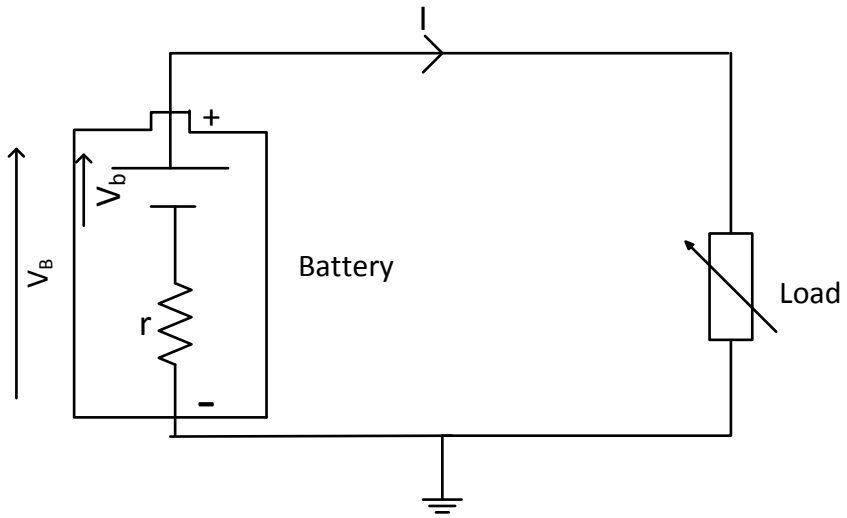

Figure 5 Battery feeding current (I) into a load.

2.3.1 Some commonly used battery terms

- **Battery capacity**: The available electrical charge stored in a battery for transfer when connected to a load. Battery capacity is usually rated in Ampere-hour (Ah). For example, a 1.5V AA Energizer L91 Lithium battery [26] is rated at 3000mAh. This means that the battery can deliver 3000mA current for one hour.

- **Energy density**: This is the energy storage efficiency of a battery, mostly expressed in Watts-hours per Kilogram (Wh/Kg) [27]. It can also refer to the ratio of the battery energy to its weight [28].
- **Depth of discharge (DOD)**: This is the amount of energy expended from the battery expressed as a percentage or fraction of its total capacity. For example, if the DOD specification of a 1000mAh battery is given as 10%, then only 10% of the battery capacity can be used by the load, i.e. 100mA can be drawn by the load in an hour.
- **Life cycle**: This term explains how long a battery can undergo charging and discharging cycles before its capacity is reduced appreciably. This depends on the DOD. A high DOD reduces the life cycle of the battery, while a low DOD increases the number of life cycles a battery can have. Fig. 6 illustrates this dependence.

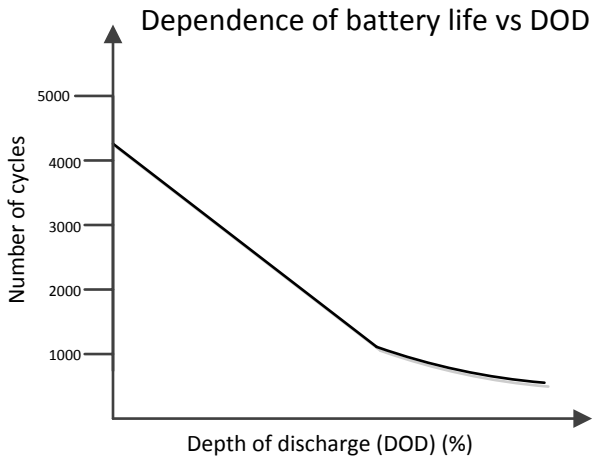

Figure 6 Dependence of cycle life on DOD.

- **Self-discharge**: This is the discharge of the battery when it is not connected to any load. A battery gradually loses its capacity when it is not even connected to a load over time. This is caused by the electrochemical reactions within the cell, which is equivalent to applying an external load [29]. The 1.5V AA Energizer L91 Lithium battery [26] has a shelf life of 15 years which indicates that the battery will lose its capacity completely over a period of 15years due to self-discharge.
- **Memory effect**: This is a term that refers to a condition where a battery temporarily loses its full capacity after discharging and charging below its full capacity over time. For instance, if a Nickel based battery is always discharged to 70% of its capacity, when it comes to a time when the battery has to be discharged below the 70% mark, the battery cannot go below that mark since it has 'forgotten' it has more capacity than that.

- **C-rate**: This term is used to describe the rated current capacity of a battery. For example, a rating of 1C means that a battery with a capacity of 1.5Ah can discharge 1.5A to a load in one hour or it can be recharged with 1.5A in one hour.
- **Specific power**: This is the ratio of the power output of a battery to its unit weight. It mostly has to do with how much current the battery can provide. A battery with a high specific power means it can deliver a large current due to its low internal resistance.

2.3.2 Battery classifications

Batteries can be classified as either primary or secondary. A primary battery is collection of electric cells which cannot be recharged once it is depleted of charge. A secondary battery is also a collection of electric cells that can be charged can be once depleted. This is because the electrochemical reactions in the secondary battery are reversible while in the primary battery, they are not.

2.3.2.1 Pros and cons of primary batteries

Primary batteries have the advantages of being inexpensive and lasting longer at smaller or intermittent current demand since they have high energy density. Primary batteries also have a low self-discharge rate which means longer storage without extensive reduction in capacity. For example, the Energizer L91 [26], which is a primary battery, has a shelf life of 15years which indicates that even after a few years of no usage, the

battery still has adequate capacity to provide power when needed. This is due to its low self-discharge rate.

However, they have the disadvantage of having a high internal resistance meaning it cannot perform well with high current demand applications. Although the initial cost is low, frequent replacement makes it expensive since it has to be discarded once the energy is depleted.

2.3.2.2 Pros and cons of secondary batteries

Secondary batteries carry the advantage of performing well under high current demand applications and having the convenience of rare replacement.

However, secondary batteries have a higher self-discharge rate compared to primary batteries meaning they cannot be stored for long periods without periodic recharging. Though the cost of using secondary batteries is lower in the long term compared to primary batteries, the initial cost is high, which arises from the cost of the batteries and the chargers associated with it.

2.3.3 Major types of battery chemistry

There are various battery chemistries when it comes to primary and secondary batteries. Zinc Carbon and Alkaline are some examples of primary battery chemistries. Nickel based, Lithium based and Lead acid are some types of secondary battery chemistries. Secondary or rechargeable batteries will be the priority in this thesis. Table 1 summarizes the different battery chemistries.

Table 1 Different battery chemistries

Primary batteries	**Secondary batteries**
Leclanchė Cells e.g. Zinc Carbon	Nickel based e.g. Nickel Cadmium
Alkaline cells e.g. Alkaline Manganese Dioxide	Lead acid e.g. Lead Calcium
Lithium based e.g. Lithium Manganese dioxide	Lithium based e.g. Lithium-ion

2.3.3.1 Nickel based batteries

There are two types of nickel based batteries, i.e. nickel metal hydride (NiMH) and nickel cadmium (NiCd). These types of batteries make use of nickel hydroxide as the cathode, either a cadmium metal or a hydrogen absorbing electrode as the anode, depending on whether it is a NiCd or NiMH battery, and an alkaline potassium hydroxide as the electrolyte.

NiMH batteries are gradually replacing NiCd batteries due to NiCd having lesser capacity or energy density and, being environmentally unfriendly. They are also more susceptible to memory effect.

Nickel based batteries have been popular over the years and are found in a number of devices, such as power tools, toothbrushes, two way radios and recently, electric vehicles. They have the advantages of operating over a wide temperature range, performing well under harsh conditions, having rapid and simple charging and the ability to be deeply discharged to almost empty without being affected. However, they are

prone to memory effect and high self-discharge rate and thus Lithium ion batteries are gradually edging them out in some areas in the global market.

2.3.3.2 Lead acid batteries

Due to its low cost and dependable service under rugged conditions, lead acid batteries account for about half of the demand of rechargeable batteries [30]. They are usually used in automobiles and standby power applications. Lead acid batteries are made up of lead dioxide as the anode, lead as the cathode and sulfuric acid as the electrolyte. There are different varieties of lead acid batteries. Some are sealed lead acid (SLA), deep cycle, lead antimony and lead calcium. SLA is designed in such a way to prevent loss of electrolyte through evaporation and hence, they are maintenance free, while deep cycle batteries are designed to be completely discharged before recharge. Lead antimony and lead calcium batteries have electrodes which have been modified with antimony and calcium respectively, to improve performance and lower cost.

Lead acid batteries have the advantages of being low cost, having no memory effect and low self-discharge rate and working well under rugged conditions. The drawbacks of lead acid batteries are their inability to be charged quickly, its heaviness and bulkiness, and the necessity of having proper storage in order to prevent sulfation (the formation of crystalline sulfur due to loss of moisture from the electrolyte), which increases its internal resistance and hence lowers performance.

2.3.3.3 Lithium based batteries

The number of battery powered applications using lithium based batteries has been growing over the years. Mobile computing, plug in hybrid electric vehicles and military applications are some major market shares in the lithium based batteries market. This is because these batteries have a high energy density, are light weighted and have a low self-discharge rate. Though lithium is the lightest of all metals, it is very unstable and can be potentially dangerous. It has to be combined with other metals to improve stability and reduce the dangers during usage and transportation.

In lithium based batteries, the anode is usually made of carbon, the cathode is a metal oxide and the electrolyte is lithium salt. The anode and cathode in lithium based batteries normally reverse roles depending on whether it is charging or discharging. The popular lithium based batteries are lithium-ion (Li-ion) and lithium ion polymer which has a solid electrolyte. These two types may have different types of metal oxide cathodes. Lithium cobalt oxide, lithium titanate, lithium manganese oxide, lithium nickel oxide and lithium iron phosphate are some types of cathodes used in Li-ion batteries. The energy density and nominal voltage vary with these different chemistries. Li-ion batteries come primarily in four basic formats, i.e. cylindrical (small and large), pouch and prismatic [31]. Small cylindrical cells are enclosed in a metal cylinder while large cylindrical cells are enclosed in a hard plastic or metal case. Prismatic cells are enclosed in a semi hard plastic case while pouch cells are enclosed in a soft foil bag.

Li-ion batteries have the advantages of having a high energy and power density, no memory effect, a low self-discharge rate and low weight. Even though Li-ion batteries are largely used in many battery powered applications, they have some shortcomings such as stringent charging requirements and degradation when deeply discharged or overcharged. These shortcomings are far outweighed by the advantages and hence its usage in a vast majority of battery powered applications. A study by TechNavio analysts forecasts a compound annual growth rate of 13.64% for the global lithium battery market in the next three years [32]. Global Information Inc. also predicts the revenue for Li-ion batteries in the transportation industry is set to grow by 700% by 2017, from $2 billion in 2011 to $14.6 billion by 2017. This is primarily driven by plug-in hybrid electric vehicles and battery electric vehicles [33]. The Li-ion battery is becoming an optimum choice for manufacturers of battery powered products; hence this thesis will focus on charging a standard Li-ion battery. Fig. 7 shows the energy densities versus battery weight of different battery chemistries. The figure shows that the Li-ion battery has high energy density at a lighter weight compared to other chemistries and hence, its gradual domination in the market shares of the battery market.

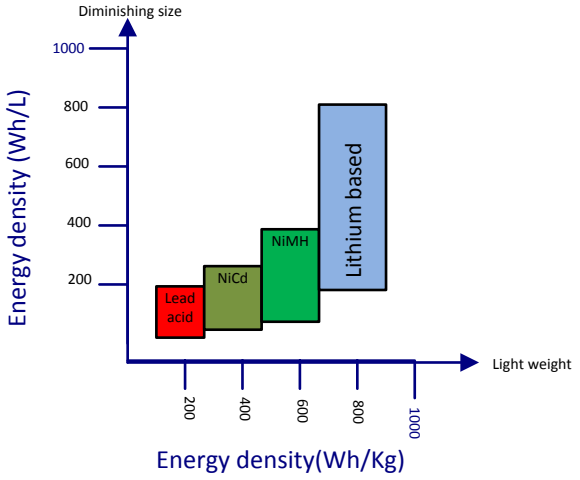

Figure 7 Comparison of battery chemistries in terms of energy density and weight.

2.4 Battery chargers

Rechargeable batteries go hand in hand with good quality chargers and with the global market for secondary batteries surging, the research and development of better quality and efficient chargers is not going to end anytime soon. Once charge is depleted from a secondary battery, the charge has to be replaced through a series of electrochemical reactions, a process called recharging. The cycle life and performance of a battery depends on how efficient and quality its charger is. Bad charging techniques destroy batteries more than any other factor.

A battery charger has three key functions, i.e. charging, optimizing the charge rate and termination, or knowing when to stop charging [34]. The charging process detects the voltage across the battery, then starts charging and keeps charging till a specified value is reached after which charging is terminated [35]. Different battery types have different

charging profiles which gives rise to the different types of charging modes. Fig. 8 provides a conceptual view of the main functions of the battery charger.

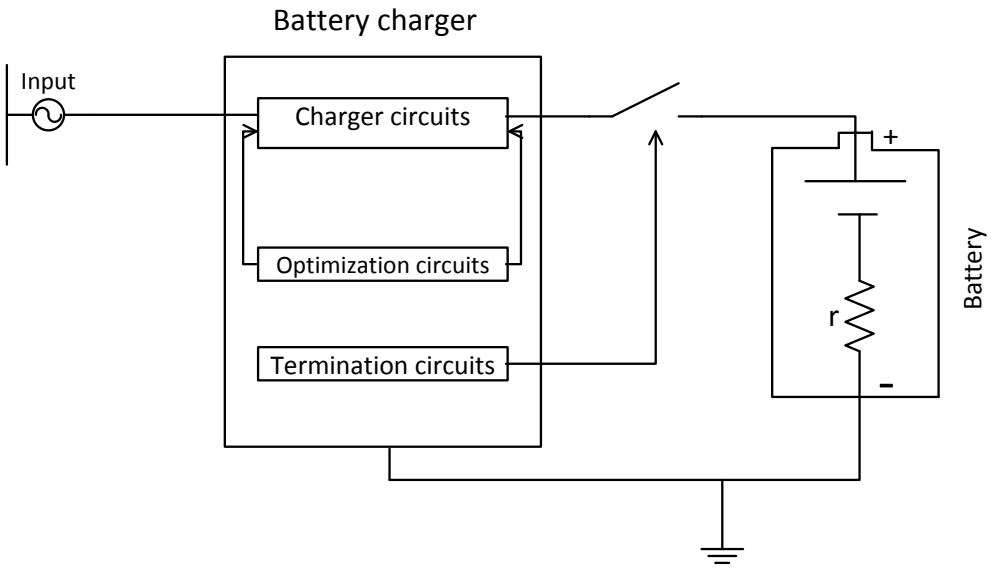

Figure 8 Conceptual view detailing the main functions of a battery charger.

2.4.1 Types of battery charging modes

Depending on the size, type and capacity of a battery, there are different modes of charging. No single mode is ideal for all types of battery. Also, some battery chargers may combine two or three different modes to suit the charging profile of the battery. Some types of charging modes are:

- **Trickle charge mode**: This is when a small and constant current is used to charge the battery. This form of charging is sometimes used when the battery is deeply discharged and needs some form of preconditioning before the main

charge cycle. A Li-ion battery for example, uses trickle charge for preconditioning when it is deeply discharged. In other instances, when a battery is fully charged, trickle charge may be used to sustain its full capacity. Fig. 9 shows the trickle charge profile.

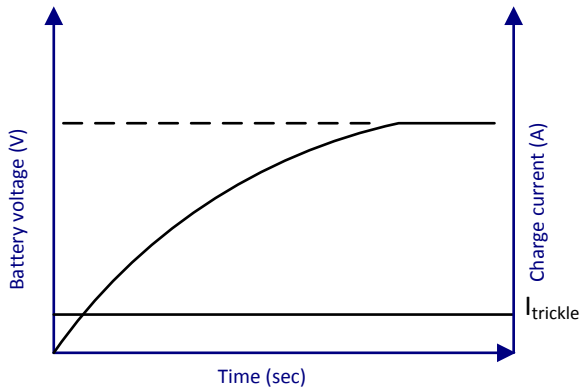

Figure 9 Trickle charge profile.

- **Constant voltage charge mode**: This is when the battery is charged at a constant voltage. Current is sourced into the battery during this mode of charging and it varies to ensure that the battery voltage remains constant. This form of charging is used for lead acid batteries. Fig. 10 shows the constant voltage charge profile.

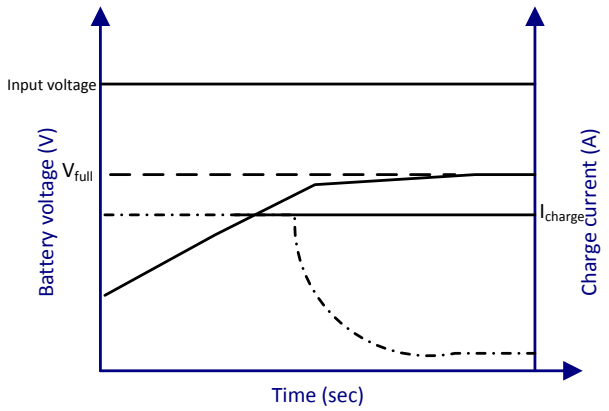

Figure 10 Constant voltage charge profile.

- **Constant current charge mode**: In this mode, the current used to charge the battery is kept constant. When the battery reaches full capacity, the current does not decrease but remains constant and if charging is not terminated, it can lead to overheating which can be potentially dangerous. This form of charging is normally used for NiCd and NiMH batteries. Fig. 11 shows the constant current charge profile.

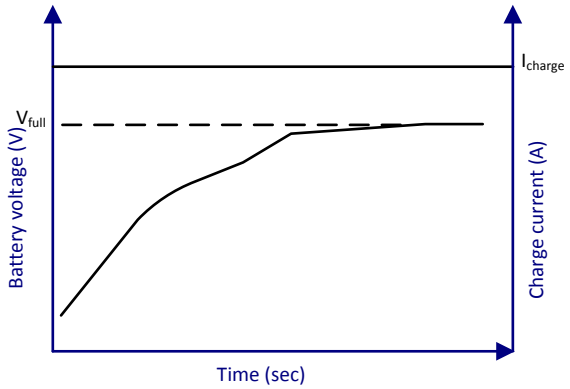

Figure 11 Constant current charge profile.

- **Pulse charge mode**: In this mode, a pulse current or voltage is applied to the battery. This pulse current or voltage has relaxation periods during which the battery has low impedance. This low impedance allows the next charge pulse to go into the battery more efficiently, preventing overheating and overvoltage gassing, thereby increasing the power transfer [36]. Pulse charge can be used for lead acid or Li-ion battery. When a discharge pulse is applied during the relaxation period of a pulse charge, it is known as burp charging. Fig. 12 shows the pulse charge profile.

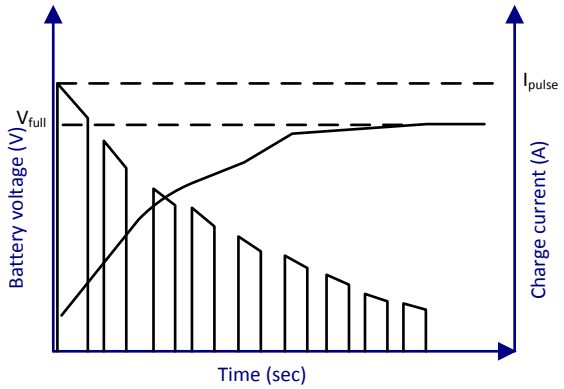

Figure 12 Pulse charge profile.

2.4.2 Li-ion battery chargers

The Li-ion battery is the battery used in this thesis considering the fact that it is the most popular battery of choice in today's portable battery powered applications. As mentioned earlier, its light weight, high energy density and low self-discharge rate makes it the perfect battery for mobile and computing applications. As the charge is depleted from the Li-ion battery, it has to be recharged so as to regain its full capacity. This is done using a Li-ion battery charger. The Li-ion battery has stringent charging requirements in order to prevent over-current and over-voltage. Over-voltage can damage the battery or reduce its cycle life, while over-current can lead to overheating, which can potentially lead to safety issues.

There are different types of chargers specifically designed for Li-ion batteries which have complex charging algorithms to meet the charging profile of the battery. A typical charge/discharge profile of a Li-ion battery is shown in Fig. 13.

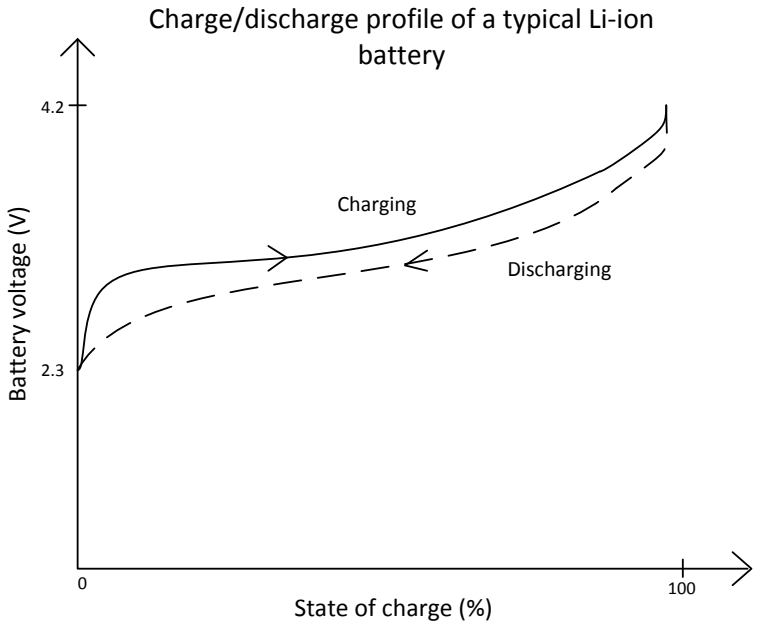

Figure 13 A typical charge and discharge profile of a Li-ion battery.

Most Li-ion battery chargers combine three charging modes, i.e. trickle charge mode, constant current mode and constant voltage mode, to ensure that the Li-ion battery is not susceptible to overvoltage which could damage it. Using only one mode of charging for Li-ion batteries could lead to potential safety issues due to its stringent charging requirements. A typical charging characteristic is shown in Fig.14.

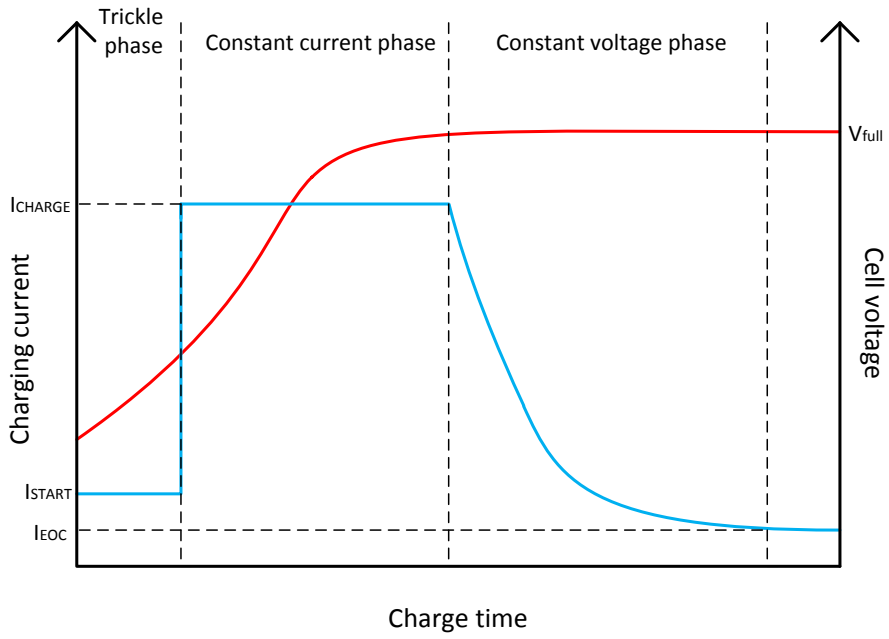

Figure 14 Charging profile of a Li-ion battery.

Trickle charge phase is used when the battery is deeply discharged and needs conditioning. A small current usually ranging from 0.025 to 0.1 of the full charge current (I_{start}) is used. If the battery is in a deeply discharged state and a high current is used for charging, it can damage the battery. This is because in this state, the rate at which electrochemical reactions take place is slower than the rate at which current is fed into the battery, hence the need for preconditioning. The preconditioning period takes a longer time than any of the other modes. Most 4.1V/4.2V rated Li-ion battery powered systems are designed such that the battery voltage does not fall below 2.3V as seen in Fig. 13. The battery management system of the charger ensures that the charger operates in such a way to prevent the battery from going into trickle charge mode, thereby ensuring the battery voltage does not fall below 2.3V. When the voltage of the battery is

above a predefined value, a constant current (from 50% to 100% of the full battery charge current, which is indicated on the battery datasheet), I_{charge}, is used to charge the battery. The constant current phase is much shorter compared to the trickle phase. However, charging with higher currents does not reduce the charging time, but instead causes the battery voltage to increase rapidly leading to over-voltage problems [37]. As the battery approaches full voltage (V_{full}), the constant current phase ends and the constant voltage phase begins. During this phase, the charging current reduces as the battery approaches V_{full} and charging is terminated when a minimum current is reached (I_{EOC}). This type of charging profile is known as the constant current-constant voltage (CC-CV) charging method.

Li-ion battery chargers can be distinguished into three main categories, i.e. linear chargers, switch mode chargers and pulse chargers. Linear and switch mode chargers uses the CC-CV method of charging while pulse charging involves feeding current pulses into the battery. The different categories of chargers are used in specific applications depending on cost, simplicity and efficiency. For example, for low power applications such as energy harvesting, switch mode chargers are used because of their low power consumption.

2.4.2.1 Linear chargers

A linear charger is similar to a linear regulator. A linear regulator usually includes a linear regulating element, which can be a resistor or a transistor. This regulating element drops the regulator input voltage to a precise output voltage. The difference between the

linear regulator and the linear charger is that the charger has added circuitry for battery charge control and protection.

Linear chargers are simple and less expensive compared to the other chargers. However, there is constant current continuously flowing through the regulating element, T_p, which causes a lot of heat dissipation, resulting in the linear charger being inefficient. Fig. 15 shows the concept of the linear charger.

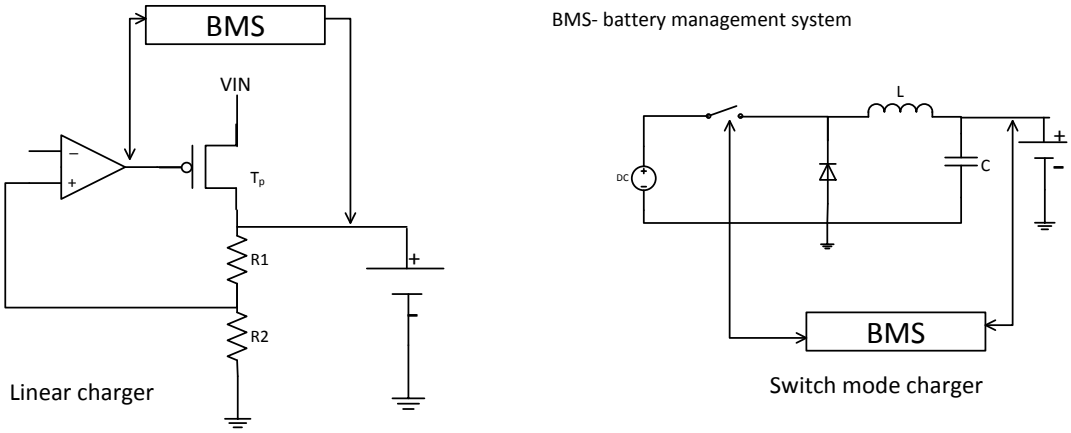

Figure 15 Linear and switch mode charger concept.

2.4.2.2 Switch mode chargers

Switch mode charges are similar to the switch mode power supplies (SMPS). SMPS usually have their output voltages regulated through a feedback system and controlling a series of switches at some frequency depending on the system operation. These power

supplies make use of DC-DC converters such as buck, boost or buck-boost depending on the input voltage. The difference between the switch mode chargers and the SMPS is that the charger incorporates a series of complex circuitry to regulate charging and provide protection for the battery.

Switch mode chargers are more efficient than linear chargers since the switches are not always on, hence dissipating less heat and consuming less power. However, they are very complex and costly compared to the linear charger. Fig. 15 shows the concept of the switch mode charger.

2.4.2.3 Pulse chargers

Pulse chargers use the pulse charge mode for charging. This involves a pass transistor between the input and output which switches on and off, pulsing current into the battery to charge it. Pulse chargers may contain added circuitry to control the pulse width and period to make charging more efficient and faster.

Pulse chargers are less complex compared to switch mode chargers and more efficient compared to linear chargers. Pulse chargers require a carefully controlled current limited input voltage. Since this requirement is stringent, there is an increase in cost associated with it. Fig. 16 shows the concept of a pulse charger.

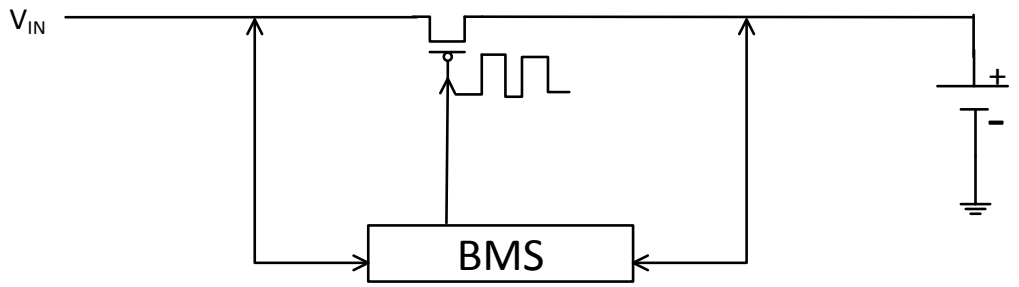

Figure 16 Pulse charger concept.

Table 2 summarizes the pros and cons of each Li-ion battery charger.

Table 2 Comparison of types of Li-ion battery charger

Charger type	**Pros**	**Cons**
Switch mode	• low power consumption • High efficiency	• Complex • Large board area
Linear	• Simple	• High power consumption
Pulse	• Simple • Efficient	• Expensive

2.4.3 Li-ion battery charger design considerations

Before designing a Li-ion battery charger, there are some system parameters that need to be considered. Some parameters such as input voltage, output voltage regulation, charge termination method [37], cell protection, cell balancing and charge control are very important considerations.

Input voltage is an important criterion when it comes to battery charger design. It enables the designer to select a topology suitable for charging. If the input voltage is higher than the battery voltage, it is important to select a charger topology that will step down and regulate the output voltage to a precise value. In such instances, a pulse/linear charger or switch mode using a buck converter can be used. When the input voltage is lower than the battery voltage, a step up converter will be needed to bring up the voltage to meet specification.

Output voltage regulation is another parameter to consider. If the output voltage is not set right, the battery can either be in under-voltage mode, reducing battery capacity or can be in over-voltage mode, raising safety concerns. The output voltage has to be set right to achieve the right battery voltage at full charge.

Charge termination methods differ according to what the designer feels best for the battery. Charge termination is important because if charging is not properly terminated, it can lead to potential safety concerns and reduced life cycle of the battery. Charge termination can be done by using a timer or by terminating when charging current reaches a certain minimum threshold.

Charge control is very essential in preventing over charging. An appropriate mode of charging should be used according to the state of the battery. When the battery is deeply discharged, an appropriate method of charging is by using a trickle charge. It is important to be monitoring the state of the battery in order to use the appropriate method for charging.

Cell protection is a very important parameter when it comes to designing battery chargers. This is to prevent potential danger to the consumer or the device. Additional circuitry is needed to monitor charger parameters such as temperature, current and voltage in order to ensure a safe charging environment.

Cell balancing is done if the charger is going to be used to charge multiple cells. This is to ensure that charge is equalized over all the cells and no cell is being undercharged or overcharged. It further increases the life cycle of the batteries and ensures efficiency when delivering power.

Table 3 summarizes the design considerations based on whether the charger is charging a single cell battery or multi cell battery.

Table 3 Design parameters depending on multi cell or single cell applications

	Design considerations					
Number of cells	Input voltage	Output voltage	Charge termination	Charge control	Cell protection	Cell balancing
Single cell	yes	yes	yes	yes	yes	no
Multi cell	yes	yes	yes	yes	yes	yes

2.5 Energy harvesting

Energy harvesting [38] is simply taking energy from the environment and converting it into electrical energy for daily use. Environmental harvesting [39] is said to be green

since it does not contribute to environmental pollution when being harnessed. Environmental harvesting systems such as hydro power plants, wind mills and solar farms have been around for a long time. The output power of these large scale energy harvesters [40] are huge and are fed directly into the electric grid system to be distributed to consumers. Small scale energy harvesters [39]-[41] which are still emerging in today's market produce very little output power and are usually used for low powered portable applications such as sensors. Micro energy harvesting [40] seeks to reduce maintenance cost in the frequent replacement of batteries, reduce pollution and enable the long term powering of devices in places that are not easily accessible. The most popular sources for micro energy harvesters include solar, thermal, vibration and radio frequency emissions [39]. The energy available from harvesting radio frequency emissions is an order of magnitude less than the other three energy harvesters [40]. All these energy harvesters need some form of power conditioning for it to be able to provide the order of power needed to power portable electronics.

2.5.1 Solar energy harvesting

This is the most popular type [42]-[44] of energy harvesting and can either be obtained from indoor lighting or the sun [45]. Solar energy harvesting is done using solar cells or photovoltaic cells which convert light energy into electrical energy. Depending on factors such as the intensity of the light, size and number of the solar cells, the output voltage and current levels may vary.

The most popular solar powered device is the solar calculator. There are emerging markets for solar powered devices such as battery chargers. An example is the Voltaic amp solar charger, which is designed to charge smart phones, tables, digital cameras and GPS [46].

2.5.2 Thermal energy harvesting

This involves the use of thermoelectric generators to produce electrical energy when there is a temperature difference across two different metals through a phenomenon called the Seebeck effect [38]-[39], [47]-[48]. The Seebeck effect is observed when a thermocouple made up of two dissimilar conductors produce electricity when the conductors are maintained at different temperatures [48]. In instances where light is not present and there is a substantial amount of heat such as in automobiles, thermoelectric generators can produce some adequate amount of power for low powered applications.

In order to obtain a considerable amount of voltage, there has to be a large temperature difference. This problem can be solved by increasing the number of generators but the drawback is that it becomes inefficient because more power is lost across the increased resistance. Recently, integrated circuits have been designed to boost the output power from these thermoelectric generators, which could open the market for wearable devices that make use of body heat. A good example is Seiko Thermic, a wristwatch powered by body heat using thermoelectric generators [49].

2.5.3 Vibration energy harvesting

This is the conversion of kinetic energy of vibrating surfaces into electrical energy. Not all vibrating surfaces can be used to produce electrical energy. To be able to convert vibrations into electrical energy, the vibrations should have a resonant frequency. Electricity produced from vibration energy is alternating and must be rectified in order to be used for portable applications. Examples of converters which convert vibrations into electrical energy are piezoelectric, electromagnetic and electrostatic transducers [48]. Piezoelectric transducers use piezoelectric materials, which have the property of generating electricity under strain or stress. Electromagnetic transducers produce electricity based on the movement of a magnet coil, while electrostatic transducers are based on the movement of the plates of a capacitor, which varies capacitance producing varying voltage.

There are commercial products, which make use of vibration energy today even though there are still challenges being faced in this industry. The Nike smart shoe is a typical example, where the speed and number of steps a person takes are wirelessly linked to a phone or some kind of application. The vibrations from movement are converted into electrical energy to power the sensors in the shoes. Also, the nPower PEG (personal energy generator), which can be placed in anything that moves, can harvest enough energy from the kinetic motions to recharge portable electronics [50].

Table 4 summarizes different energy sources and their estimated harvested power.

Table 4 Energy sources and their estimated harvested power

Energy source	**Harvester**	**Estimated harvested power [40],[48]**
Human motion	Piezoelectric transducers	$4\mu W/cm^2$
Industrial machine vibrations	Electromagnetic/electrostatic transducers	100-800 $\mu W/cm^2$
Thermal	Thermoelectric generators	25-60 $\mu W/cm^2$
Direct sunlight	Solar panels	10-100 mW/cm^2
Indoor light	Solar panels	10-100 $\mu W/cm^2$
Radio frequency	Antennas	$< 1\ \mu W/cm^2$

2.6 The battery and the supercapacitor

The battery and the supercapacitor, also known as electrochemical or ultracapacitor, complement each other in systems where both are present. The supercapacitor differs from conventional capacitors by not having an intervening dielectric material between electrodes [51]. A supercapacitor has its two electrodes immersed in an electrolyte with a separator between the electrodes [52]. The electrodes have much higher surface area and decreased distance between them, hence having much higher capacitance and energy than the conventional capacitors [53]. Fig. 17 shows the conventional capacitor versus the supercapacitor in terms of operation and equivalent circuit. A supercapacitor can be modeled to the first order as a conventional capacitor but due the porous material used to make its electrodes, it exhibits a behavior closely related to transmission lines [54].

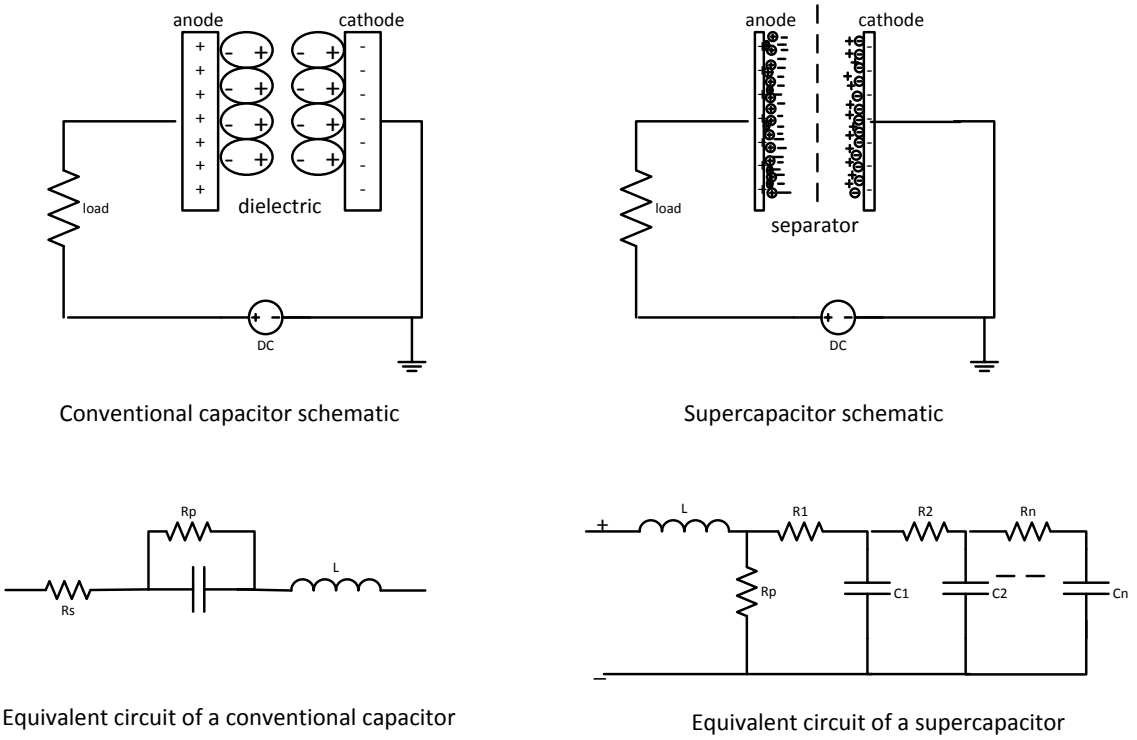

Figure 17 Conventional capacitor versus supercapacitor.

A battery can store more energy than a capacitor, i.e. high energy density, but it cannot deliver it quickly, i.e. low power density, hence supercapacitors are ideal for applications such as sensors where short peak current pulses are needed. Supercapacitors have the advantage of having the ability to be charged rapidly and hence they are ideal for energy harvesting applications. They also have a longer shelf life and can perform well under rugged conditions, such as relatively higher and lower temperatures, compared to batteries. They can undergo many charge and discharge cycles without affecting their capacity because energy is stored in their electric field compared to a battery which stores energy based on a chemical reaction. Despite these wonderful characteristics, they

cannot replace batteries since they have high self-discharge rates and are expensive. This can be explained by comparing the equivalent circuit of the battery, shown in Fig. 5, to that of the supercapacitor (Fig. 17). The resistance, R_p, is negligible in the battery but present in the supercapacitor, and is responsible for high leakage current between the electrodes.

A battery cannot deliver short term peak currents to a load, while a supercapacitor cannot meet the demands of long term peak current. This is because a supercapacitor stores energy in its electric field and not due to chemical reactions and hence can deliver power quickly from its electric field. Therefore, a battery-supercapacitor combination allows peak current pulses to be delivered to a load whenever needed and at the same time sustaining longer term load power demand. This ensures the battery runs longer, safer and at reduced output impedance, which prevents unwanted transients [53]. These two energy storage elements will therefore complement each other in the charging system designed in this thesis.

2.7 Overview of charging system

The main aim of this thesis is to design a battery charging system, which can be used with an energy harvesting systems, USB applications and wall adapters and also reconfigurable to be used as a constant current or trickle charger. This charging system should be able to support sensors in remote locations, i.e. ensuring that battery life lasts longer. Typical voltages for sensors to be used as load for this charging system range from 2.7V to 5.5V, hence a Li-ion coin or prismatic cell with voltages of 3V or 4.2V

respectively will be the target cell to be charged. The charging system seeks to add additional blocks to improve functionality in order to support an energy harvesting system. These additional blocks are a step down DC to DC converter and a switching network system to enable the charging of the battery from an energy harvesting system.

2.7.1 Description of charging system block diagram

A block diagram of the charging system is shown in Fig. 18. The energy harvesting system (EHS) is treated as a black box providing a certain output current and voltage in this project. It is treated as another input source.

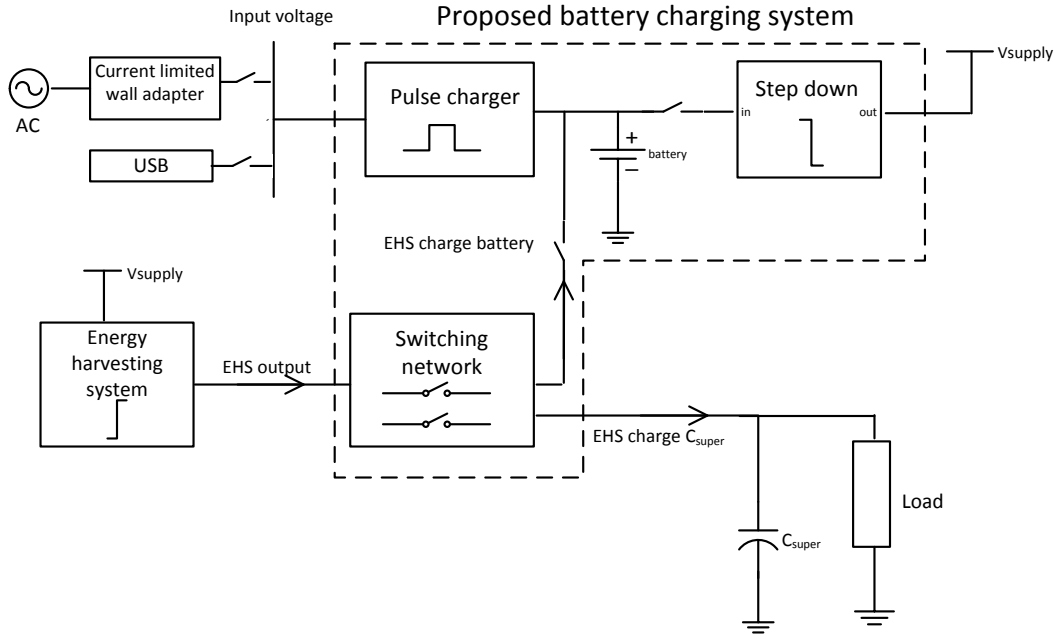

Figure 18 Charging system with DC-DC converter and switching network.

A pulse charger is chosen due to its simplicity, faster charging and less power consumption. The pulse charger will take its input either from a current limited wall adapter or from a USB. It will then charge the battery to its full voltage and monitor system parameters such as input and battery voltage, charge current and temperature to ensure safe charging and battery protection.

The step down DC-DC converter is needed to down convert the battery voltage to an ideal voltage suitable to be used as supply for the energy harvesting system. Energy harvesters provide output voltages that are very low, i.e. microvolts or millivolts. These small voltages are then boosted by charge pump circuits or boost converters to a higher voltage, which can then be used to power an electronic circuit. These booster circuits make use of complementary metal-oxide semiconductor (CMOS) transistors or bipolar junction transistors (BJT) which need a relatively higher voltage for operation. The low voltages produced by the harvesters are not enough to power up the CMOS transistors or BJTs, therefore an initial battery voltage is needed to kick start the system. The step down DC-DC converter is necessary to achieve this initial voltage for startup. The converter can also produce a voltage which might be needed somewhere in a larger system.

To prevent reduced efficiency, the switching network system is designed to bypass the pulse charger and enable battery charging directly from an EHS. It also enables the supercapacitor being charged by the energy harvesting system to deliver short term peak current to a load when needed without affecting the battery, thereby enabling both the

battery and supercapacitor to complement each other. This block ensures that the EHS and the pulse charger operate independently from each other and each can be used as a standalone device.

2.7.2 Description of charging system flow process

When the charging system recognizes that an input voltage, i.e. USB or wall adapter is present, it prevents the battery from being charged from the energy harvesting system. The battery is then charged to a certain voltage which can support the EHS. This is achieved by stepping the battery voltage down. This voltage serves as power supply to power up the EHS to charge the supercapacitor. When the supercapacitor voltage is high enough to support the load and the wall adapter and USB inputs to the pulse charger are not available, the switching network system turns on to charge the battery from the energy harvesting system. When both battery and supercapacitor voltages are good, the switching network system has the option to operate in such a way as to use the supercapacitor for peak load currents and the battery for constant load demand. The above description is shown in the flow chart in Fig. 19.

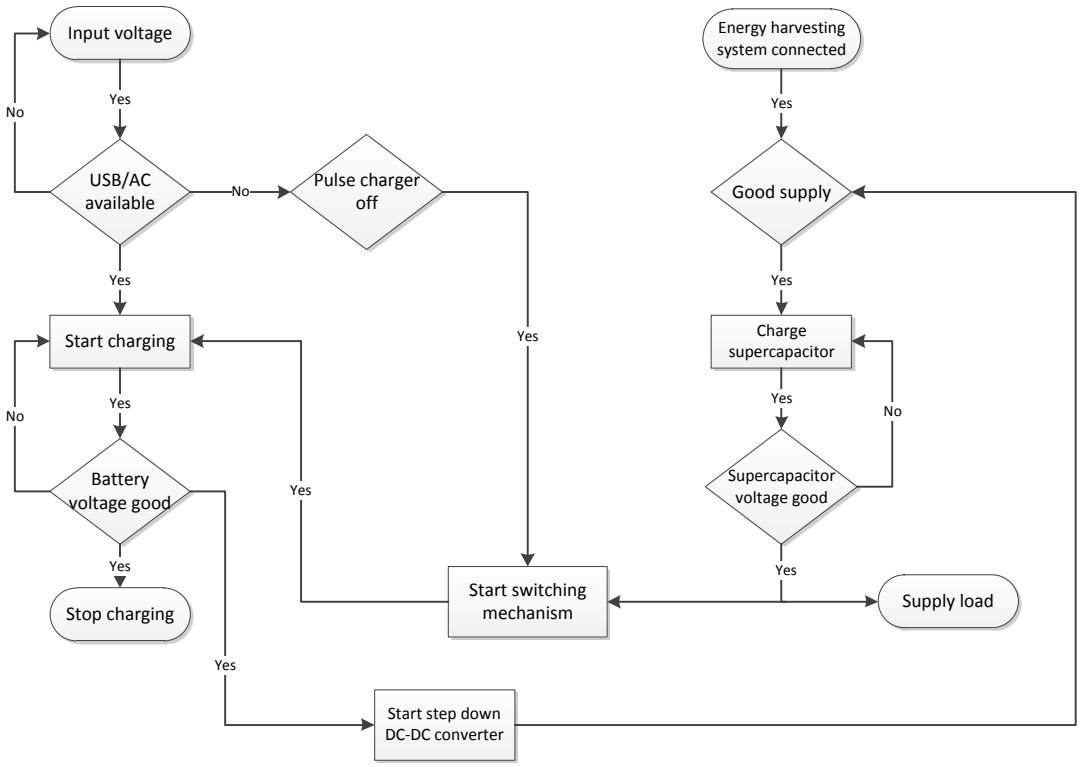

Figure 19 Flow chart showing the operation of the battery charging system.

3. PULSE CHARGER

The type of battery charger designed in this thesis is the pulse charger. It is chosen over the switch mode and linear chargers because of its lower power consumption and simplicity. Pulse charging can be applied to both nickel based batteries and Li-ion batteries. This thesis looks at both NiMH and Li-ion batteries. Tests performed by [55] indicate that pulse charging eliminates concentration polarization, increases power transfer rate and lowers charge time by getting rid of the constant voltage charging phase. Concentration polarization is when ion mobility is hindered in the electrolyte of the battery, increasing internal resistance and voltage drop, thereby preventing the full voltage of the battery from being reached. In pulse charging, the period between pulses allows the chemical reactions in the battery to stabilize before charging begins, enabling the electrochemical reactions to keep pace with the rate of electrical energy input [34]. Pulse charging seems to be an effective method for increasing the life cycle of a battery and achieving a higher discharge capacity [55]. This makes it an ideal choice for the application in this thesis. This section introduces some previous works and commercially available pulse chargers, the conceptual idea of the proposed pulse charger, a description of the block level diagram, a detailed transistor level design and finally presents simulation results to prove the proposed charger design works.

3.1 Previous works

Published works making use of the pulse charging strategy to charge Li-ion batteries include the phase locked battery charger proposed in [56] which uses a phase-locked

loop (PLL) to charge a 4.2V, 600mAh Li-ion battery. The phase locked battery charger makes use of the inherent properties of a PLL, such as auto locking, auto tracking and high accuracy, to charge the battery. A PLL consists of a phase comparator, a low pass filter and a voltage controlled oscillator. The battery is incorporated in the low pass filter in order to construct a fast, safe and cheap battery charge system. In this published work, the charging process consists of three phases: a constant current charge phase where an upper bound current is used to charge the battery, a variable current charge phase where a decreasing current is used for charging and a float charge phase where a small current is used to maintain the battery at a preset voltage. In this work, the 600mAh Li-ion battery is able to charge to 4.2V in 150 minutes proving that though the designed circuit is simple, it can provide a suitable charge current, making the PLL a perfect battery charge circuit topology [56]. Fig. 20 shows the block diagram of the proposed phase locked battery charger.

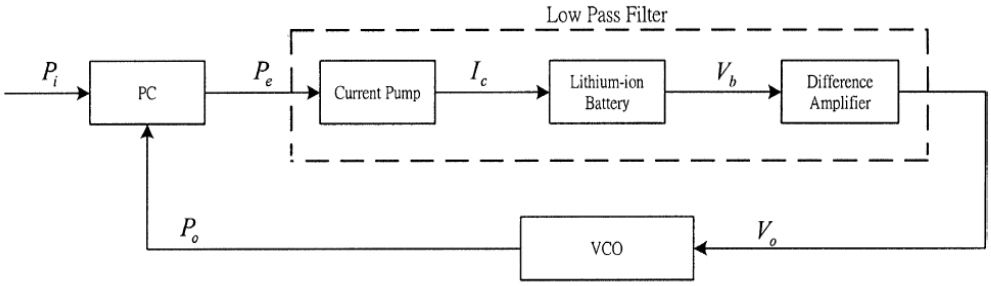

Figure 20 Proposed block diagram of phase locked battery charger.

A variable frequency pulse charge system (VFPCS) is presented in [57] that can dynamically track the optimal charge frequency to improve battery-charge response. This work seems to overcome the trial and error method used in commercial battery pulse charge systems to determine the optimal frequency of the pulse charges. The VFPCS can determine what optimal pulse charge frequency is needed during charging and supply that optimal charge pulse to increase charge speed. The VFPCS is implemented using a microprocessor to detect and control the frequency optimally. A voltage regulator, transistors and a sensing resistor serve as a variable frequency pulse generator. Experimental results verified the performance of the VFPCS by charging a 600mAh Li-ion battery. It showed an improvement of 24% in charge time compared to the standard constant voltage-constant current (CC-CV) charging, proving that the VFPCS can provide pulses with an optimal frequency to charge a battery at a reduced charge time [57]. Fig. 21 shows the implementation of the proposed VFPCS.

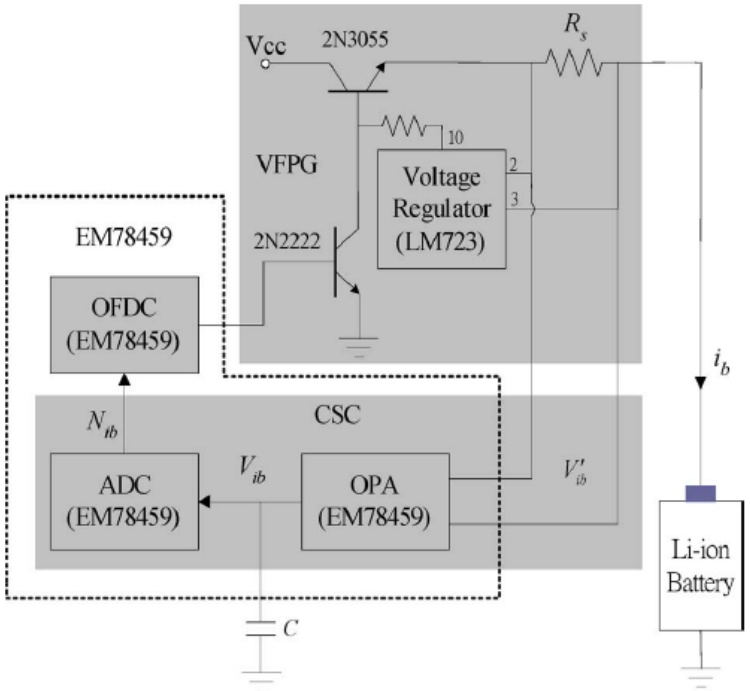

Figure 21 Implementation of VFPCS.

A duty varied voltage pulse-charge strategy (DVVPCS) is proposed in [58] to detect and dynamically track the suitable duty of the charge pulse to improve battery charge performance. Commercial battery pulse charge systems use a trial and error method which might not be suitable. The DVVPS therefore detects the suitable charge pulse-charge duty and supplies that suitable charge pulse to the battery to decrease charge time and improve efficiency. The DVVPCS consists of a controller, a duty varied pulse generator (DVPG), an average current sensor and two analog-to-digital (ADC) converters. The controller and ADC are implemented using a microprocessor to detect the charging modes of the battery. The average current sensor is implemented using an

operational amplifier, a current sensing resistor and a capacitor to detect the average charging current. When the charge current is determined, a corresponding duty, generated by the DVPG, is obtained to increase battery charging speed and efficiency. Experimental results proved that the charge speed of the DVVPCS is improved by 14% compared to the standard CC-CV method. The results indicate that the DVVPCS can actually provide charging pulses with suitable pulse-charge duty for Li-ion battery to obtain fast-charge process. Fig. 22 shows the block diagram of the proposed DVVPCS.

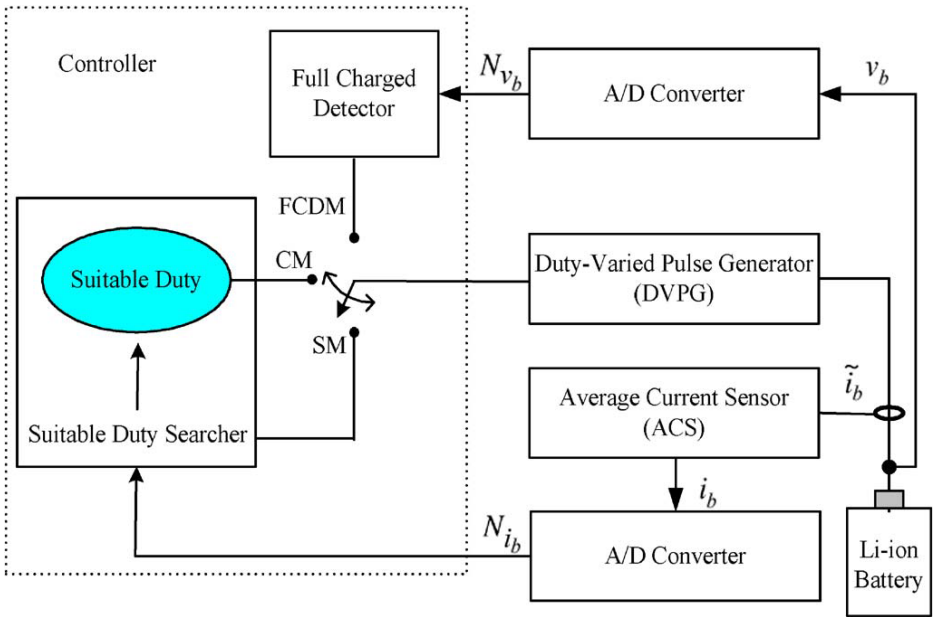

Figure 22 Block diagram of DVVPCS.

Commercial pulse chargers for portable applications on the market today include the LTC4052, LTC1730 and MAX1879. LTC4052 integrated circuit (IC) is a complete standalone pulse charger with an integrated metal oxide semiconductor field effect

transistor (MOSFET) for single cell Li-ion batteries. It is ideal for cell phones and handheld computers. This IC has over-current protection, a thermal shutdown, defective battery detection and a programmable charge termination. The charge current is set by the wall adapter. It has a trickle charge mode which activates when the battery is below 2.45V. The charger goes into a full charge mode when the battery goes above this voltage. When the battery approaches the programmed float voltage, the MOSFET begins switching with a gradually decreasing duty cycle and termination is achieved by a programmable timer [59]. Fig. 23 shows the block diagram of the LTC4052.

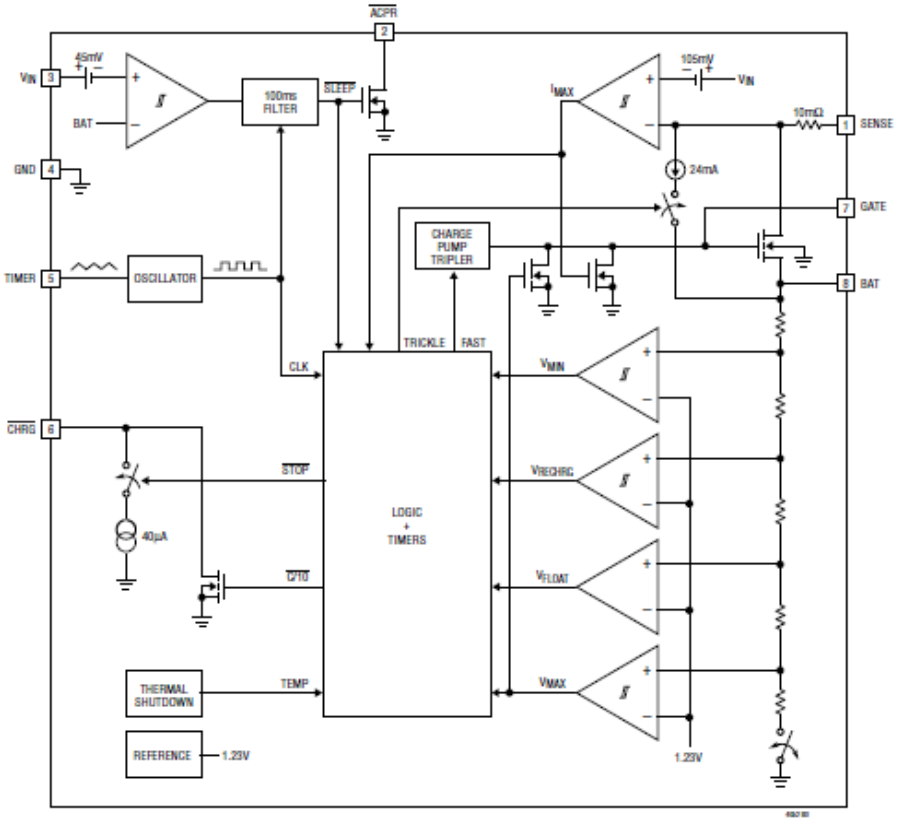

Figure 23 LTC4052.

LTC1730 is a complete pulse charger for single cell Li-ion batteries. It can charge a completely discharged cell by allowing the current limited input power source to provide charge current to the battery through the internal MOSFET. It has the ability to either charge a 4.1V or 4.2V battery by setting the SEL pin. Its trickle charge mode will only activate when the battery voltage is less than 2.45V, after which full charge mode operation starts. This is when the internal MOSFET is turned on. It also has over-current protection, thermal shutdown and a programmable charge termination timer [60]. Fig. 24 shows the block diagram of the LTC1730.

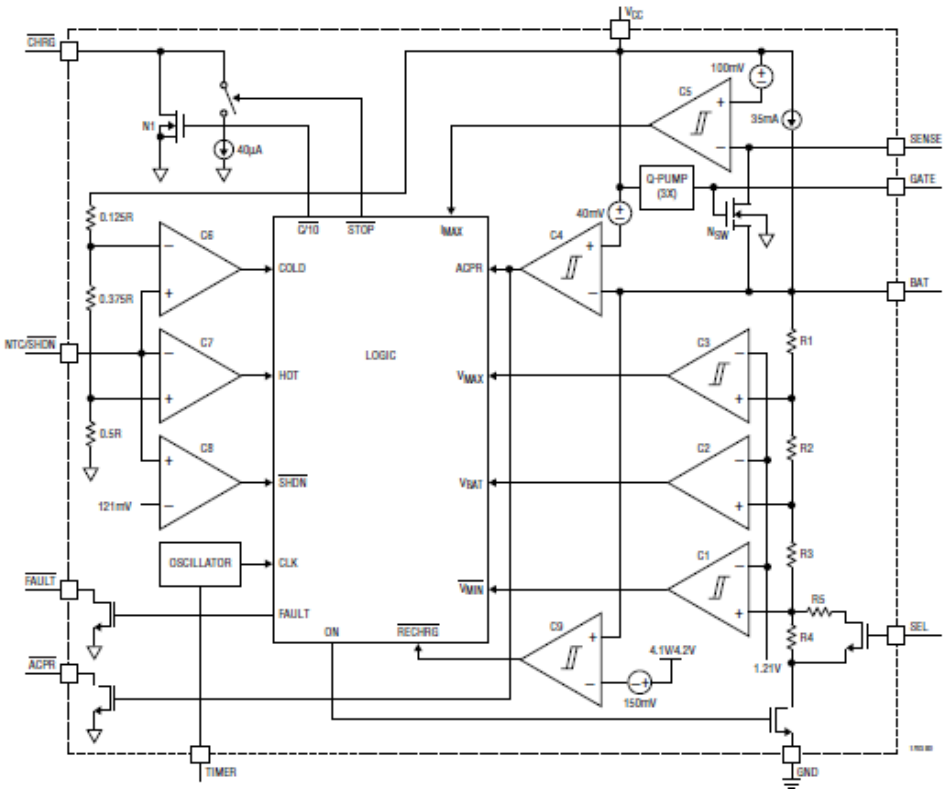

Figure 24 LTC1730.

MAX1879 is a single cell Li-ion battery charger which uses pulse charging strategy to minimize power consumption. It combines the efficiency of switch mode chargers and low power consumption of linear chargers. The IC monitors voltage and temperature continuously and has a preset charger time out function. It can automatically shut down when it detects that input power has been removed to minimize the current drain of the battery. It also has the ability to charge deeply discharged cells and restart charging at 4V. It can be used in many handheld devices, such as cell phones, digital cameras and pagers [61]. Fig. 25 shows the functional diagram of the MAX1879.

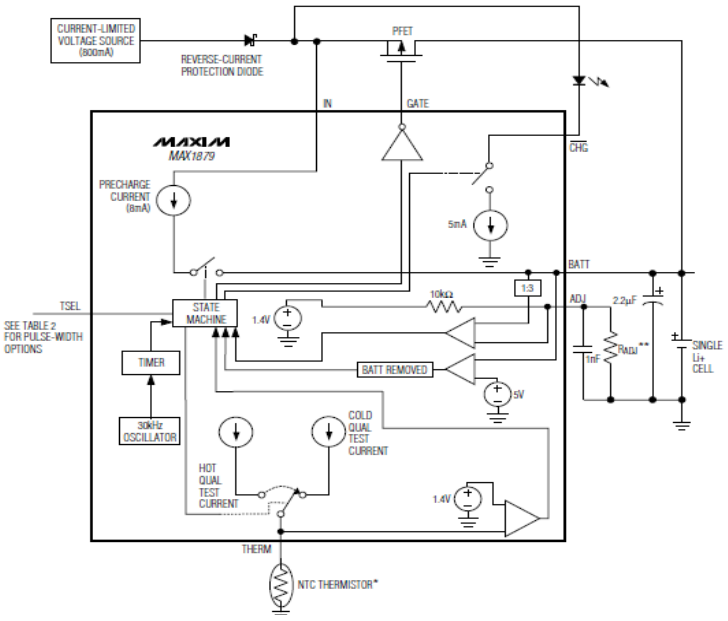

Figure 25 MAX1879.

Table 5 summarizes a comparison of the previous works and commercial pulse chargers discussed above.

Table 5 Comparison of previous works

	VFPCS [57]	**DVVPCS [58]**	**PLL based [56]**	**MAX1879 [61]**	**LTC4052 /LTC1730 [59],[60]**
Control loop	PFM	PWM	-	PWM	PWM
Cell Voltage	4.2V	4.2V	4.2V	4.2V	4.2V/4.1V
User programmable	no	no	no	Partially	partially
Precondition phase	Not indicated	Not indicated	Not indicated	present	present
Over temperature protection	Absent	Absent	absent	present	present
Design implementation	Software/ discrete	Software/ discrete	discrete	analog	analog
Power consumption	-	-	-	minimal	minimal
Charge current	Average current	Average current	Average current	User defined	User defined

3.2 Conceptual idea of proposed pulse charger

The main idea behind this work is to make the pulse charger completely versatile. [56]-[58] propose pulse chargers which reduce charging time. It does not address the issue of a deeply discharged Li-ion battery and also it is discretely implemented. The proposed pulse charger designed in this thesis not only addresses fast charging but also provides a pre-conditioning phase for deeply discharged cells. [59]- [61] are commercial pulse chargers with provision for deeply discharged cells and have important safety mechanisms in place to protect both the user and the battery. However, these chargers can only be used as pulse chargers and does not have the versatility of the pulse charger designed in this thesis. The proposed pulse charger can be used as a standalone pulse charger, a constant current charger or a trickle mode charger. It also seems to provide the user with full programmability options. The trickle current, for example, in [56] - [58] is preset during design and cannot be changed by the user. The charger designed in this thesis provides an option to the user to set the value of the trickle current. The full charge current is set by the current limited wall adapter, similar to that in [59] - [61]. Fig. 26 shows the conceptual idea of the proposed pulse charger.

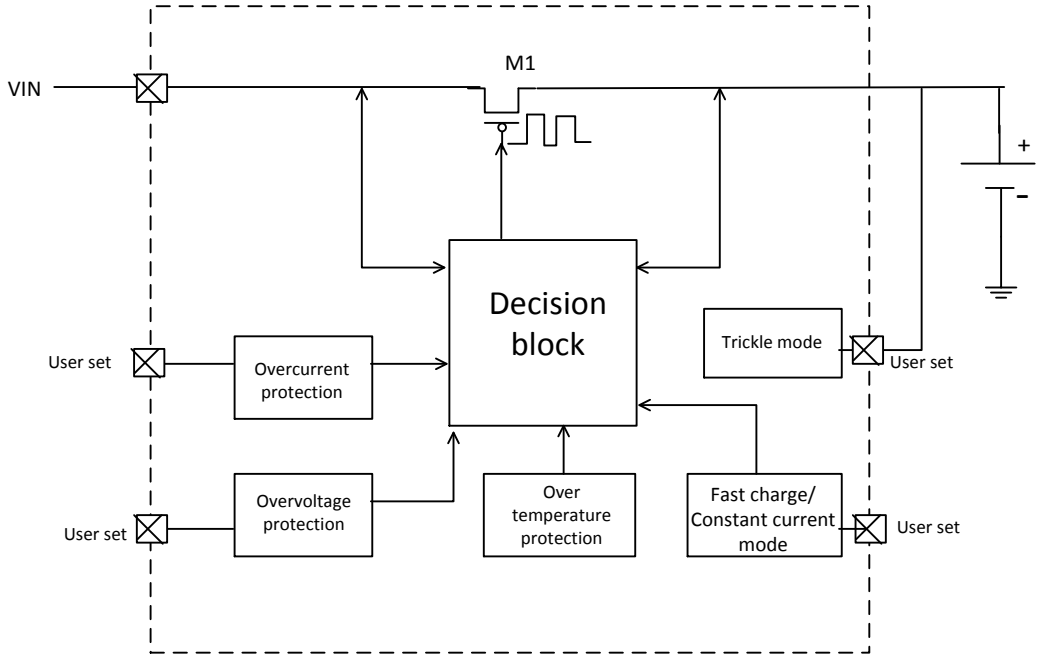

Figure 26 Conceptual block diagram of proposed pulse charger.

Most pulse chargers have a control loop that controls the current pulses and that loop is not accessible to users. They use a form of empiricism to determine the duty cycle. The proposed pulse charger seeks to give control of the period and frequency of the current pulses to the user of the device. The charge current, overvoltage set point, over temperature set point, pre-charge current, power good set point and current limiting can all be user set. This is to enable a wider range of Li-ion coin, prismatic and cylindrical cells with different nominal voltages to be charged and possibly nickel based batteries. The proposed pulse charger is set to charge a maximum of 3.3V rated battery. This is because the maximum voltage rating of transistors used in the design is limited to 3.6V. To prevent permanent damage or device failure, the proposed pulse charger must limit

its input voltage to 3.6V. Specifications of the 3.3V/2.3Ah/7.6Wh OlevinPower Li-ion single cell battery (A123) [62] is used to set design parameters in this thesis.

3.2.1 Flow chart of proposed pulse charger

A flow chart of the proposed pulse charger is shown in Fig. 27.

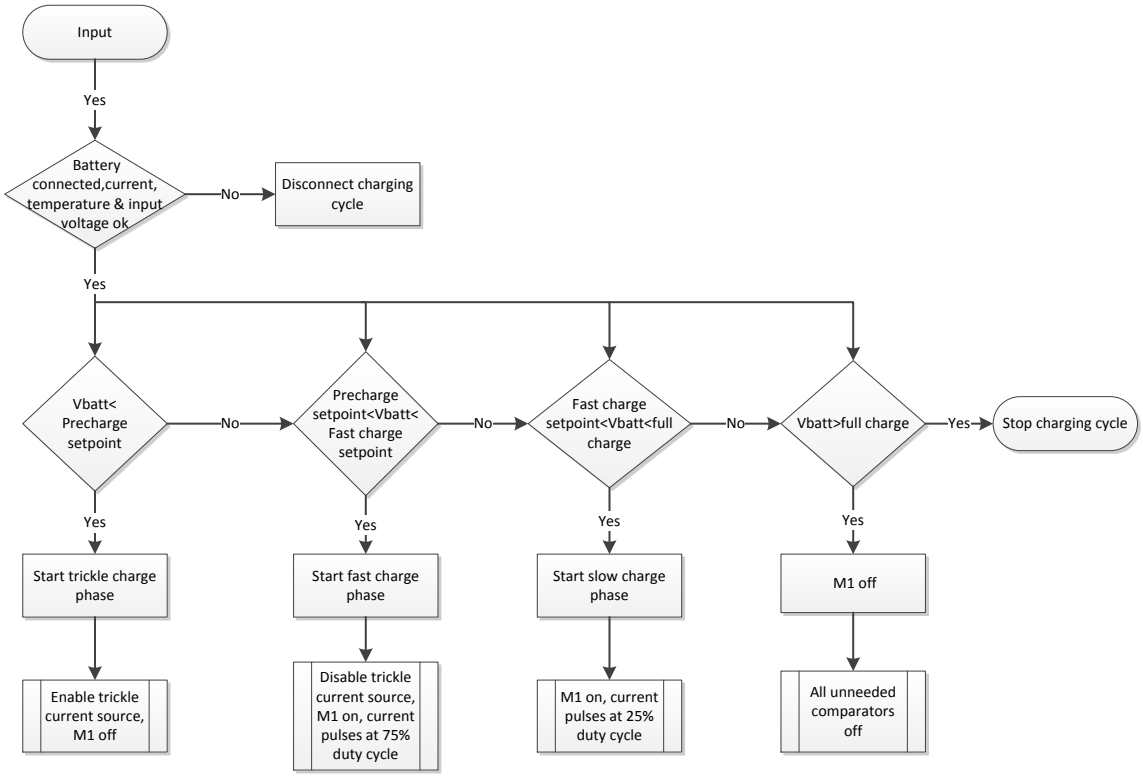

Figure 27 Pulse charger flow chart.

When the input is connected, i.e. a current limited wall adapter, the input current, voltage and current temperature of the device is checked to ensure that they are all within the safe operating range (SOR). If these parameters are within the SOR and a battery is

detected, the charger is given the green light to proceed with charging. These parameters are continuously checked throughout the entire charging process and when any of the parameters fall outside the SOR, the charger is instantly disconnected to prevent any damage.

When charging commences, the battery voltage is determined to see which charging phase is appropriate. If the battery voltage is less than the user set pre-charge voltage, the trickle charge phase is initiated. During this phase, the main power switch, M1 is off. This is to allow an internal current source to pre-charge the battery to a voltage set by the user. The current for pre-charging is also user set and this portion of the device can be used as a trickle charger by disconnecting all other phases.

Once the battery voltage is above the set pre-charge point, the current source for pre-charging is turned off and M1 becomes operational. If the battery voltage is above the set pre-charge voltage, the charger determines whether the battery voltage is above the fast charge voltage set point or below. If it is below, the charger proceeds with charging with a higher duty cycle. During this phase, the input current is pulsed at 75% duty cycle into the battery. This ensures a faster charge time and at the same time enables electrochemical reactions to keep pace with the input of electrical energy. When the battery voltage approaches full charge, i.e. above the fast charge set point, the input current is pulsed at 25% duty cycle to ensure that maximum capacity is achieved and battery charge efficiency is increased. The user can decide on the frequency of the pulses

by providing a clock with a desired frequency. This clock pin can be manipulated to enable the pulse charger serve as a constant current charger.

Termination occurs when the battery voltage crosses the full charge set point, which is also user set. When termination occurs, M1 and all unneeded comparators are turned off to reduce power consumption if the input is still connected.

3.2.2 Description of block diagram

The block diagram of the proposed pulse charger based on the flow chart is shown in Fig. 28. In Fig.28, the pulse charger is in normal mode and has three charging phases, i.e. pre-charge, fast charge and slow charge. The pre-charge phase includes the current source, $I_{T,}$ and the comparator, TC. The fast and slow charge phase is controlled by the FC comparator and a series of logic circuits in the decision block of the charger. Termination is achieved by the OV comparator in connection with logic circuits in the decision block to ensure the battery is not overcharged. M1 is the main power transistor which switches on and off to pulse the input charge current into the battery. M2 is a fractional size of M1 and in combination with M3, comparator C1 and error amplifier C2 form the current limiting branch. The current limit is set by connecting a resistor to the RLIM pin. The PG comparator ensures that the input voltage is always good enough for charging while the temperature sense block ensures that the circuit does not operate under high temperature conditions which can cause device failure. Table 6 shows the specifications of the pulse charger.

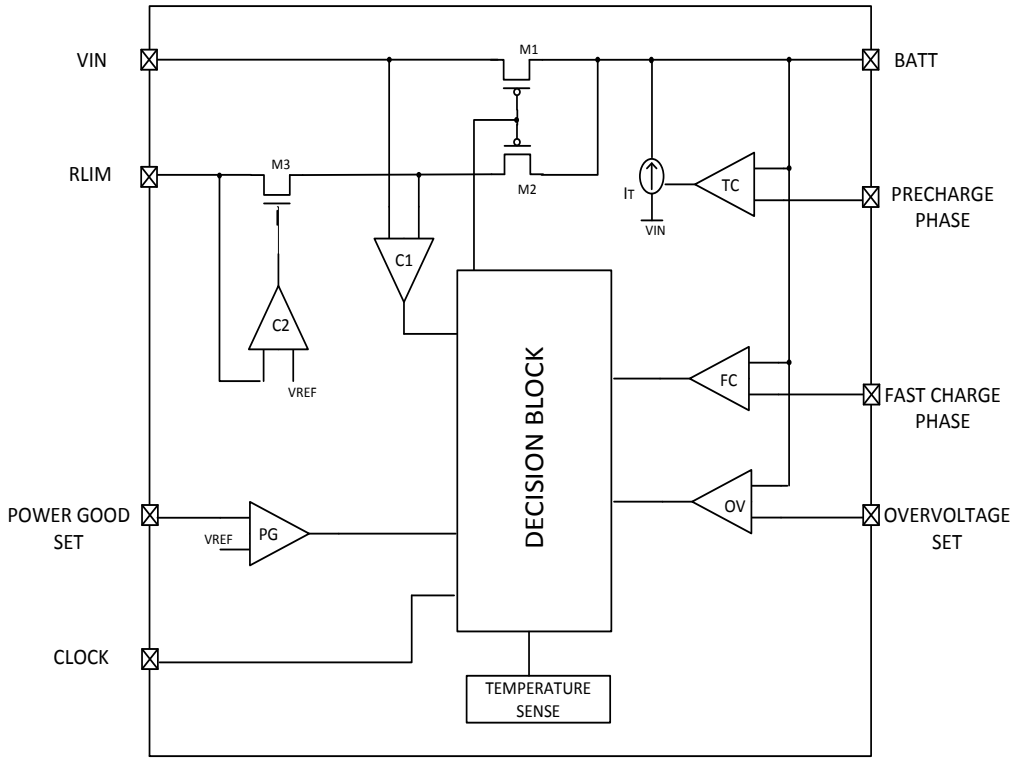

Figure 28 Block level diagram of pulse charger.

Table 6 Specifications of pulse charger

SPECIFICATION	**Min**	**Typ**	**Max**	**UNIT**
Input voltage, V_{in}	3.3	3.3	3.6	V
Input current, I_{in}		200	500	mA
High temperature cutoff, T_{off}			85	^{o}C
Pre-charge current, I_T	5	10	20	mA
Battery voltage, V_{batt}	3	3	3.3	V
Reference voltage, V_{ref}		1.2		V

3.3 Circuit level implementation

This section seeks to describe the building blocks of the pulse charger in more detail. The basic building blocks, including the comparator, which is part of every decision

making block and the duty cycle generator, which forms the core of the fast charging phase of the charging process, are discussed. Secondary building blocks, such as the trickle and fast charging blocks, are also discussed in more detail. Circuits such as the current limiting and over temperature blocks which ensure protection and safety during operation of the pulse charger are also presented. Simulation results showing the operation of each building block are also provided.

3.3.1 Design of basic building blocks

The main basic circuit, which must have good properties due to its frequent use in the charger, is the comparator. The comparator is used at every stage of the charging process and also in the protection schemes. It is necessary to ensure that the designed comparator achieves low power consumption. The duty cycle generator is another basic block for the charger. It is used in the fast charging phase to ensure a smooth transition from one phase to another.

3.3.1.1 Design of comparator

Comparators are circuits that output either a low or high signal depending on the two input signals it receives. Comparators can be classified as open loop comparator, regenerative or a combination of both. An open loop comparator employs an operational amplifier with no compensation while regenerative comparators employ positive feedback. Fig. 29 shows a regenerative comparator using resistors in positive feedback.

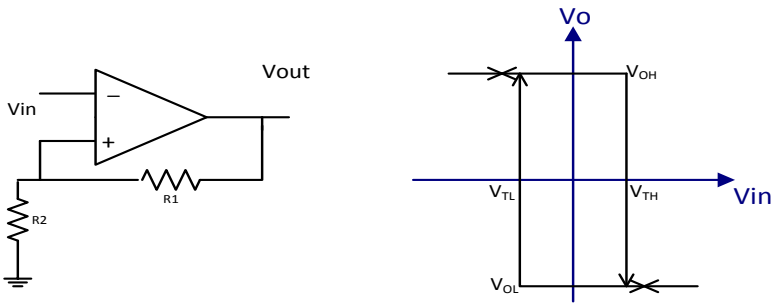

$$hysteresis\ window = \frac{R_2}{R_2 + R_1}(V_{OH} - V_{OL})$$

Figure 29 Regenerative comparator showing hysteresis.

Fig. 30 shows an open loop comparator with two analog input signals, V_+ and V_-, and a binary output signal, V_{out} .

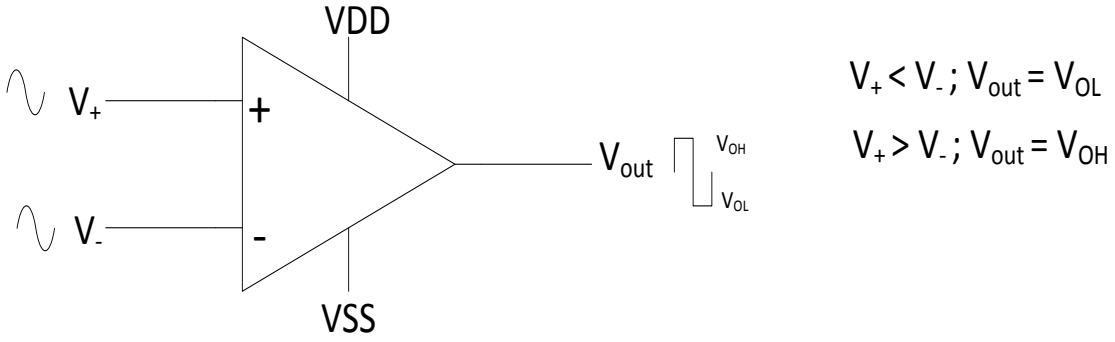

Figure 30 Open loop comparator.

If V_+ is greater than V_-, the comparator outputs a high voltage, V_{OH}, and when V_- is greater than V_+, the comparator outputs a low voltage, V_{OL}. In this project, the

comparators are used in decision circuits to ensure smooth transition from one charging phase to another. The comparator can therefore be seen as a single-bit analog to digital converter.

One important feature needed in the comparator is hysteresis. Hysteresis is the difference between input signals at which the comparator outputs stays at either a high or low voltage depending on its value before it entered the hysteresis window. The window of hysteresis is shown in Fig. 31. The figure also shows an analog input signal superimposed with noise and as it crosses the reference voltage, multiple transitions are triggered at the output of the comparator. If a comparator is designed with hysteresis, the output signal retains its value in the hysteresis window, V_{TH}-V_{TL}, even if the signal crosses the reference voltage many times. The output of the comparator will change once the input signal crosses one of the thresholds, i.e. V_{TH} or V_{TL}. Hysteresis ensures that a noisy signal does not cause these undesirable multiple transitions between states when the input signal is at the switching threshold, hence providing some form of filtering.

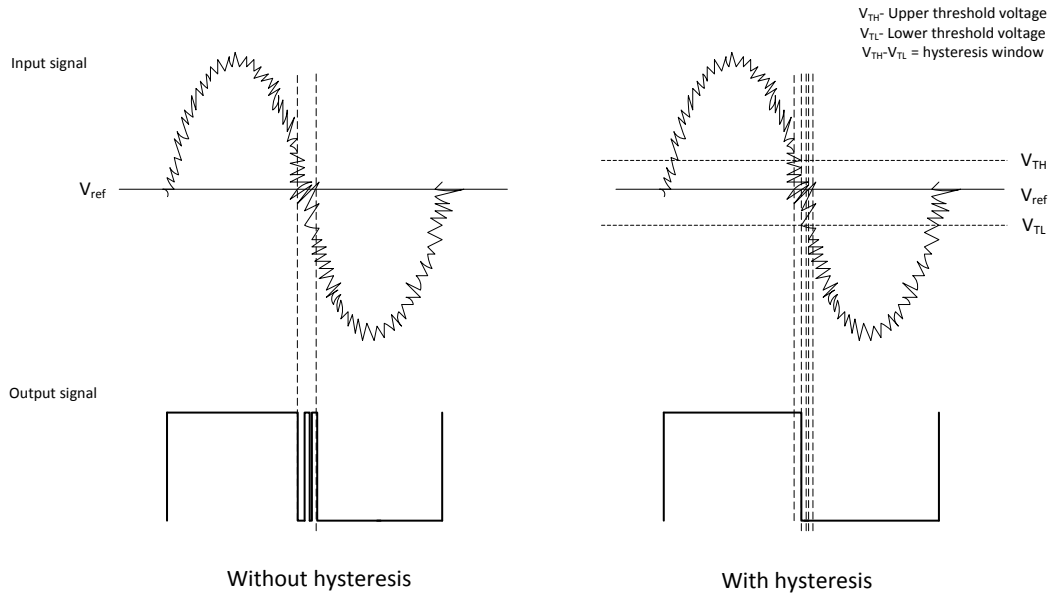

Figure 31 Advantage of hysteresis window.

In this thesis, the comparator designed is shown in Fig. 32. It is composed of a single stage operational amplifier with low offset and enough gain, a CMOS Schmitt trigger to provide hysteresis and a latch to provide stability and a sample and hold function [63].

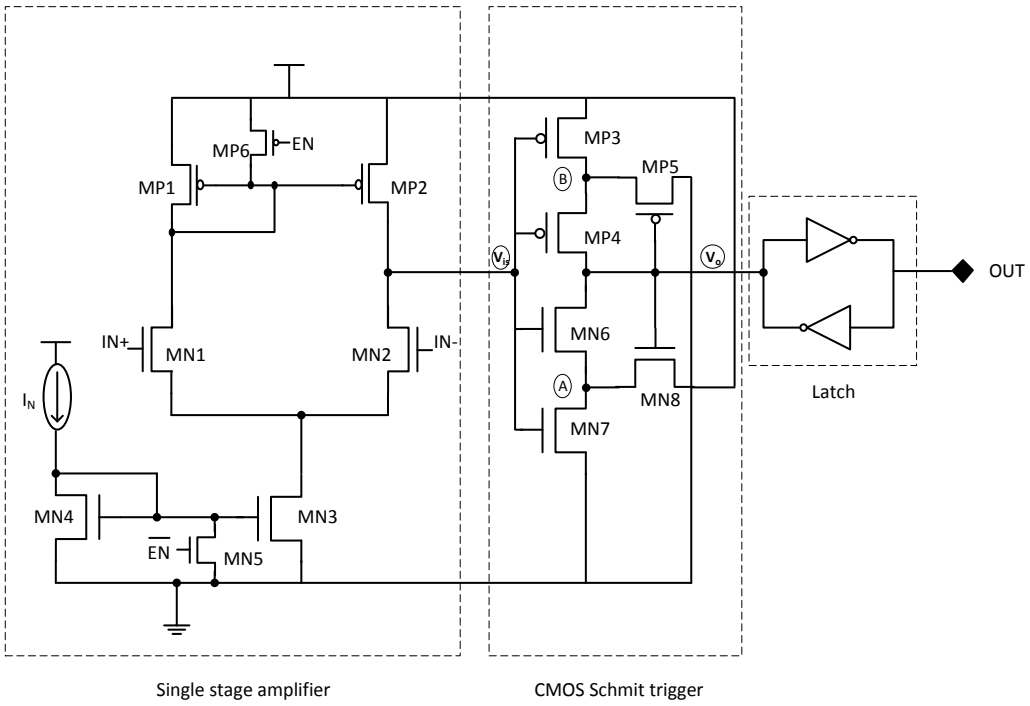

Figure 32 Transistor level diagram of comparator.

The single stage amplifier is designed to incorporate an enable/disable function, have low power consumption, a gain greater than 40dB and a low offset voltage. To improve matching in the current mirrors (MP1, MP2, MN3 and MN4), long length devices are used. MP6 and MN5 implement the enable/disable function. If the input signal to MP6 is low, the transistor turns on and shuts off the current mirror load (MP1 and MP2). Likewise, if the input signal to MN5 is high, it turns on and shuts off the current mirror (MN3 and MN4). This function ensures the comparator is turned off at a time it is not needed in order to reduce power consumption in the entire pulse charger. Another technique to ensure low power operation is to design in the subthreshold or weak inversion region.

In the subthreshold region, the MOSFET gate is held below the threshold voltage and diffusion current dominates as compared to drift current in saturation region [64]. Diffusion current is the flow of current from the source to the drain of the transistor while drift current is the flow of current controlled by a voltage applied to the gate of the transistor. Equation 2 shows that the drain current, I_{ds}, in the subthreshold region is independent of the drain to source voltage, V_{ds} if V_{ds} is greater than the thermal voltage, V_T [65]. The transconductance equation, shown in equation 3, shows a linear relationship between the transconductance, g_m and drain current. The transconductance to drain current ratio for a MOSFET is maximized in subthreshold operation [66].Hence, a moderate gain, low noise and low power consumption can be achieve in this area of operation. Gain, A_v is increased and noise, v_n^2 is decreased as gm is increased as seen in equations 4 and 5 respectively.

$$I_{ds} = K_{p,n}\frac{W}{L}(m-1){V_T}^2\left(e^{\frac{V_{gs}}{mV_T}}\right)\left(1-e^{\frac{-V_{ds}}{V_T}}\right) \tag{2}$$

$$g_m = \frac{I_{ds}}{mV_T}\ (m>1) \tag{3}$$

where m is the body effect coefficient and $K_{p,n}$ is a process parameter.

$$A_v = g_m R_o \tag{4}$$

where $R_o = 1/\lambda I_{ds}$.

$${v_n}^2 = \frac{8}{3}\frac{kT}{g_m} + \frac{k_f}{2\mu C_{ox}}\frac{1}{WL}\frac{1}{f} \tag{5}$$

where K_f is a fitting parameter, f is frequency, T is temperature, C_{ox} is gate oxide capacitance, R_o is output impedance, W and L are width and length of transistor respectively.

MN1 and MN2 are designed in sub threshold with an inversion level of one. This is because higher inversion level means smaller area and higher speed, but higher power consumption. At smaller inversion levels, power consumption is low but circuit operation is slow, hence an inversion level optimizing area, speed and power conversion is appropriate. This can be inferred from Fig. 33 which shows that at the higher inversion region, transistor sizes are small, i.e. small area, but there is a large consumption of power and higher speed. At smaller inversion region, power consumption is low while area is large and speed is smaller due to a smaller bandwidth of operation. Between the inversion levels of 0.1 and 10 where there is just a slight change in power consumption; a smaller area with better bandwidth operation can be picked. Fig. 33 shows that a good inversion level can be chosen at the intersection of the normalized power consumption, area and speed curves.

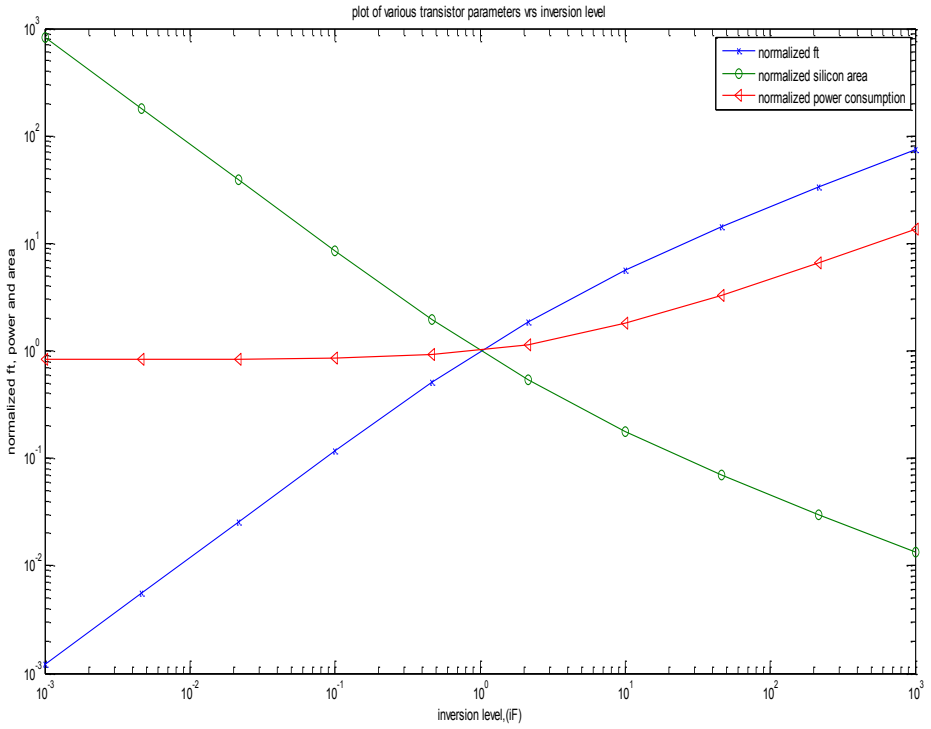

Figure 33 Plot of various transistor parameters versus inversion level.

With a gain of 40dB, I_{ds} of 1uA, the g_m of the transistors can be calculated by following the procedure below.

For an inversion level of one, i.e. i_f=1,

$$gm = \frac{2I_{ds}}{\Phi_t n(1+\sqrt{1+i_f})} \tag{6}$$

$$g_{mN1,N2} = \frac{2 * 1\mu A}{26mV * (1+\sqrt{1+1})} = 31.8\mu\frac{A}{V}$$

The dimensions of the transistors can be calculated as follows,

$$\frac{W}{L} = \frac{g_{mN1,N2}}{\mu C_{ox}\Phi_t(-1+\sqrt{1+i_f})} \tag{7}$$

$$\frac{W}{L} = 32.8$$

After obtaining the initial dimensions of the transistors, the circuit is adjusted to achieve a good gain at low power consumption. The final transistor dimensions are shown in table 7. The gain and phase margin plot is shown in Fig. 34.

Table 7 Comparator first stage transistor dimensions

Transistor	**W/L (um)**
MN1	4/1.5 * 1
MN2	4/1.5 * 1
MN3	4/1.5 * 3
MN4	4/1.5 * 3
MN5	4/1.5 * 3
MP1	4/1.5 * 4
MP2	4/1.5 * 4
MP6	4/1.5 * 2

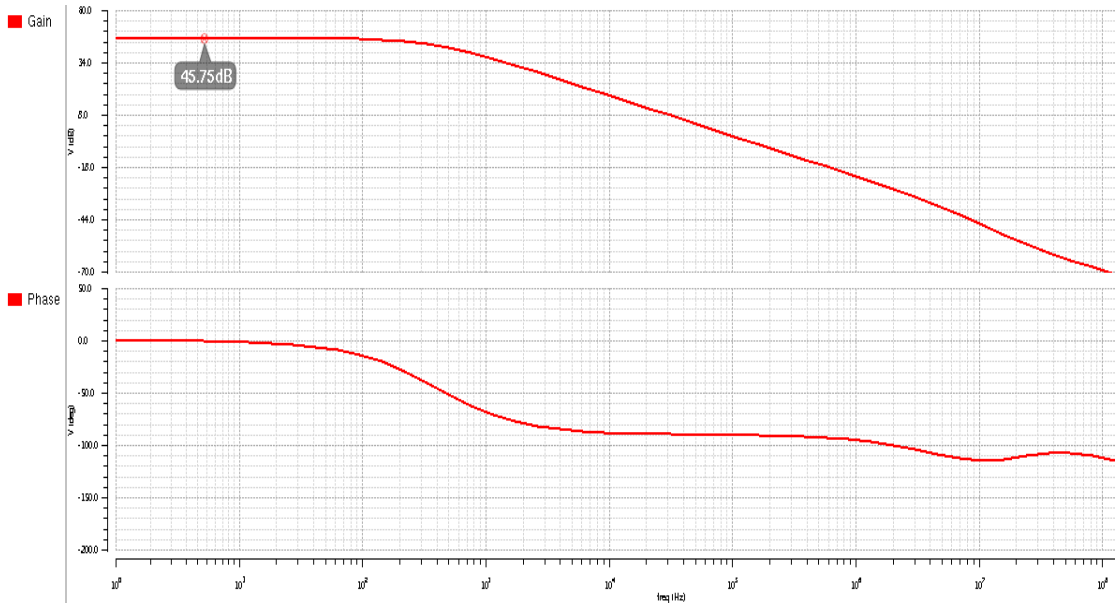

Figure 34 Gain and phase plot of amplifier stage in comparator.

The CMOS Schmitt trigger, shown in Fig. 32, is added to introduce hysteresis into the comparator. Transistors MP5 and MN8 introduce hysteresis by operating as source followers providing some form of positive feedback where they feedback the output voltage, V_o to node B and A respectively [63]. When the input, V_{is}, to the CMOS Schmitt trigger is low, transistors MP3, MP4 and MN8 are on operating in the triode region, while MN6, MN7 and MP5 are off and V_o is equal to the supply voltage. As V_{is} increases to a value above the threshold voltage, MN7 begins to turn on. At this point, both MN7 and MN8 are on and form a biasing network to bias MN6. The condition of the P transistors does not change. The voltage at node A, V_A begins to decrease. When V_{is} reaches the upper threshold voltage, V_{TH}, MN6 turns on fully and transition starts with V_o starting to go low. MP4 and MP3 start to turn off when MP5 turns on, further reducing V_o due to the source follower operation. The cycle then repeats itself when the

input goes low again [63], [67]. The hysteresis at the output of the latch is shown in Fig. 35.

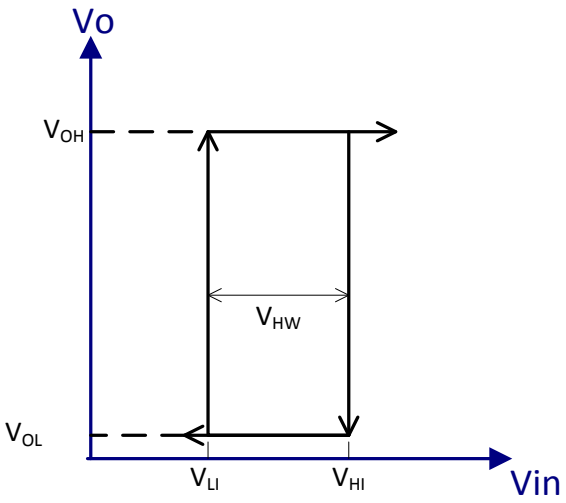

Figure 35 Hysteresis of comparator.

V_{OH} and V_{OL} is the maximum and minimum output voltage respectively. V_{OH} and V_{OL} are dependent on saturation levels of the amplifier. V_{HI} is the input voltage at which output switches from V_{OH} to V_{OL} and V_{LI} is the input voltage at which the output switches from V_{OL} to V_{OH}. V_{HW} is the hysteresis window. To determine the V_{OH}, V_{OL}, V_{LI} and V_{HI}, the following equations are used [68].

At the time when the output is switching from high to low, MN7 and MN8 are in saturation and MN6 is off,

$$I_{dMN8} = \frac{\beta_{MN8}}{2}(V_{GS} - V_{THN8})^2 = \frac{\beta_{MN8}}{2}(V_{DD} - V_{in} + V_{THN6} - V_{THN8})^2 \quad (8)$$

where β is the transconductance parameter of the transistors if $V_{THNN6} = V_{THN8}$.

$$I_{dMN8} = \frac{\beta_{MN8}}{2}(V_{DD} - V_{in})^2 \tag{9}$$

$$I_{dMN7} = \frac{\beta_{MN7}}{2}(V_{in} - V_{THN7})^2 \tag{10}$$

The current through MN7 and MN8 is the same and both are in saturation.

$$I_{dMN8} = I_{dMN7}$$

$$\frac{\beta_{MN8}}{2}(V_{DD} - V_{in})^2 = \frac{\beta_{MN7}}{2}(V_{in} - V_{THN7})^2 \tag{11}$$

From equation 11, V_{HI} from Fig. 35 can be determined if $V_{HI}=V_{in.}$

$$V_{HI} = \frac{\left[V_{DD} + \left(\sqrt{\frac{\beta_{MN7}}{\beta_{MN8}}} * V_{THN7}\right)\right]}{1 + \sqrt{\frac{\beta_{MN7}}{\beta_{MN8}}}} \tag{12}$$

To determine V_{LI}, just before the output switches again, MP3 and MP5 are in saturation.

Similarly,

$$I_{dMP5} = \frac{\beta_{MP5}}{2}(-V_{LI} + V_{THP4} - V_{THP5})^2 \tag{13}$$

If $V_{THP4} = V_{THP5}$,

$$I_{dMP5} = \frac{\beta_{MP5}}{2}(V_{LI})^2 \tag{14}$$

$$I_{dMP3} = \frac{\beta_{MP3}}{2}(V_{LI} - V_{DD} - V_{THP3})^2 \tag{15}$$

Similarly, the current through MP3 and MP5 is the same and both are in saturation.

$$I_{dMP3} = I_{dMP5}$$

$$\frac{\beta_{MP3}}{2}(-V_{LI} + V_{DD} - V_{THP3})^2 = \frac{\beta_{MP5}}{2}(V_{LI})^2 \tag{16}$$

$$V_{LI} = \frac{\sqrt{\frac{\beta_{MP3}}{\beta_{MP5}}}(V_{DD} - V_{THP3})}{\left(1 + \sqrt{\frac{\beta_{MP3}}{\beta_{MP5}}}\right)} \quad (17)$$

$$V_{HW} = V_{HI} - V_{LI}$$

For a V_{LI} of 1.45V, V_{HI} of 1.55V and a V_{HW} of 100mV, using equations 12 and 17, the transistor dimensions can be determined.

$$\frac{(W/L)_{MN7}}{(W/L)_{MN8}} = \frac{\beta_{MN7}}{\beta_{MN8}} = \frac{(V_{DD} - V_{HI})^2}{(V_{HI} - V_{THN7})} = 2.77$$

$$\frac{(W/L)_{MP3}}{(W/L)_{MP5}} = \frac{\beta_{MP3}}{\beta_{MP5}} = \frac{(V_{LI})^2}{(-V_{LI} + V_{DD} - V_{THP3})^2} = 1.15$$

The transistor dimensions of the Schmitt trigger are shown in table 8. Fig. 36 shows that the comparator has a hysteresis window of 100mV.

Table 8 CMOS Schmitt trigger transistor dimensions

Transistor	**W/L (µm)**
MP3	4/0.5 *4
MP4	4/0.5 *4
MP5	4/0.5 *5
MN6	4/0.5 *2
MN7	4/0.5 *2
MN8	4/0.5 *2

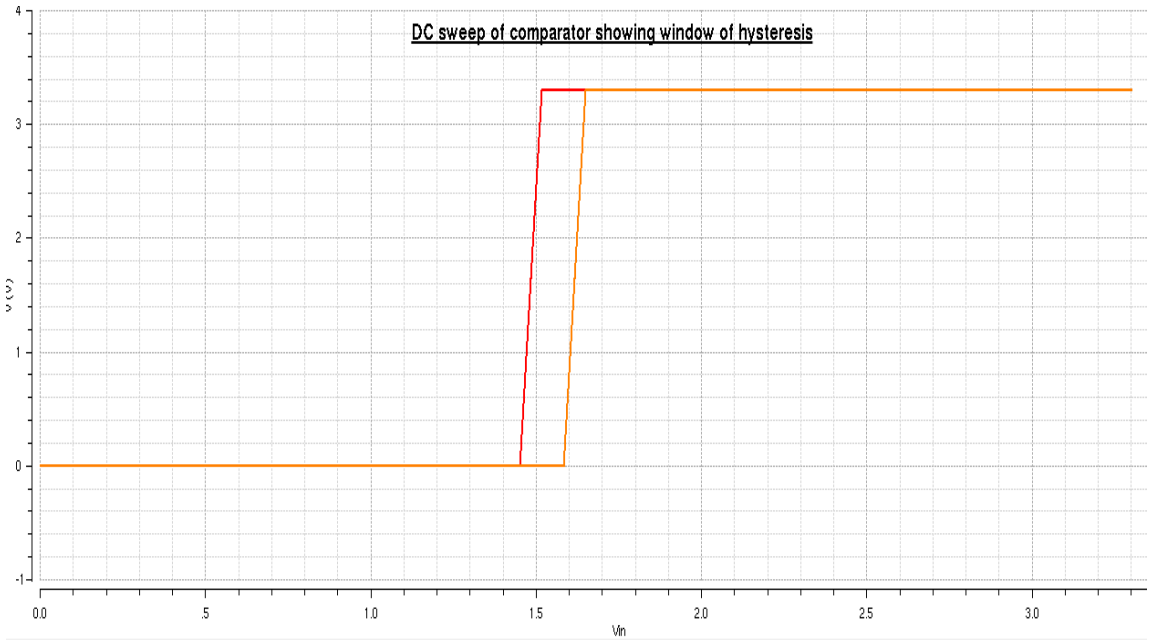

Figure 36 Hysteresis window of designed comparator.

3.3.1.2 Design of duty cycle generator

In many pulse chargers, users do not have access to the switching frequency of the main power switch. The duty cycle and frequency of the charge pulses are normally obtained through a trial and error method [57]. This can cause the main switch to be on for longer periods than needed and might contribute to extra power consumption or even overcharging. There is no clear literature to specify the optimum duty cycle for pulse chargers. Most internal regulation loops are similar to a pulse width modulation (PWM) or pulse frequency modulation (PFM) system, which varies the pulse width or frequency, respectively, with respect to the battery voltage to achieve a fully charged battery.

A study by [69] indicated that better charging response is obtained when lower frequencies are used for pulse charging. In [70], it was suggested that charging at low frequencies is faster than charging at high frequencies. It also suggests that higher duty cycle pulses are more efficient in charging batteries than lower duty cycle. A higher duty cycle will result in faster charging but will cause the battery to be prone to overcharging and overvoltage conditions, while a lower duty cycle will result in longer charge time but good battery charge efficiency. It is therefore normal to conclude that the best duty cycle is 50%. This conclusion is unacceptable since the electrolyte concentration differs at different times during charging [58]. Thus, it is necessary to provide a method where faster charging can be achieved and at the same time achieve a good battery charging efficiency without entering overvoltage or overcharge condition. In order to do this, the charging phase is divided into two parts: one part to provide a fast charging time using a higher duty cycle and the other part using a lower duty cycle to enable better battery charging efficiency. Due to the stringent charging requirements of a Li-ion battery, a duty cycle of 0.7 or higher is appropriate for the initial stage of charging which then reduces as full charge is approached. The duty cycle for faster charge is set at 0.75 while that for better charge efficiency is set at 0.25. This can be generated using a duty cycle generator. A conceptual idea of the duty cycle generator (DCG) is presented in Fig. 37.

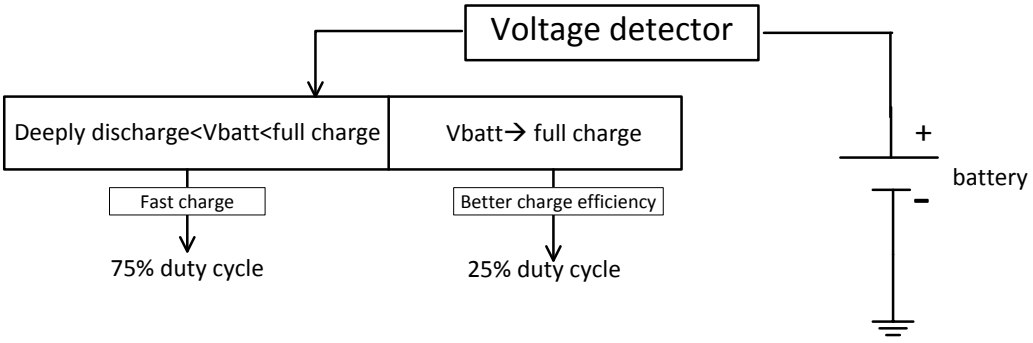

Figure 37 Conceptual idea of DCG.

To provide versatility, giving the user access to the frequency at which the switch is pulsed and also providing options to use the pulse charger as other type of chargers, a duty cycle generator is designed and added to the proposed pulse charger. The duty cycle generator uses flip flops. A flip flop is a memory device that is controlled by a clock signal. It stores only one bit of data. A positive edge triggered D flip flop operates by changing state at the positive or rising edge of the clock input. If the data bit, D, is high when a clock pulse is applied, the output, Q, is also high, i.e. the flip flop sets. Likewise, if D is low when the clock pulse is applied, Q goes low and the flip flop resets. The set and reset, also known as clear, inputs take precedence over the clock input, i.e. the flip flop will only operate if both set and clear are high. Fig. 38 shows the timing diagram and truth table of the positive edge triggered D flip flop.

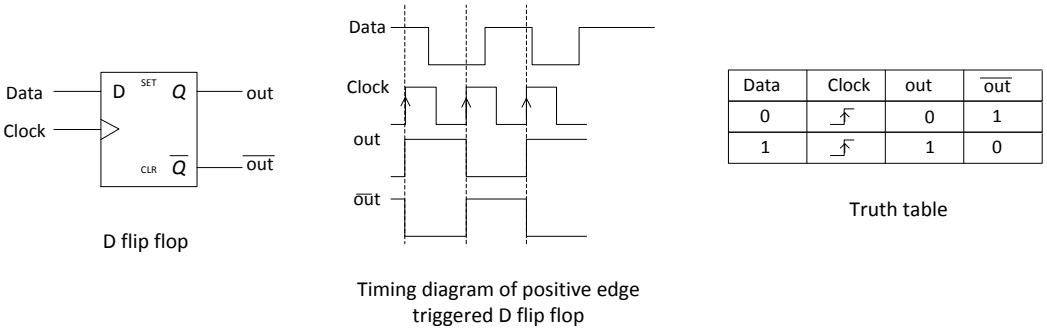

Figure 38 Positive edge triggered flip flop operation.

The duty cycle generator circuit, shown in Fig. 39, consists of two positive edge triggered D flip flops. The first flip flop divides the frequency of the clock by two at node A, while the second flip flop serves as a modulo two divider using the divided clock from the first flip flop at its clock input [71]. The NAND gates will then generate the waveforms with 25% and 75% duty cycle. Fig. 40 shows the waveforms at node A, B, C and D. The proposed pulse charger clock input frequency should be less than 1 KHz since charging at lower frequencies shows some superiority to higher frequencies [70].

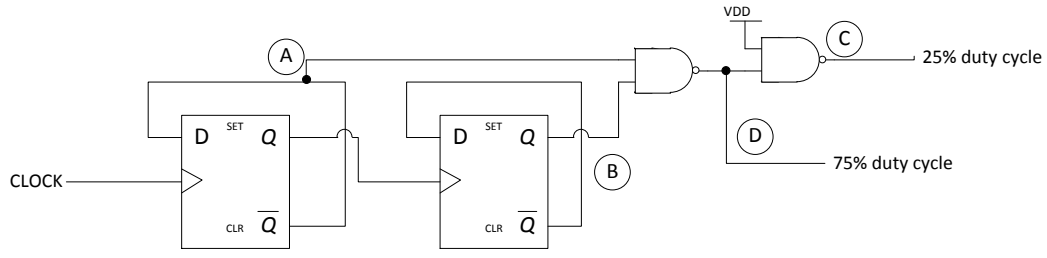

Figure 39 Duty cycle generator.

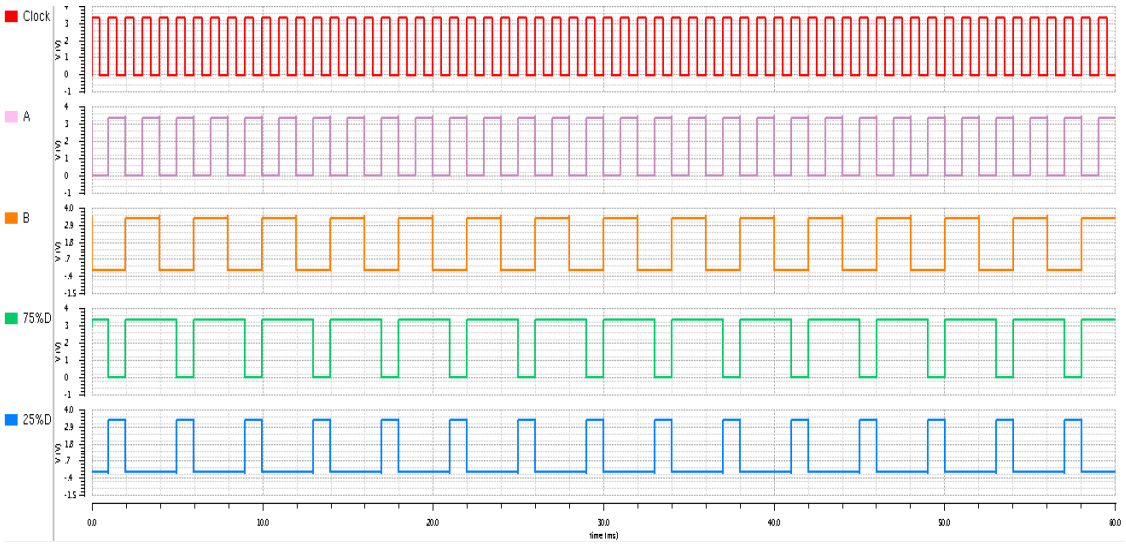

Figure 40 Waveforms of duty cycle generator.

3.3.2 Design of trickle charging phase

Deeply discharged cells have reduced capacity and hence many battery management systems have protection circuits in place to prevent cells from attaining a deep discharge state. However, there are times when a cell might be deeply discharged and will have to be charged to its full capacity. If the Li-ion battery is in a deeply discharged state and a high current is initially used for charging, the battery could become damaged so typically, a small current, about ten percent of full charge current, is used to charge the battery until a moderate voltage is reached after which full charge current, 1C, can be used.

The trickle charging phase is included in the design primarily for the preconditioning of deeply discharged Li-ion cells. From table 6, a maximum of 20mA can be supported

during this phase. The trickle charge phase is shown in Fig. 41 and is only enabled during normal mode if the following conditions exist: die temperature is below 85^{o}C (T_{die}), input voltage is present (PG) and at a good level (the input voltage ranges from 3.3V to 3.6V), the battery is not in overvoltage state (OV) and the battery voltage is less than a predefined threshold, V_{TS}, which can be set by the user. V_{TS} is also the minimum voltage below which the battery becomes deeply discharged. Recommended V_{TS} for the OlevinPower 3.3V Li-ion battery [62] is 2V.

Since the trickle charge phase had to be enabled by the factors mentioned above, the NOR gate can be used for implementation. Equation 18 shows that the trickle charge phase will only be enabled (PMOS enable) if all inputs are low and will immediately be disabled when any of the inputs go high.

$$Trickle_{enable} = \overline{PG + T_{die} + OV + TC_{out}} \tag{18}$$

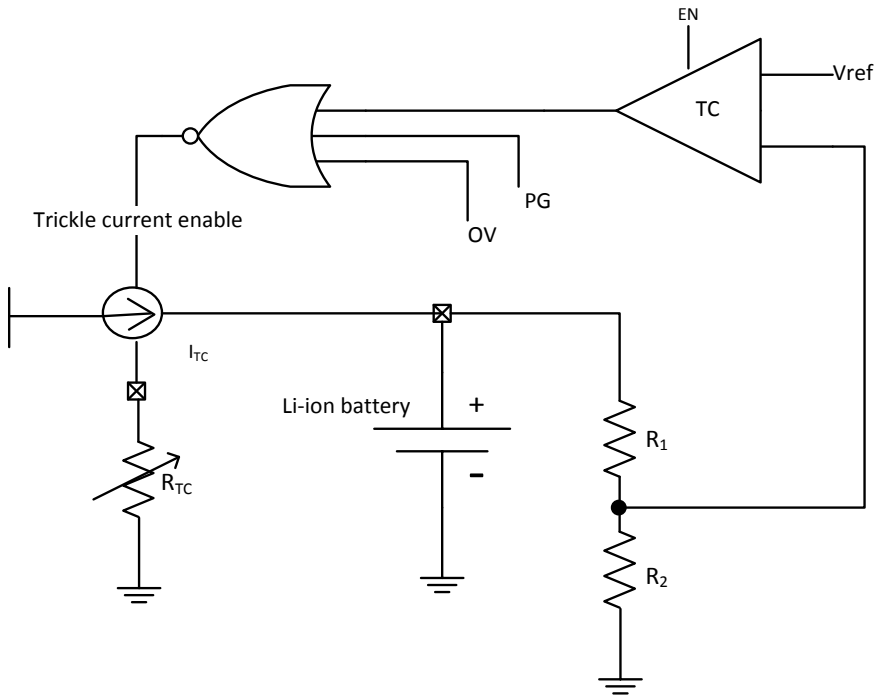

Figure 41 Trickle charging phase block diagram.

The current source, I_{TC}, is designed to have large output impedance and sized to handle at most 25mA. Long channel length devices are used to reduce the effects of mismatch. Resistors R_1 and R_2 set the V_{TS} by using equation 19.

$$V_{TS} = 1.2\left(1 + \frac{R_1}{R_2}\right) \tag{19}$$

If V_{TS} is 2V,

$R_1 = 0.67R_2$

Using commercial resistor values (5% tolerance), $R_1 = 820\text{K}\Omega$ and $R_2 = 1.2\text{M}\Omega$

The current into the Li-ion battery can be varied from 5mA to 20mA by changing the resistance of the potentiometer, R_{TC}. The trickle currents and its corresponding

resistance can be obtained from table 9. The error in current using commercial resistor values is less than 5%. Fig. 42 shows the characterization of trickle current source IT with respect to varying resistance values.

Table 9 Trickle currents and corresponding resistor values

Commercial Resistor value (5%)	**I_{TC}**
1.5KΩ	20mA
2.2KΩ	15mA
3.9KΩ	10mA
10KΩ	5mA

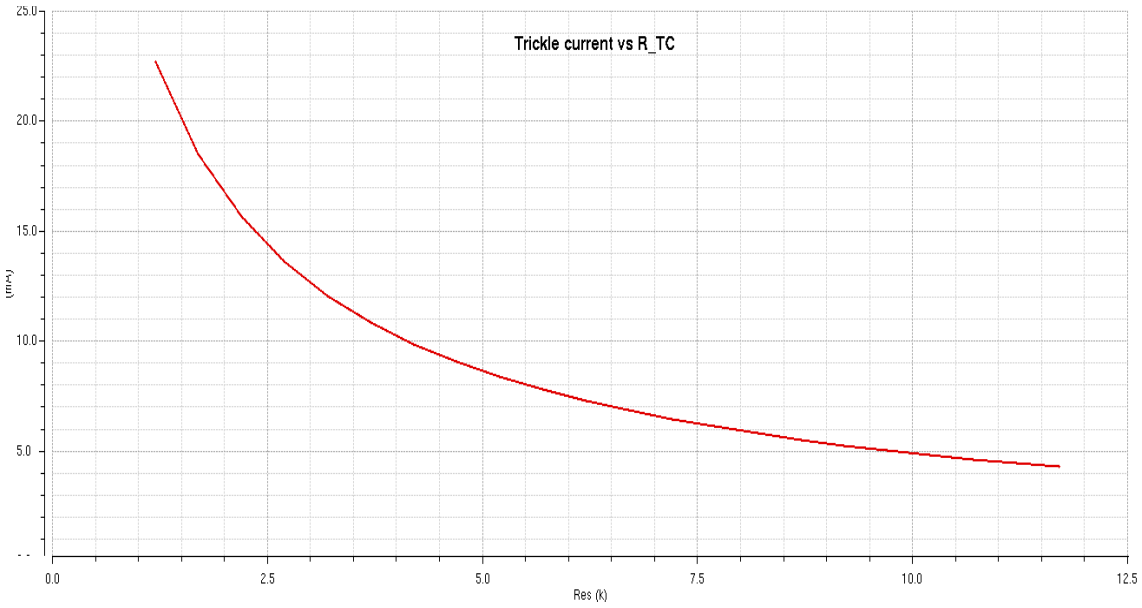

Figure 42 Trickle current, ITC, versus resistance, RTC.

Fig. 43 shows the signals OV, PG, trickle current enable, the output of the comparator, TC_out, the battery voltage, V_{batt} and then the trickle current. Modeling the battery as a 10mF capacitor in series with a 100mΩ resistor, the trickle current is set to 10mA and V_{TS} is 2V. From the figure, when V_{batt} is less than 2V, the input power is good, PG, and the battery is not in overvoltage, OV, the trickle charging phase is active and the battery is charged with a 10mA current. Immediately, the battery voltage exceeds VTS, at point A, the trickle phase is disabled.

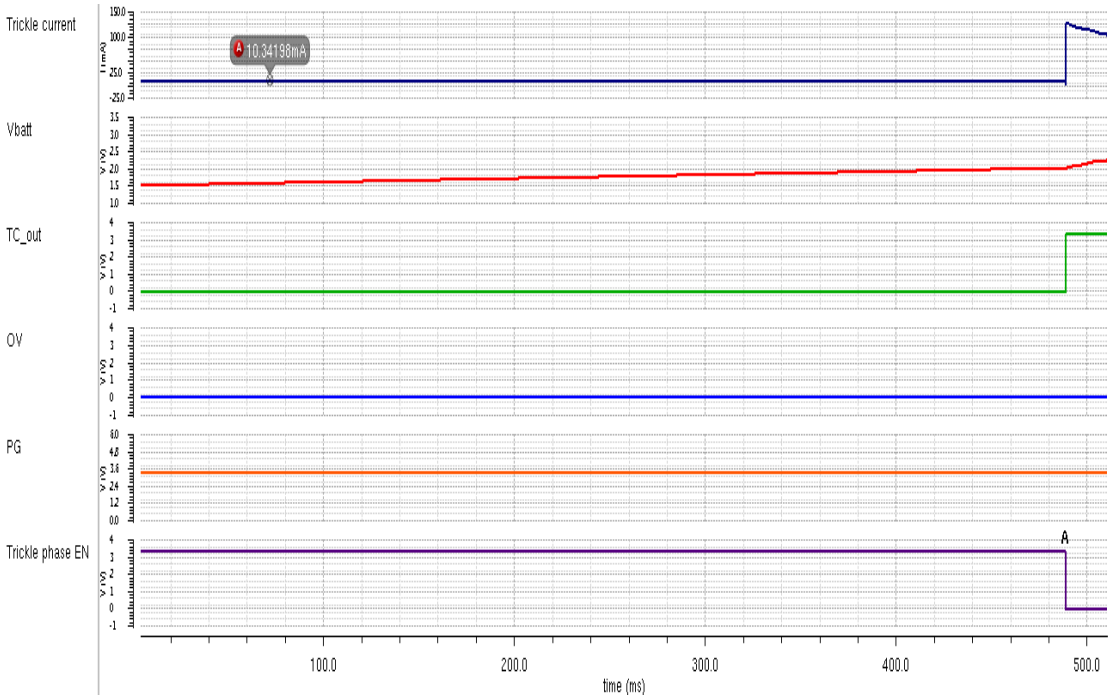

Figure 43 Trickle charging phase operation signals.

3.3.3 Design of fast charging phase

Pulse charging decreases battery charge time at the same time increasing the life cycle of batteries. It provides rest periods during which the battery electrolyte's ions has the opportunity to be distributed evenly in order to obtain better battery charge efficiency [57]. This phase seeks to combine fast charging with increased battery charging efficiency by using a large duty cycle, 0.75, initially to decrease charge time and a small duty cycle, 0.25, to achieve better battery charging efficiency.

The process begins when the Li-ion battery reaches V_{TS}. Charging at large current is done during this phase. The fast charging phase is divided into two stages, i.e. charging at 0.75D and charging at 0.25D. These two different duty cycles are generated using the duty cycle generator (DCG) discussed. For this phase to be triggered, the battery should not be in overvoltage state. Also, the die temperature, the temperature of the Li-ion battery, the input voltage (PG) and input current (I_{in}) must all be within specifications. If any of these parameters fall outside the specified range, the fast charging phase will not be enabled. This is to protect the IC and the battery from damage. The designed pulse charger has a maximum allowable charge current of 500mA during the fast charging phase. This current is set by the current limited input adapter.

Once the fast charging phase is enabled, the battery voltage is determined. If the voltage lies between V_{TS} and V_N, where V_N is nominal voltage and can also be user set, the duty cycle generator provides pulses at 0.75D to drive the PMOS switch, $M_{1,}$ which then pulses the charge current from the input adapter into the battery at 0.75D. The output of

the SW comparator serves as the select signal for the multiplexer. Depending on whether the battery voltage is below V_N or not, 0.75D or 0.25D is selected to drive M_1. Chemical reactions in the battery are stabilized during rest periods allowing electrochemical reactions to keep pace with the rate of input of electrical energy input [34]. This increases power transfer rate and lowers charge time [55]. When the battery is approaching full charge, i.e. above V_N, M_1 is driven at 0.25D, hence pulsing charge current at 0.25D into the battery. The lower duty cycle is to ensure full charge is reached without causing overvoltage concerns and also achieve better battery charging efficiency. As long as the battery voltage is between V_N and OV, the battery is charged at 0.25D. In the case of the OlevinPower 3.3V Li-ion single cell battery, V_N is 2.8V and OV is 3.3V. V_N is set by R_3 and R_4 by using equation 20. V_{TS} and V_N can be changed to reflect what the user wants.

$$V_N = 1.2\left(1 + \frac{R_3}{R_4}\right) \tag{20}$$

If V_N is 2.8V,

$R_3 = 1.33R_4$

Using commercial resistor values (1% tolerance), $R_3 = 2.67\text{M}\Omega$ and $R_4 = 2\text{M}\Omega$

The operation of the fast charge phase can be summarized using equations 21-23. The output of the DCG will pass to drive M1 as long as the mux_enable signal is high, pulsing at 0.75D or 0.25D depending on the voltage of the battery, determined by the output of comparator SW (SW_{out}). The fast charging phase block diagram is shown in Fig. 44.

$$\left(\overline{PG} \cdot TC_{out} \cdot I_{in} \cdot T_{die} \cdot TS\right) \cdot \overline{OV} = mux_{enable} \tag{21}$$

$$DCG_{out} = SW_{out} \cdot 0.25D + SW_{out} \cdot 0.75D \tag{22}$$

$$mux_{enable} \cdot DCG_{out} = M1_{drive} \tag{23}$$

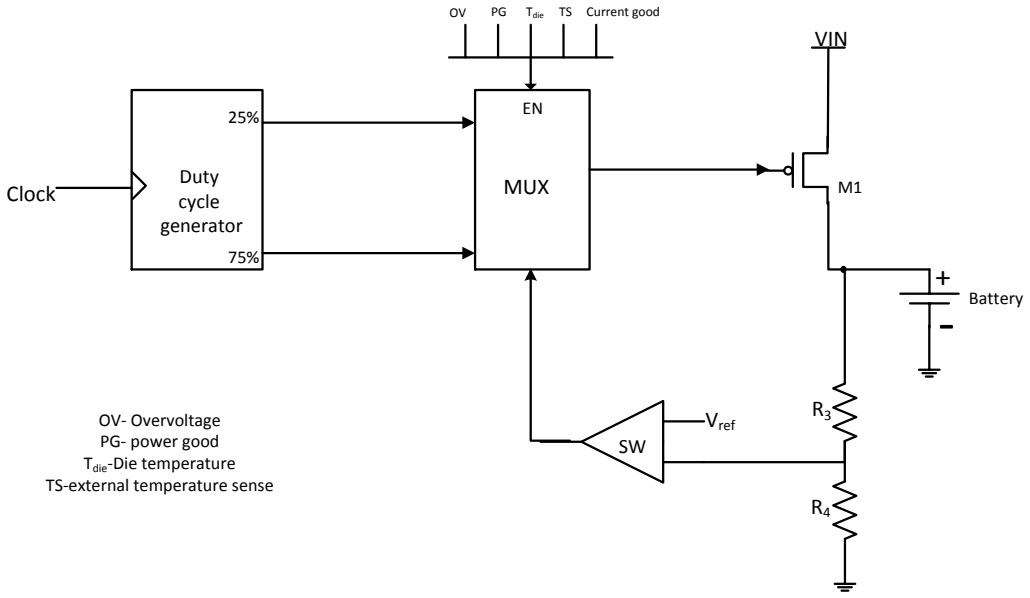

Figure 44 Fast charging phase block diagram.

Fig. 45 shows the operation of the fast charging phase. Before, V_{batt} reaches V_{TS}, the trickle charging phase is in operation. Once, V_{batt} reaches V_{TS}, point A in the figure, the pulse charger switches to the fast charging phase, where a charge current of 125mA is pulsed into the battery at 0.75D. The signal to the gate of the PMOS switch, M1, is out_mux. When V_{batt} reaches V_N, point B, the charge current is pulsed at 0.25D and the battery gradually approaches full charge. The OV signal goes high, point C, when the

battery attains full charge. This turns M1 and all unneeded comparators off. Input power, PG, and die temperature, Temp, must be within specifications during this charging phase.

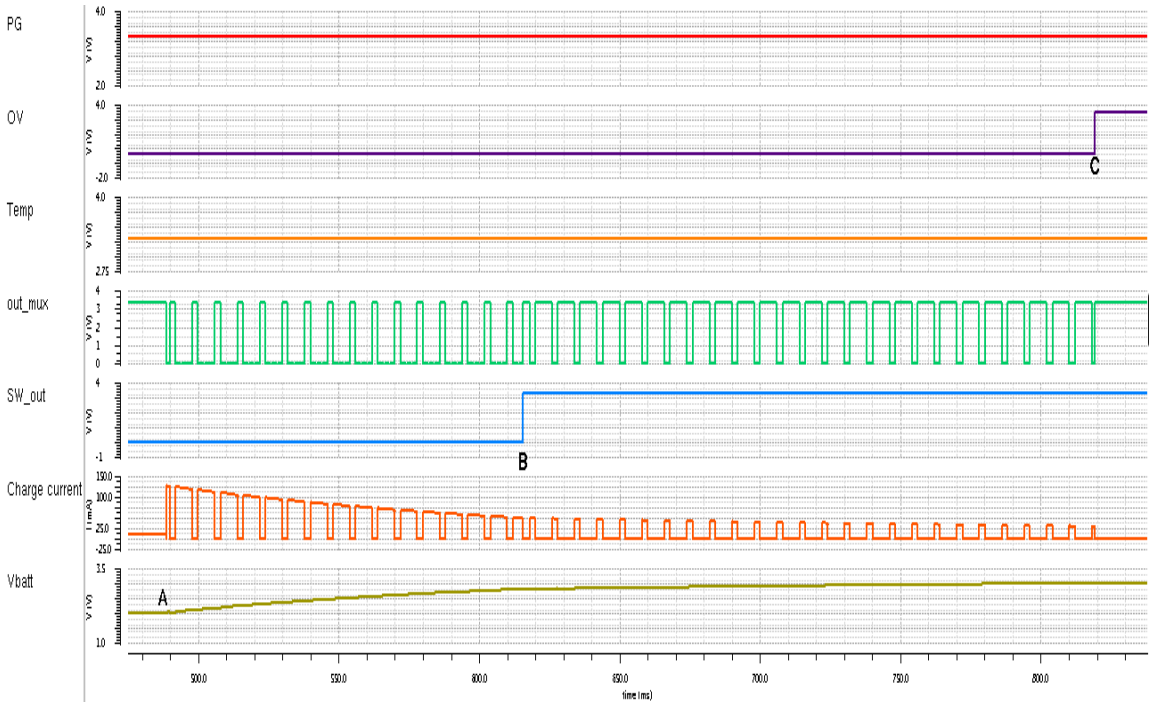

Figure 45 Fast charging phase operating signals.

3.3.4 Protection schemes

The designed pulse charger includes protection schemes to ensure safe operation within specified limits. It is very important to charge the battery within the specified limits and at the same time ensuring the battery temperature is also within a safe operating region. These protection schemes are external and internal temperature sense circuitry and

overvoltage and overcurrent protection. These circuits ensure that both the Li-ion battery and IC are protected from abnormal conditions that can cause battery and circuit failure. Fig. 46 shows the safe mode operating region of the battery and the circuit.

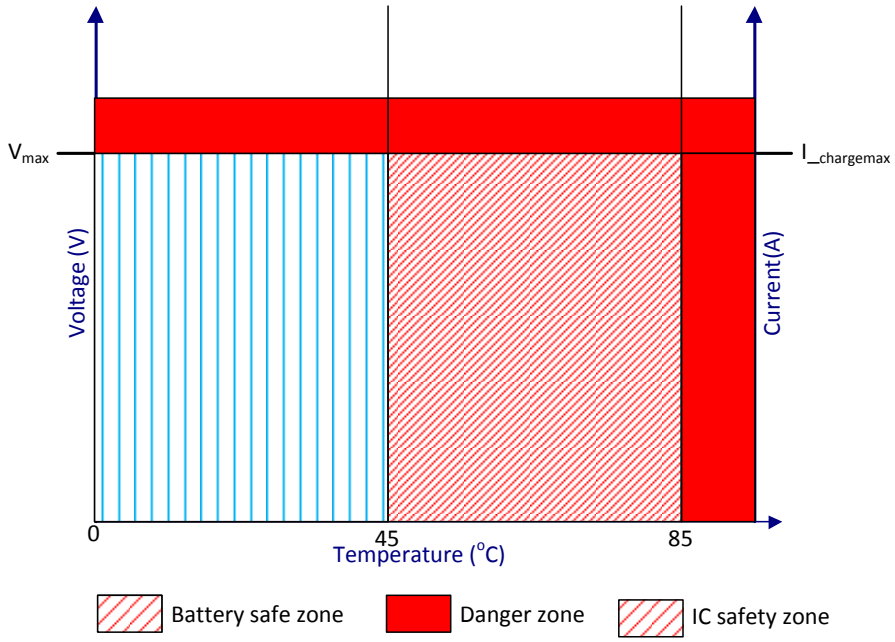

Figure 46 Safe operating region of circuit and battery.

Temperature wise, the Li-ion battery must be charged within the safe operating temperatures of 0°C to 45°C [72]. Also, the internal operating temperature of the IC, i.e. die temperature, must not exceed the specification of 85°C. Overvoltage and overcurrent protection ensures that the battery voltage and charging current respectively does not exceed their specified limits. Fig. 22 also shows the danger region where the battery and IC are most likely to fail when they operate outside the designed specifications.

3.3.4.1 Overcurrent protection

To prevent damage in case of the charge current exceeding a set threshold, a current limiting block is added to the design. This block serves as an overcurrent protection circuit. The overcurrent threshold is set by the $R_{\_LIM}$ resistor which tries to limit the charge current through M1 in case the charge current tries to exceed the preset threshold.

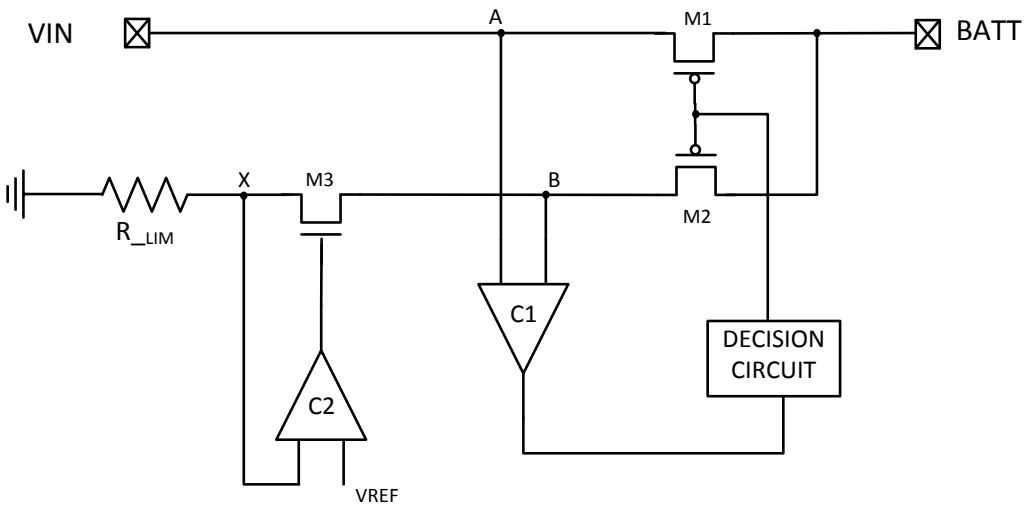

Figure 47 Overcurrent protection circuit.

The current limiting circuit is shown in Fig. 47. The circuit consists of a current sensing FET, M2, which is connected to M1 to mirror the charging current. M1 is 1500 times M2. $R_{\_LIM}$ is used to set the limiting current through M3 and M2, thereby setting the overcurrent threshold. When the current through M1 is greater than 1500 times the current through M2, the comparator, C1, comparing the nodes A and B outputs a signal to the decision circuit to turn M1 off. This always ensures the charge current through M1

is below the preset threshold. The amplifier, C2, is used to force the voltage at node X to be equal to V_{REF}, hence the limiting current, $I_{\_LIM}$, is set by using equation 24. This current can be user set and must not exceed 300μA.

$$I_{\_LIM} = \frac{V_{ref}}{R_{\_LIM}} \tag{24}$$

Since M1 must handle a maximum current of 500mA. It has to be sized as such with minimum on-resistance ($1/g_{ds}$) to reduce power consumption during operation.

$$g_{ds1} = K_p \frac{W}{L}(V_{in} - |V_{TH}|) \tag{25}$$

If V_{in}=3.3V and g_{ds}<10Ω^{-1}, then from equation 25,

$$\left(\frac{W}{L}\right)_1 = 59523$$

Also,

$$\left(\frac{W}{L}\right)_2 = \frac{1}{1500}\left(\frac{W}{L}\right)_1$$

C2 is shown in Fig. 48. The one stage amplifier has a better gain than the regular single stage amplifier comprising of a differential pair and current mirror load. This is because the current mirror used as load for the differential pair has its output impedance boosted by the current amplifier which consists of MP5, MP6, MN2 and MN3. The amplifier has two feedback loops, i.e. a negative loop that decreases the impedance at node x and a positive loop that increases the impedance, Z at node y. By including the current amplifier with a gain of A_c, the overall transconductance, g_m of C2 is increased and

hence the one stage amplifier can provide a relatively large gain of $A_c g_m Z$. This amplifier is presented in [73].

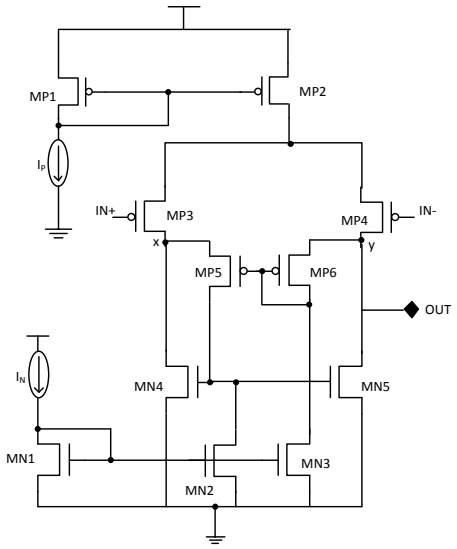

Figure 48 Error amplifier, C2, with boosted output impedance.

The amplifier gain is expressed as,

$$Voltage\ Gain\ = A_v = \frac{2g_{mP3,4}}{g_{oP4} + g_{oN5}} \frac{g_{mP4}\, A_c}{g_{oN4}} \tag{26}$$

where g_o is the output conductance of the transistor.

For i_f=10 and I_ds=1μA, using equation 6,

$$g_{mP3,P4} = \frac{2 * 1\mu A}{26mV * (1 + \sqrt{1 + 10})} = 38.5\mu A/V$$

The dimensions of the transistors can be calculated using equation 7,

$$\left(\frac{W}{L}\right)_{P3,P4} = 12.77$$

The transistor dimensions are shown in table 10.

Table 10 Transistor dimensions of C2

Transistor	**(W/L)µm**
MP1	(4/2)*4
MP2	(4/2)*4
MP3	(4/2)*4
MP4	(4/2)*4
MP5	(4/2)*1
MP6	(4/2)*1
MN1	(2/1.5)*2
MN2	(2/1.5)*2
MN3	(2/1.5)*2
MN4	(4/1.5)*2
MN5	(4/1.5)*2

3.3.4.2 Thermal protection

Thermal protection includes internal and external temperature sense circuitry. The internal temperature sense circuitry monitors the die temperature of the IC to prevent it from exceeding the predetermined limit of 85^{o}C. This is to prevent the die temperature from rising to a point where the IC can become damaged. When die temperature increases, leakage currents increase which can cause the circuit to fail. Extreme temperatures accelerate circuit aging and reduce circuit performance.

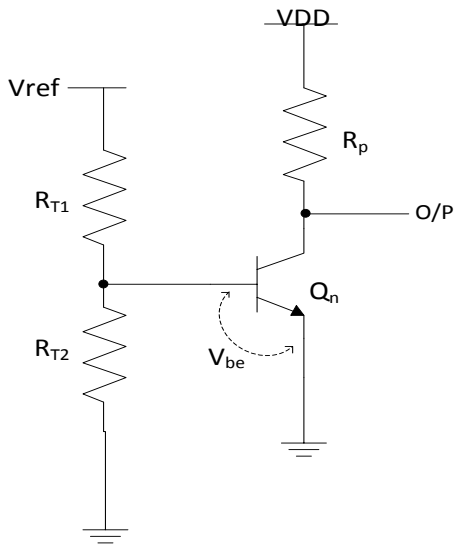

Figure 49 Temperature sense circuit.

Fig. 49 shows the temperature sense circuitry. The circuit consists of a bipolar NPN transistor, Q_n, whose base-to-emitter voltage, V_{be}, has a negative temperature coefficient. The resistors, R_{T1} and R_{T2}, set the voltage at the base of Q_n such that at a particular temperature, Q_n turns on and pulls the output, O/P, to ground. In normal operation, Q_n is off and O/P is pulled high through R_p. O/P can be used as a logic signal to either turn the IC off or on. Using equations 27 and 28, R_{T1} and R_{T2} are preset to set the base voltage of Q_n at 0.484V which corresponds to a cut off temperature of 85°C.

$$V_{be} = \frac{KT}{q} ln \frac{I_c}{I_s} \tag{27}$$

where I_c is the collector current, I_s is the reverse saturation current and $KT/q = V_T$ is the thermal voltage. For a constant Ic, the temperature dependence of V_{be} is

$$\left.\frac{\partial V_{be}}{\partial T}\right|_{I_c} = -2mV/^oC$$

To set the temperature at which the IC shuts off, i.e. 85°C, the V_{be} of Q_n at that temperature must be determined.

$$V_{be}|_{cut-off} = V_{be}|_{27^oC} + \left(T_{cut-off} - T_{27^oC}\right) * \left.\frac{\partial V_{be}}{\partial T}\right|_{I_c} \quad (28)$$

where $V_{be}|_{cut-off}$ is the base-emitter voltage at which the temperature sense circuitry shuts off the IC, $V_{be}|_{27^oC}$ is base emitter voltage at room temperature which is 0.6V and $T_{cut-off}$ and T_{27^oC} are cut off and room temperatures respectively.

$V_{be}|_{cut-off} = 0.6 + (85 - 27) * -0.002 = 0.484V$

At room temperature, V_{be} is 0.6V, which implies at 85°C, V_{be} will be equal to 0.484V. Based on this voltage, R_{T1} and R_{T2} can be determined by using equation 29 when V_{ref} is 1.2V.

$$2.479 = 1 + \frac{R_{T1}}{R_{T2}} \quad (29)$$

Fig. 50 shows the output signal of the circuit across temperature. The signal goes low as the temperature approaches 85°C. This signal is fed into the decision block of the pulse charger to turn it off.

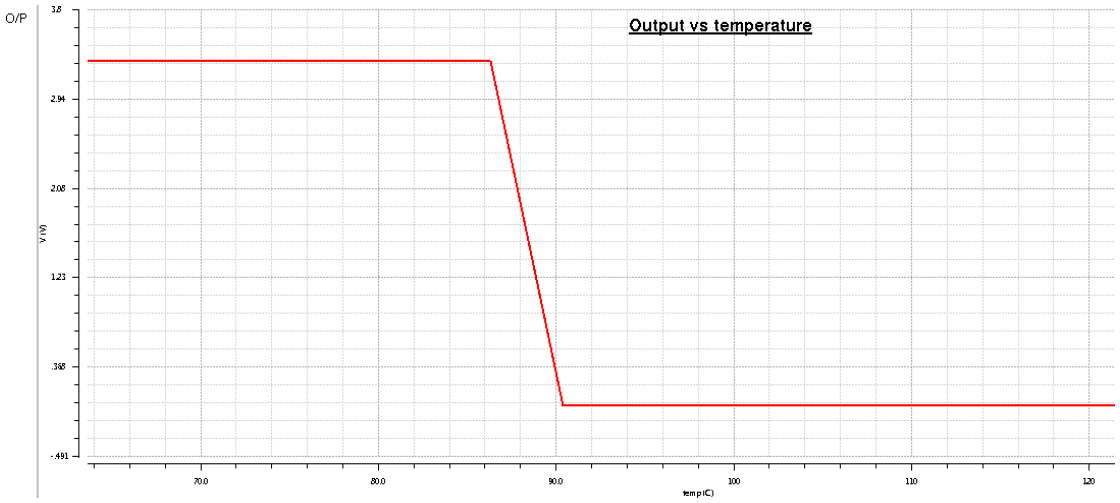

Figure 50 Output signal of temperature sense circuit.

External temperature sense ensures that the battery temperature is within safe operating limits during charging. A pin is provided so that the user can connect a battery temperature sense circuitry if needed. This external temperature sense circuitry senses the ambient temperature, ensuring that any factor that might cause rise in battery temperature such as internal battery fault or ambient temperature does not cause harm to the battery. In cases where the battery is exposed to high temperatures, this serves as a protection scheme to prevent the battery from charging when its electrolyte is too cold to charge without damage or too hot to safely charge [74]. Thermistors can be used to serve as external temperature sense circuits. They are temperature sensitive resistors which can either have a positive temperature coefficient (PTC) or a negative temperature coefficient (NTC). They convert sensed temperatures to voltage signals which can be used to control the charger, i.e. to turn it off or on depending on battery condition.

3.3.4.3 Overvoltage protection

Overvoltage leads to overcharging which can lead to reduced life cycle of batteries. Overcharging can also lead to thermal runaway. Battery thermal runaway is the rapid repetitive increase in temperature of the battery due to overheating or overcharging which can lead to fire or explosion. Heat generation during overcharge is almost proportional to charging current [75]. This occurs due to increase in gases produced during overcharge reactions in the battery [75] – [76]. Therefore, there must be measures in place to prevent this from happening. In this design, the overvoltage protection circuit serves two purposes, i.e. battery charge termination and overvoltage protection. Most pulse charger designs use timers to terminate charge [59] – [61]. One problem with this is that if the timers are not correctly programmed, overcharging can occur which can accelerate the failure rate of the battery. To prevent this, battery charge termination and overcharge are incorporated in the overvoltage protection block. Fig. 51 presents the conceptual idea.

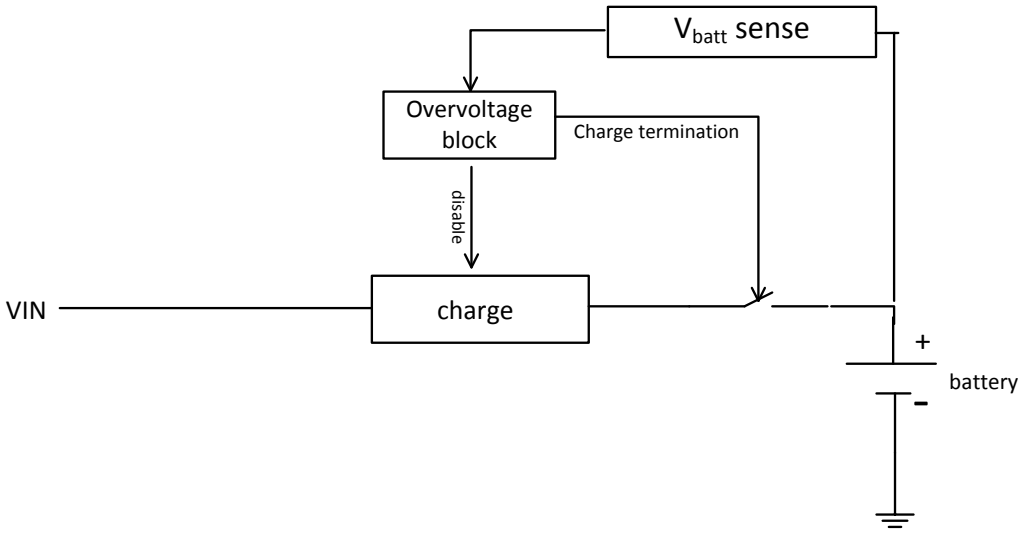

Figure 51 Conceptual idea of overvoltage protection.

The comparator, OV, shown in Fig. 52 will monitor the output voltage of the battery and once the threshold is reached, sends a signal to M1 to shut it off. Signals are also sent to unneeded comparators and circuits to shut off in order to reduce power consumption.

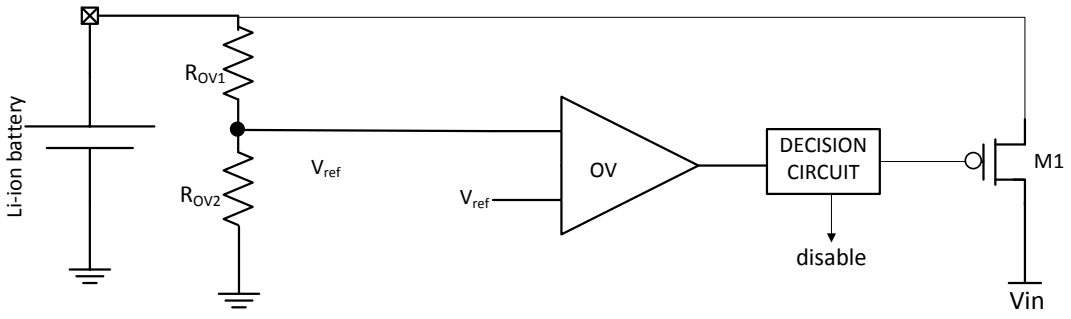

Figure 52 Overvoltage protection and termination.

The overvoltage threshold is set by resistors R_{OV1} and R_{OV2} by using equation 30. Based on the specifications of OlevinPower 3.3V Li-ion single cell battery, the overvoltage threshold is set to 3.3V.

$$V_{OV} = 1.2\left(1 + \frac{R_{OV1}}{R_{OV2}}\right) \tag{30}$$

If V_{OV}=3.3V, using commercial resistors (1% tolerance), R_{OV1}=1.74MΩ and R_{OV2}=1MΩ.

3.4 The pulse charger

A detailed block diagram of the designed pulse charger with the relevant pins is shown in Fig. 53. The use of each pin is shown in table 11. All the charging phases are combined and simulation results are presented. The pulse charger can be operated as a trickle or constant current charger to serve as an overnight or NiMH battery charger. This brings versatility to the design.

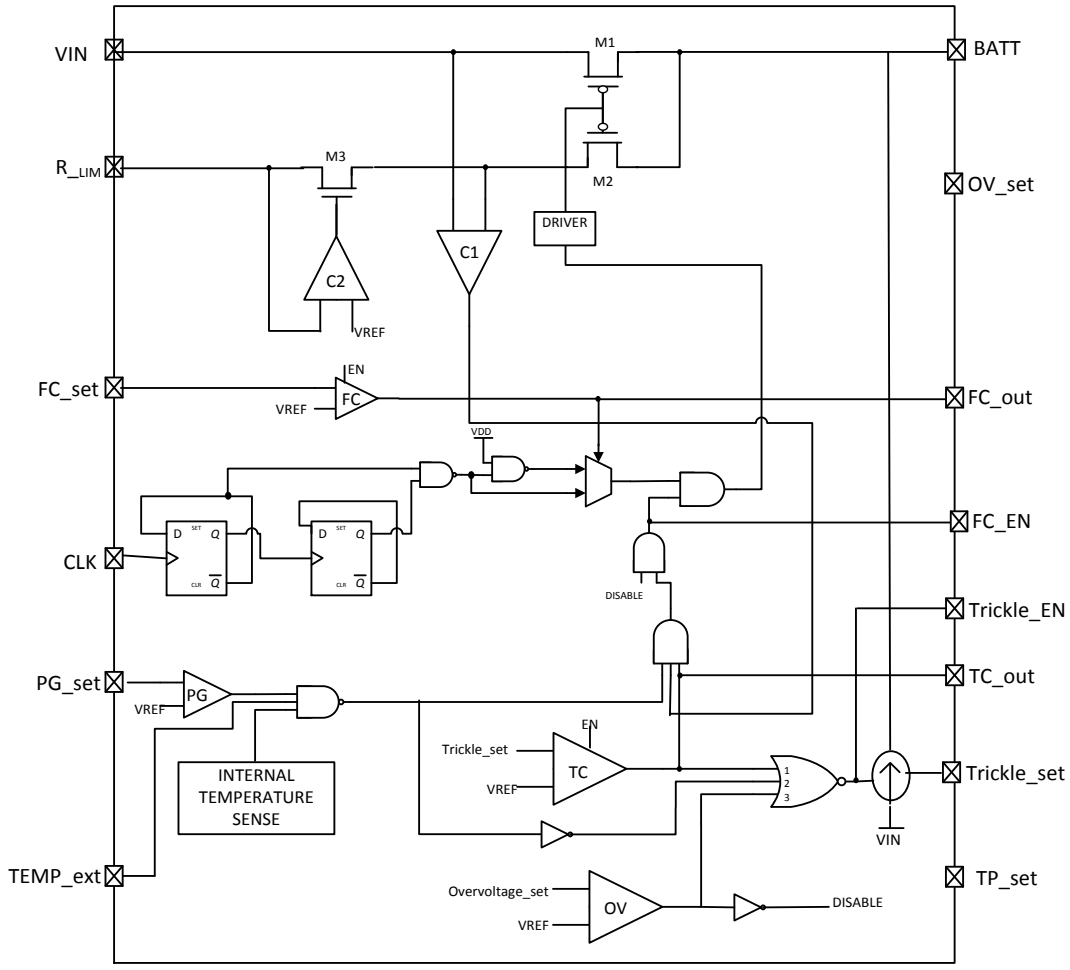

Figure 53 Detailed block diagram of pulse charger.

Table 11 Pulse charger pin descriptions and maximum ratings

Pin	**Usage**	**Maximum specification**
VIN	Connection to adapter	3.6V/500mA
R_{LIM}	Set overcurrent threshold	300μA
FC_set	Set nominal battery voltage	Battery specification
CLK	Clock input	<1KHz
PG_set	Input voltage monitoring	3.6V
TEMP_ext	Battery temperature monitor	Battery specification
OV_set	maximum battery voltage	3.3V
Trickle_set	Set trickle current	20mA
TC_out	Set constant current charger	3.6V
Trickle_EN	Enable trickle phase	3.6V
TP_set	Set trickle phase	Battery specification
FC_out	Set constant current charger	3.6V
FC_EN	Fast charge enable	3.6V
BATT	Battery connection	3.3V

Fig. 54 shows the configuration of the pulse charger in normal mode. The 3.3V OlevinPower Li-ion single cell battery specifications are used to set the parameters for the pulse charger during simulation. The input voltage, overvoltage, fast charge and trickle charge thresholds are set at 3.6V, 3.3V, 2.8V and 2V respectively. The charge current is set to 155mA and a clock frequency of 1 KHz is used during simulation. The Li-ion battery is modeled as a 100mF capacitor in series with a 100mΩ resistance. The simulation results are shown in Fig. 55 and 56.

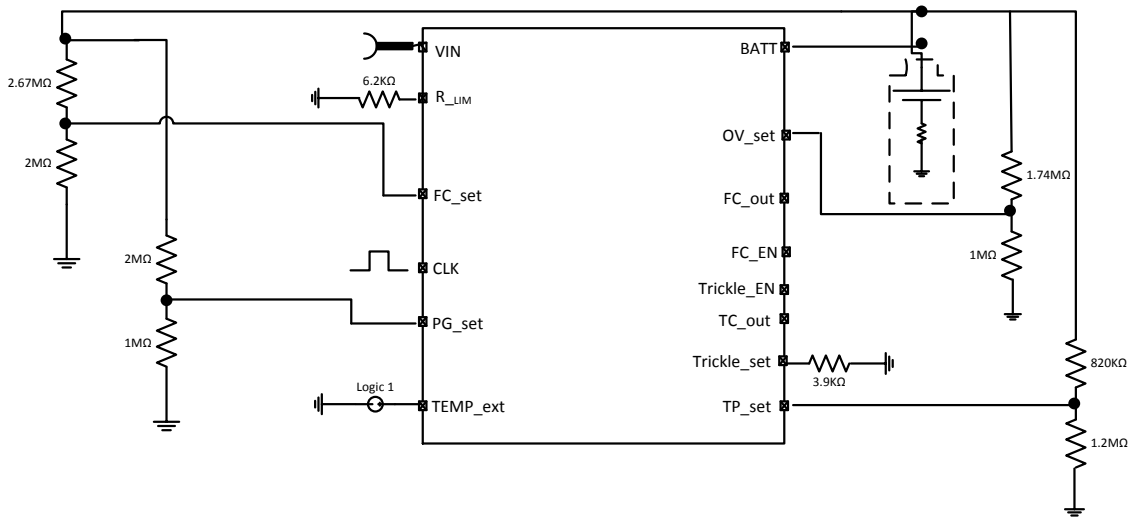

Figure 54 Pulse charger in normal operation connection diagram.

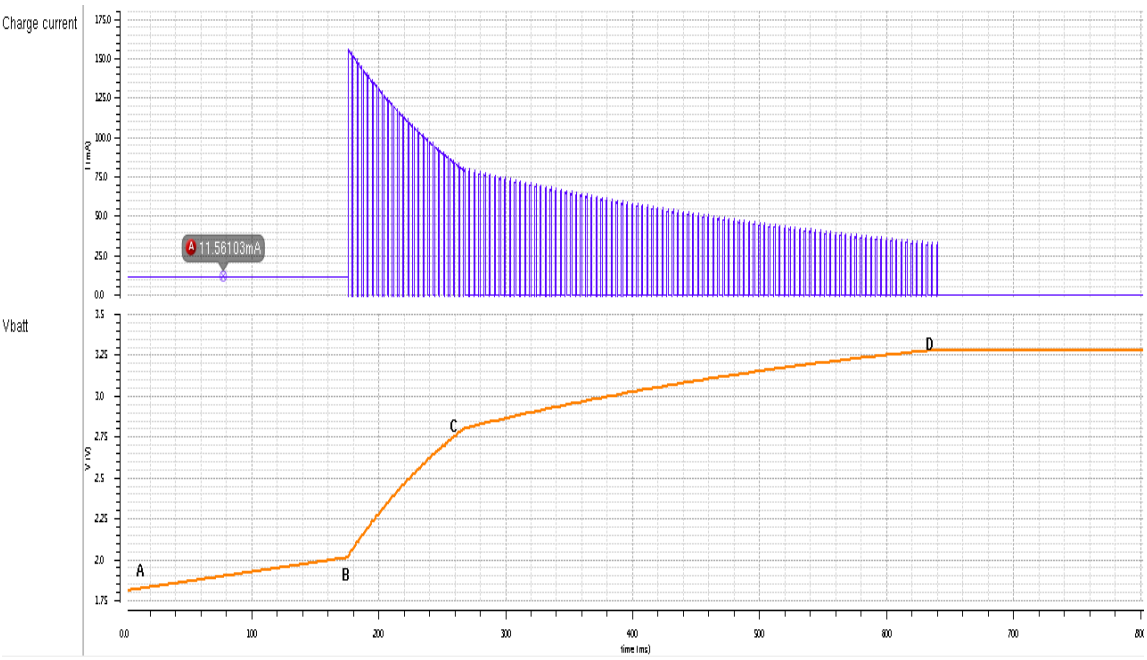

Figure 55 Battery charging using pulse charger.

Fig. 55 shows the charging of the battery going through all the charge phases. When the battery is less than 2V, it is trickled charged with a current of 11mA. When it reaches this voltage, point B, the charge current, 155mA, from the current limited wall adapter is pulsed into it at 0.75D. After, the nominal voltage is reached, 2.8V, the duty cycle changes to 0.25 to allow increase in battery charge efficiency. It is noticed that fast charging occurs between point B and C. The user can change the nominal voltage to suit a fast charge application if needed. Battery charging is terminated when the battery attains full charge at point D.

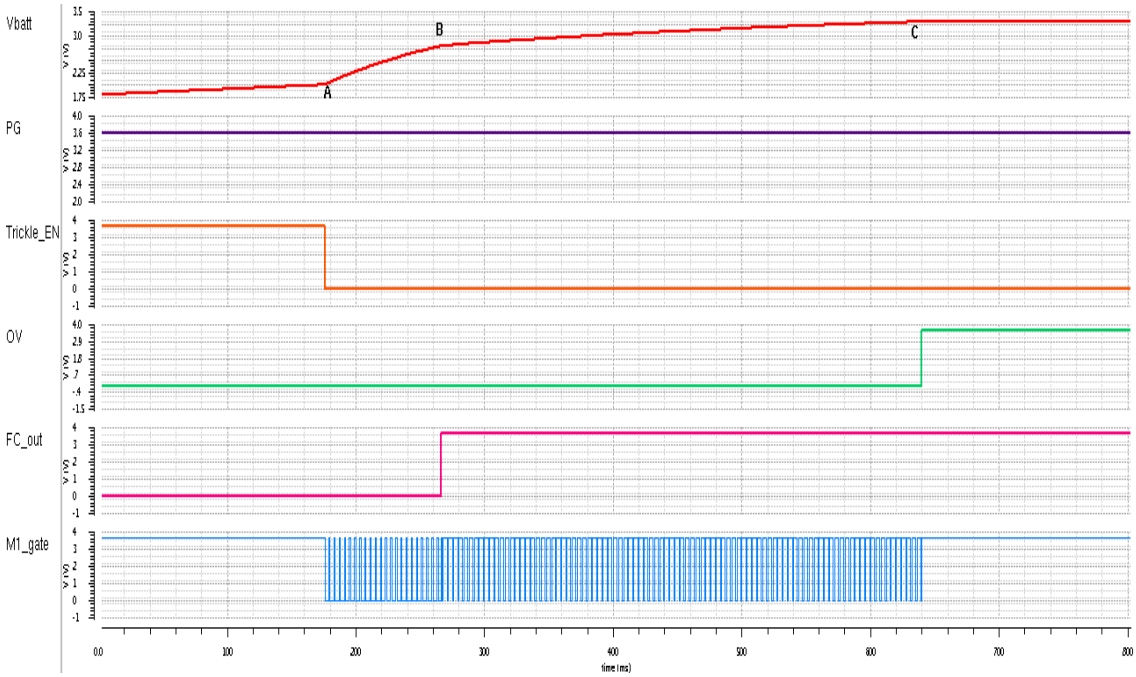

Figure 56 Waveforms showing operation of pulse charger.

Fig. 56 shows the relevant signals of the pulse charger during operation. It is seen that up to point A, the Trickle_EN signal is high. This shows that the battery is in a deeply discharged state. At point B, FC_out goes high to switch to a lower duty cycle. M1_gate shows the driving signals which enable the switch to pulse current into the battery. From point A to B, the pulses are at 0.75D and from point B to C, they are at 0.25D. Charge termination occurs at point C when the OV signal goes high. This means the battery has attained full charge. During this whole charging process, the PG signal is high and it is constantly monitored. This shows that the input voltage is suitable for charging.

3.4.1 Transformation of pulse charger to trickle charger

To setup the pulse charger to work as a trickle charger the FC_EN pin and TC_out pins are connected to ground. The CLK pin is connected to VIN. In this configuration, the fast charge phase is off, which means M1 will not be turned on at any time. To prove the concept works, the battery was modeled as a 100μF capacitor in series with a 10mΩ resistor. OV was set to 3V with an input of 3.3V. The trickle current was set at 5mA. Fig. 57 shows operation of the pulse charger in trickle charger mode.

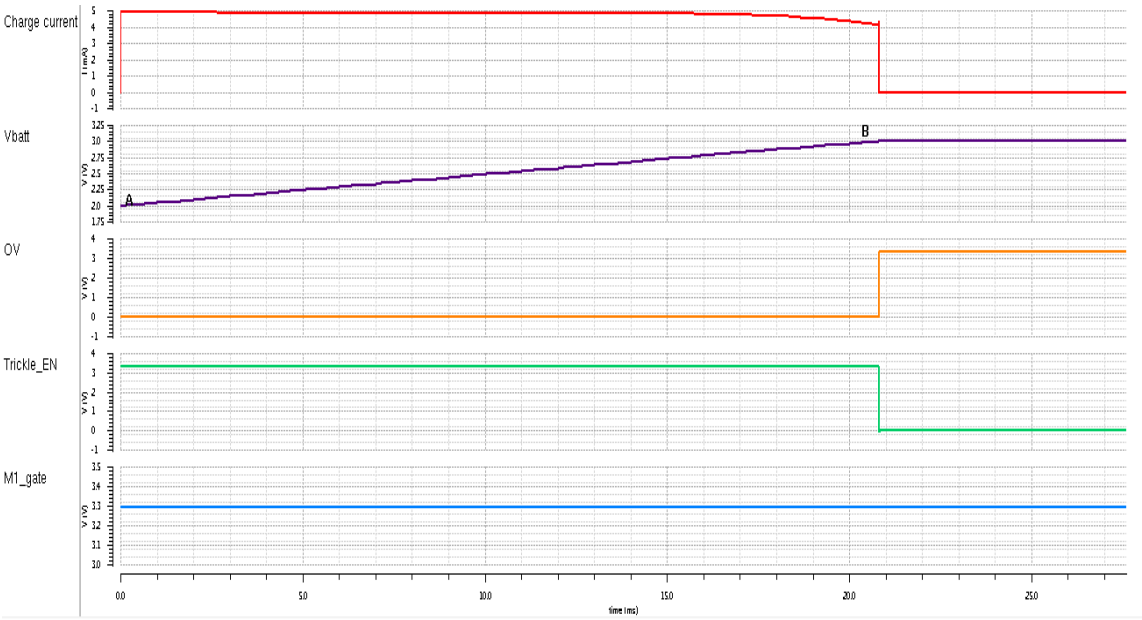

Figure 57 Operation of pulse charger as trickle charger.

In trickle charger operation mode, the signal at M1_gate is equal to VIN, which ensures M1 is never on. As long as the battery voltage is less than 3V, the charge current is set to 5mA and the battery is charged till it reaches point B. At this point, full charge is attained, the Trickle_EN goes low to turn off the internal current source, I_T. OV goes high to terminate charging completely.

3.4.2 Transformation of pulse charger to constant current charger

Constant current charging can be used for NiMH batteries. This configuration extends the functionality of the pulse charger to charge another type of battery apart from the Li-ion. To configure the pulse charger to work as a constant current charger, the Trickle_EN and FC_out are connected to ground, while the TC_out and CLK pins are connected to VIN. These connections force the trickle charging phase to be non-

operational and M1 to be always on during charging. To prove the concept works, the battery is still modeled as a 100µF capacitor in series with a 10mΩ resistor. OV was set to 3V with an input of 3.3V. The constant current was set at 155mA. Fig. 58 shows the simulation results of this configuration.

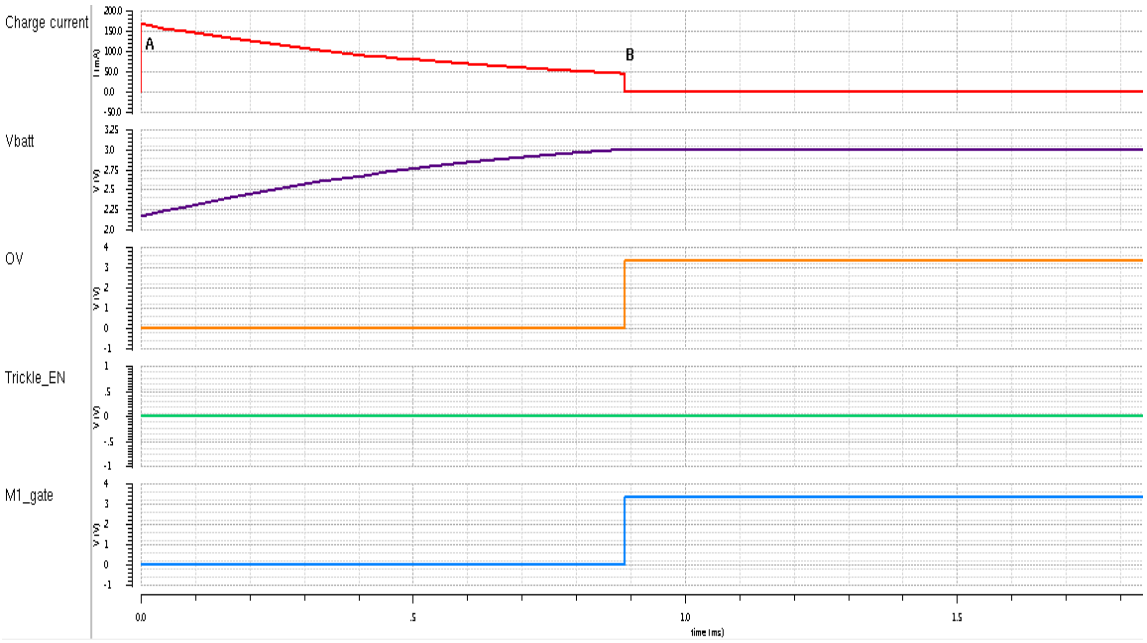

Figure 58 Operation of pulse charger as constant current charger.

Fig. 58 shows the relevant signals of the pulse charger when operating as a constant current charger. M1_gate signal shows that the main switch is on until full charge is attained. Comparing to Fig. 56, there is no pulsing. This is because it is in constant current mode of operation. At point A, the charger senses the battery voltage and begins charging with a constant current of 155mA which reduces as full charge is approached.

At point B, battery has reached full charge, OV goes high and charging is terminated. It is noticed that the trickle phase is off during the entire charging process.

4. STEP DOWN DC-DC CONVERTER AND SWITCHING NETWORK SYSTEM

For the system to support energy harvesting applications, additional blocks have to be designed. These blocks are the step down DC-DC converter and a switching network system. The step down converter serves as a DC supply for the energy harvesting system (EHS) while the switching system creates a path for the battery to be charged from the EHS. The switching network system also provides an option for the battery and the supercapacitor to complement each other in supplying power to the load. These two blocks together with the pulse charger form the battery charging system. This section looks at the different types of DC-DC step down converters, the reason why a particular topology is chosen, a detailed design procedure of the converter and simulation results showing the operation of the converter. The flow chart detailing the operation of the switching network system and the transistor level design is discussed. Finally, simulation results are presented. The EHS is considered to be a black box, providing a certain output current and voltage, and requiring a certain DC supply voltage. The specifications of the EHS are presented in table 12.

Table 12 Specifications of the EHS

Parameter	**Specification**
Supply voltage /current	1.8V/10mA$_{max}$
Output voltage/current	3.3V/200μA$_{max}$

4.1 Step down DC-DC converter

Energy harvesting systems with no start up circuit need an initial DC supply to kick start the system [77]. This is because the voltage harvested, by the energy harvesters, is very small and is not able to power up the CMOS circuits in the system. Hence, an initial DC voltage is needed to kick start the CMOS circuits into operation. This initial DC supply is provided by a battery but in most cases, the battery voltage is too high for the operation of the system and needs to be reduced to a level which can be used by the EHS. The circuit that performs this step down function is known as a step down DC-DC converter. Step down DC-DC converters are used in almost any portable electronic device. They are required because different sub circuits in devices may require different voltage levels for operation. During circuit operation, the battery voltage is likely to diminish, hence to allow constant operation of sub circuits during diminishing battery voltage level, step DC-DC converters provide output voltage regulation, which allows the supply voltage to remain constant under different load conditions and varying battery voltage.

The main types of step down DC-DC converters are linear regulators, switched inductor and switched capacitor converters [78]. Linear regulators, e.g. low-dropout (LDO) regulator, are very popular due to its simplicity and low cost. However, they are inefficient because the power transistor, T_p, used to drop the input voltage, V_{in}, to the required level, V_o, is always on and at high load currents, heat dissipation is high and hence, power consumption goes up. The LDO is shown in Fig. 59.

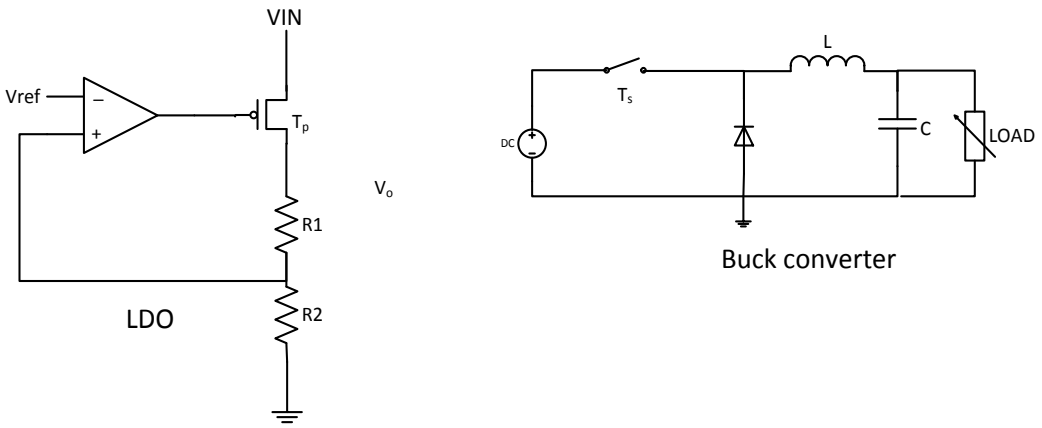

Figure 59 Linear regulator (LDO) and switch inductor converter (buck).

Switched inductor converters, such as buck converters, offer high efficiency at increased cost and complexity. Increased cost is due to additional external components, i.e. inductors and capacitors, which take up board space, and complexity due to the control loop needed to achieve good output voltage regulation. The main switch, T_s, is not always on, but switching constantly depending on output voltage levels to ensure reduced power consumption. The buck converter is shown in Fig. 59.

Switched capacitor converters combine the benefits of linear regulators and switched inductor converters, i.e. simplicity and high efficiency respectively. A switched capacitor converter consists of a series of switch networks and capacitors, which can be connected in different configurations, to obtain different output voltages from one input voltage.

Table 13 shows the comparison between the different step down converters in terms of area and power. For the purposes of in this thesis, a switched capacitor converter is chosen.

Table 13 Comparison of different step down converters

Converter type	**Area**	**Quiescent power**
LDO	small	high
Buck	huge	low
Switched capacitor	moderate	low

4.1.1 Switched capacitor converter

For smaller board space due to few external components, lower power consumption due to the switching action of the converter and low current application, the switched capacitor converter is chosen over the other step down DC-DC converters. It combines the benefits of the switched inductor converter and the linear regulator, making it an ideal choice for the step down function in this project. There are also no magnetic components, hence less noisy.

The switched capacitor converter can be designed to have different gain configurations [79] – [80]. Based on the supply voltage specification for the energy harvesting system, the switched capacitor circuit should be able to step the battery voltage down from 3V or 3.3V to 1.8V. To do this, the converter makes use of two flying capacitors, C_1 and C_2,

which is used to store and transfer energy to the output capacitor, C_{out}. By detecting the output voltage, the control loop in Fig 60 is able to generate pulses at Ø1 and Ø2 to produce a gain setting of 2/3.

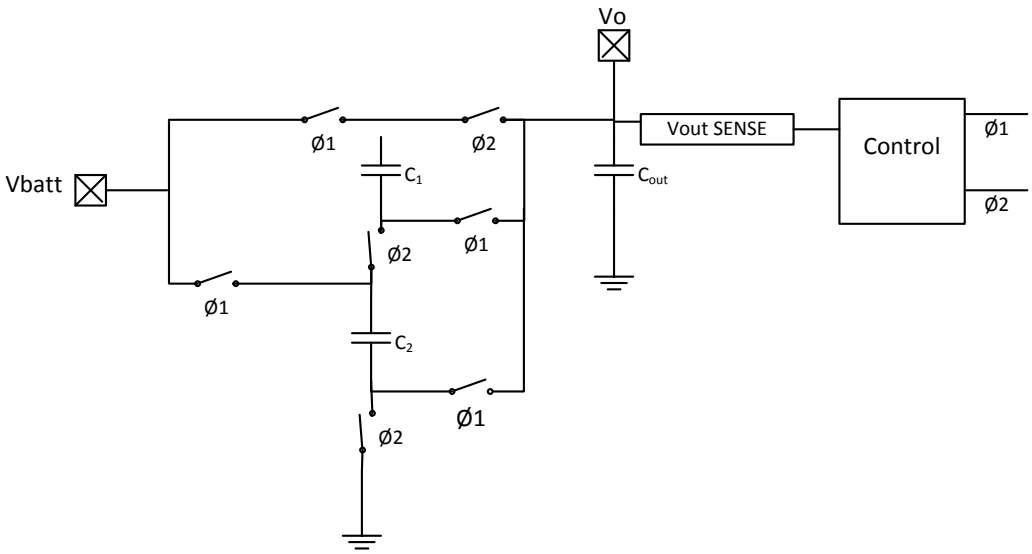

Figure 60 Switched capacitor converter.

In Fig.61, at the end of Ø2, the flying capacitors, C_1 and C_2, are connected in series together, and in parallel with C_{out}. During Ø1, they are connected in parallel, and in series with C_{out}. These series-parallel configurations are made possible by the control loop which controls the different clock phases, i.e. Ø1 and Ø2.

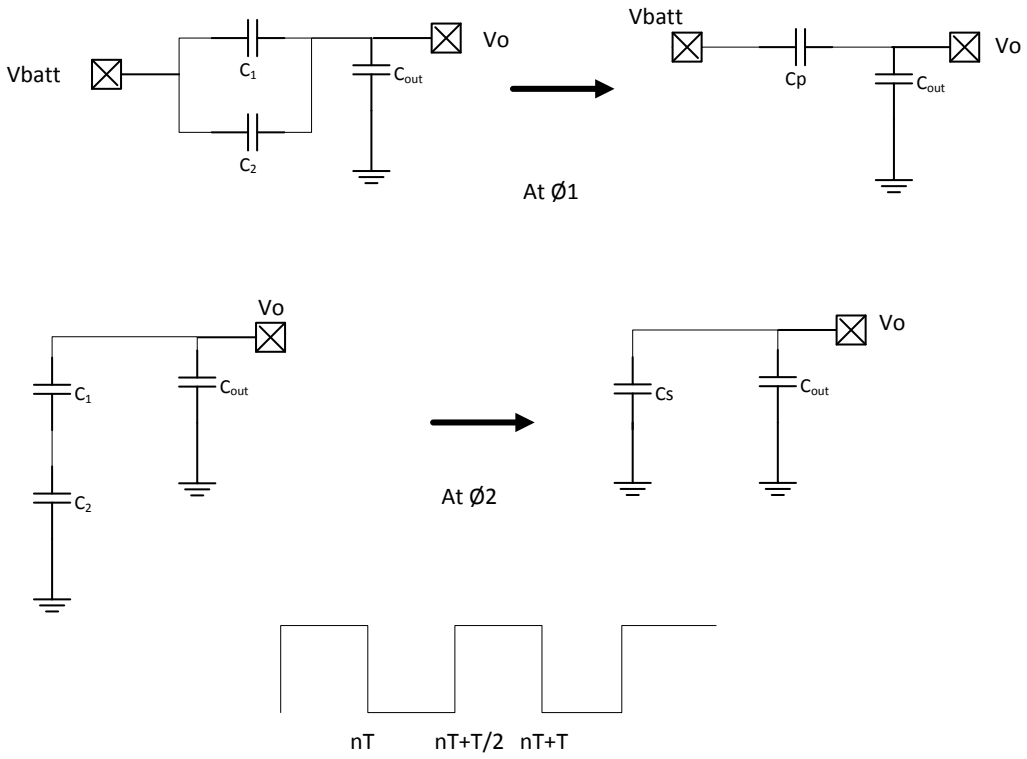

Figure 61 Operation of switched capacitor converter during different clock phases.

The analysis of this switched capacitor converter based on charge conservation [78] is presented in equations 31 to 43.

At the end of Ø2, i.e. time nT, capacitors C_s and C_{out} have the following charge equations.

$$Q_{cout}(nT) = C_{out}V_o(nT) \tag{31}$$

$$Q_{cs}(nT) = C_sV_o(nT) \tag{32}$$

At the end of Ø1,

$$Q_{cout}\left(nT + \frac{T}{2}\right) = C_{out}V_o\left(nT + \frac{T}{2}\right) \tag{33}$$

$$Q_{cp}\left(nT+\frac{T}{2}\right)=C_p\left(V_{batt}-V_o\left(nT+\frac{T}{2}\right)\right) \tag{34}$$

The theory of the law of charge conservation states if two capacitors are connected together, the total charge on the parallel combination is equal to the sum of the original charge on the capacitors [81]. Based on this theory, using equations 31 to 34,

$$Q_{cout}\left(nT+\frac{T}{2}\right)-Q_{cp}\left(nT+\frac{T}{2}\right)=Q_{cout}(nT)-Q_{cs}(nT)$$

$$C_{out}V_o\left(nT+\frac{T}{2}\right)-C_p\left(V_{batt}-V_o\left(nT+\frac{T}{2}\right)\right)=C_{out}V_o(nT)-C_sV_o(nT)$$

$$V_o\left(nT+\frac{T}{2}\right)=\frac{C_p}{C_{out}+C_p}V_{batt}+\frac{(C_{out}-C_s)}{C_{out}+C_p}V_o(nT) \tag{35}$$

Therefore,

$$Q_{cout}\left(nT+\frac{T}{2}\right)=\frac{C_{out}C_p}{C_{out}+C_p}V_{batt}+\frac{C_{out}(C_{out}-C_s)}{C_{out}+C_p}V_o(nT) \tag{36}$$

$$Q_{cp}\left(nT+\frac{T}{2}\right)=\frac{{C_p}^2}{C_{out}+C_p}V_{batt}+\frac{C_p(C_{out}-C_s)}{C_{out}+C_p}V_o(nT) \tag{37}$$

At time nT+T, using the law of conservation at Ø2,

$$Q_{total}(nT+T)=Q_{cout}\left(nT+\frac{T}{2}\right)-Q_{cp}\left(nT+\frac{T}{2}\right)\Rightarrow V_o(nT+T)=\frac{Q_{total}(nT+T)}{C_{out}+C_s}$$

$$V_o(nT+T)=\frac{{C_p}^2-C_{out}C_p}{(C_{out}+C_p)(C_{out}+C_s)}V_{batt}+\frac{(C_{out}-C_s)(C_{out}+C_p)}{(C_{out}+C_p)(C_{out}+C_s)}V_o(nT) \tag{38}$$

If $m=\frac{{C_p}^2-C_{out}C_p}{(C_{out}+C_p)(C_{out}+C_s)}$ and $n=\frac{(C_{out}-C_s)(C_{out}+C_p)}{(C_{out}+C_p)(C_{out}+C_s)}$, then

$$V_o(nT+T)=mV_{batt}+nV_o(nT)$$

At nT+2T,

$$V_o(nT+2T) = mV_{batt} + nV_o(nT+T)$$

$$V_o(nT+2T) = mV_{batt} + n\big(mV_{batt} + nV_o(nT)\big) = m(1+n)V_{batt} + n^2V_o(nT) \quad (39)$$

At nT+3T,

$$V_o(nT+3T) = m(1+n+n^2)V_{batt} + n^3V_o(nT) \quad (40)$$

At nT+KT, as K varies from 0 to infinity

$$V_o(nT+KT) = m(1+n+n^2+n^3+\cdots+n^{K-1})V_{batt} + n^KV_o(nT)$$

$$V_o(nT+KT) = mV_{batt}\left(\frac{1-n^K}{1-n}\right) + n^KV_o(nT) \quad (41)$$

where $n = \frac{(C_{out}-C_s)(C_{out}+C_p)}{(C_{out}+C_p)(C_{out}+C_s)} < 1$.

Hence as $K \to \infty$,

$$V_o(nT+KT) \cong mV_{batt}\left(\frac{1}{1-n}\right) \quad (42)$$

Substituting m and n into equation 42,

$$V_o(nT+KT) = \frac{{C_p}^2 - C_{out}C_p}{(C_{out}+C_p)(C_{out}+C_s)} * \left(\frac{1}{\left(\frac{(C_{out}-C_s)(C_{out}+C_p)}{(C_{out}+C_p)(C_{out}+C_s)}\right)}\right)V_{batt}$$

$$\frac{V_o(nT+KT)}{V_{batt}} = \frac{{C_p}^2 - C_{out}C_p}{2C_sC_{out} + 2C_pC_s} \quad (43)$$

Then, if $C_2 = C_1, C_p = 2C_1, C_s = \frac{C_1}{2}, C_{out} = C_1$

$$\frac{V_o}{V_{batt}} = \frac{2}{3}$$

The efficiency, η, of the switched capacitor circuit [78] is approximated as,

$$\eta = \frac{3}{2}\frac{V_o}{V_{batt}} \tag{44}$$

This efficiency is maximized when the battery is at 2.7V for an output voltage of 1.8V. If the battery voltage is more than 2.7V, the efficiency of the converter reduces and the output voltage is obtained with an error. For the purposes in this thesis, the battery nominal voltage cannot exceed 3V and hence at that voltage, the converter can output a voltage with an error that does not exceed twelve percent.

4.1.1.1 Transistor-level implementation

Fig. 62 shows the transistor level implementation of the switched capacitor converter with a gain of 2/3. There are two 1µF flying capacitors and seven switches, five of which are PMOS and the other two, NMOS. During Ø1, P1, P2, P4 and P5 are on and N1, N2 and P3 are off. The vice versa occurs during Ø2. This switching action of these combinations of switches, which are driven by control signals, Ø1 and Ø2, produce an output gain of 2/3.

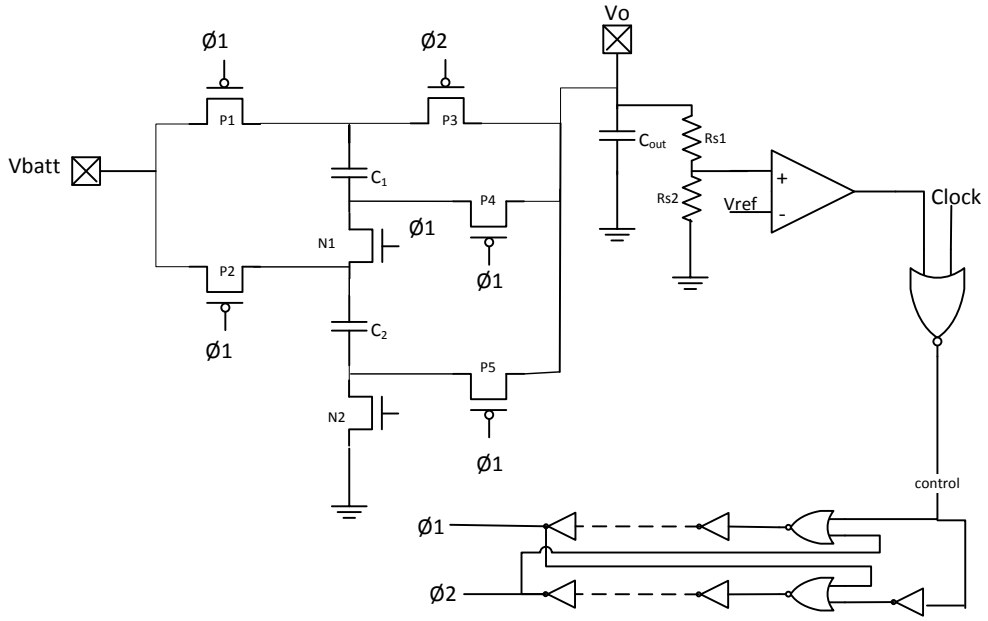

Figure 62 Transistor level implementation of switched capacitor converter.

Both the NMOS and PMOS switches are designed to have low on resistance (r_{on}) in order to reduce voltage drop and improve efficiency during operation. Equation 45 details how the PMOS switches are sized.

If $r_{on}<1\Omega$, then $g_{ds} < 1\Omega^{-1}$.

$$g_{ds1} < K_p \frac{W}{L}(V_{in} - |V_{TH}|) \tag{45}$$

If $V_{in}=3V$ and $g_{ds}<1\Omega^{-1}$, then

$$\left(\frac{W}{L}\right)_1 > 10000$$

Ø1 and Ø2 are generated by the control loop, which consists of an output voltage detector and a non-overlapping clock. The output voltage detector consists of a comparator and a resistor feedback network. The resistors detect the voltage level of the

output and the comparator outputs a high or low logic signal depending on whether the detected output voltage is less than or equal to 1.8V. The output of the comparator is combined with a clock signal using a NOR gate to produce a signal to control the non-overlapping clock generator. A non-overlapping clock is used to ensure that Ø1 and Ø2 do not have the same logic value at the same time.

To determine the values of the resistors, R_{s1} and R_{s2}, the following equation is used,

$$V_o = 1.2\left(1 + \frac{R_{s1}}{R_{s2}}\right) \tag{46}$$

If V_o is 1.8V,

$$R_1 = 0.5R_2$$

Fig. 63 shows the operation of the switched capacitor circuit at no load conditions.

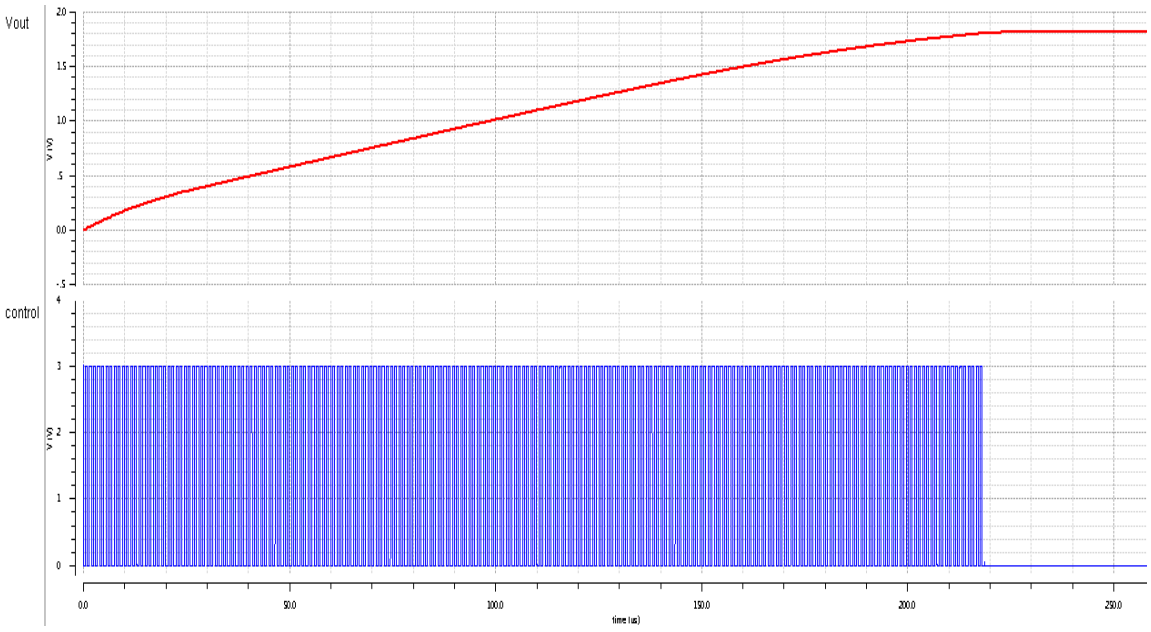

Figure 63 Operation of switched capacitor converter with V_{batt}=3V at no load.

It is seen from Fig. 63, that with a clock frequency of 1MHz, the control signal to the non-overlapping clock generator is continuously pulsing until the output reaches 1.8V for a battery voltage of 3V at no load conditions. C_{out} gradually charges during this period till it achieves 1.8V.

Fig. 64 shows the variation of the output voltage with load current. As load current increases, the converter's output voltage drops, indicating that it is able to source a load current less than 30mA. Since the application is for low load currents, this does not pose a problem because the output voltage remains constant when operating under the required specifications of the EHS, i.e. a maximum of 10mA.

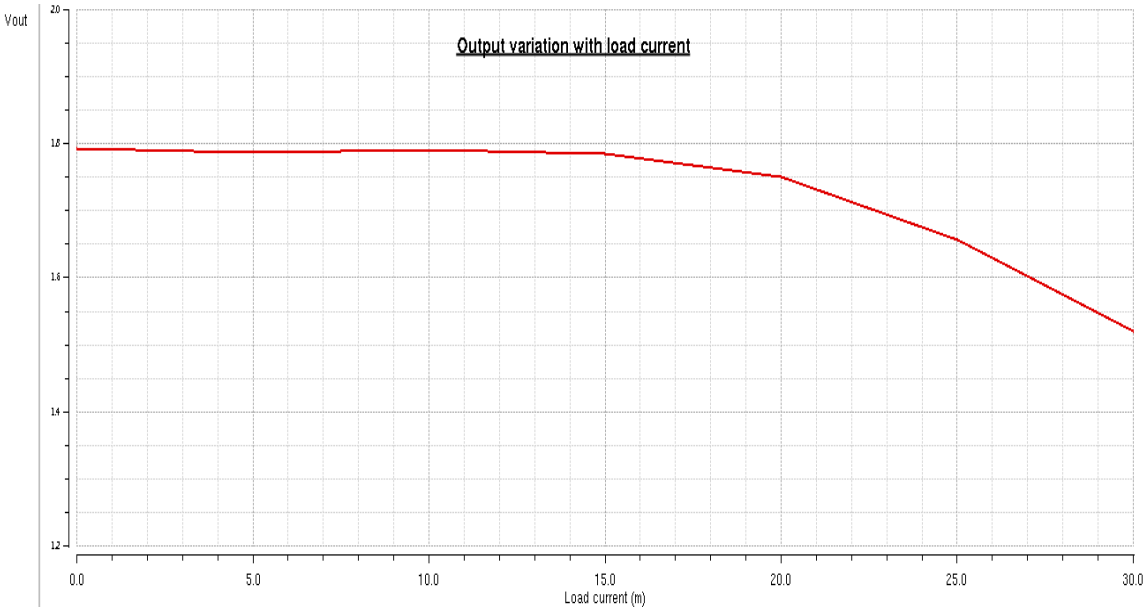

Figure 64 Converter's output voltage variation with load current.

Fig. 65 shows the variation of the output voltage of the converter under varying battery voltage. As voltage decreases, the output voltage also decreases. The converter's output voltage will remain stable as long as the battery voltage is above 2.7V.

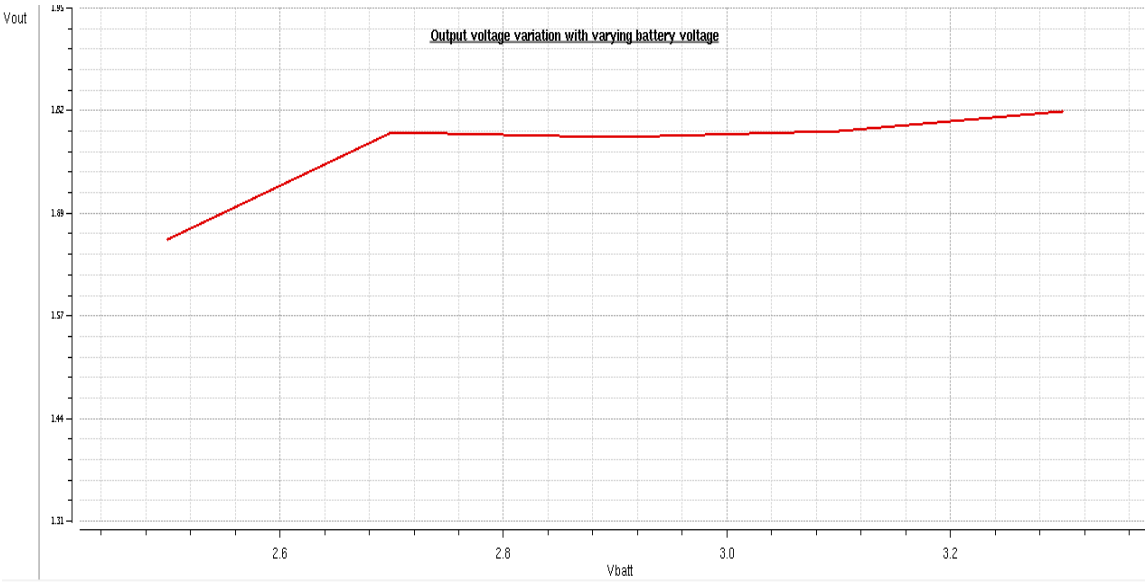

Figure 65 Converter output variation with varying battery voltage.

The efficiency of the converter is shown in Fig. 66. As load current increases, the converter's efficiency starts decreasing. This is because the converter cannot support the current demand, i.e. above 20mA, and the output voltage drops, causing efficiency to also decrease.

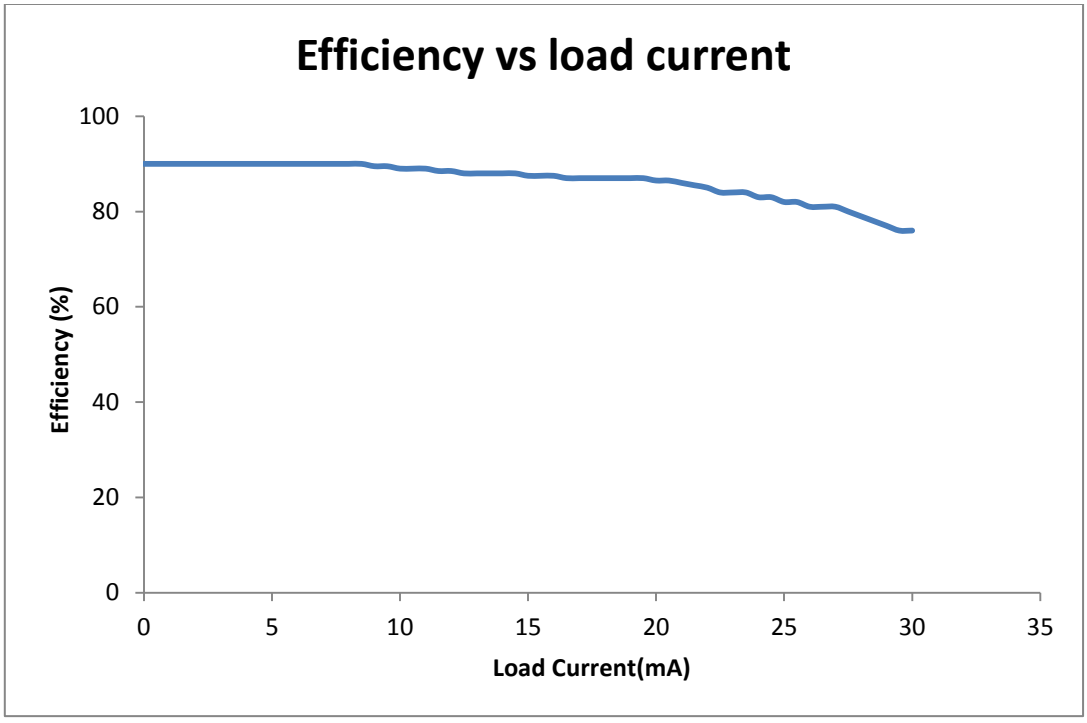

Figure 66 Efficiency of switched capacitor converter at 3V input.

4.2 Switching network system

The current sourcing capability of the EHS is not enough to meet the power requirements of the pulse charger. The specifications of the EHS, shown in table 12, indicate that, it can provide a maximum of 200µA at the output. The pulse charger needs at least 1mA to operate. To prevent reduced efficiency, the switching network system is designed to bypass the pulse charger and enable battery charging directly from an EHS. It also has the option to enable the supercapacitor, being charged by the EHS, to deliver short term peak current to a load when needed without affecting the battery, thereby enabling both the battery and supercapacitor to complement each other. This block

ensures that the EHS and the pulse charger operate independently from each other and can each be used as a standalone device.

A battery-supercapacitor combination allows peak current pulses to be delivered to a load whenever needed and at the same time sustain long term load power demand. The supercapacitor is the main power supply to the load while the battery serves as a backup. When AC/DC input or USB is not available, the battery can be charged from the EHS and when the supercapacitor is not able to support the load, the battery can provide power to the load. This switching network being part of the battery charging system provides options to make the system adaptable to load and input power conditions.

4.2.1 Implementation of the switching network system

The switching network will only be connected to the battery when AC/DC input or USB is not available. When the block determines that these inputs are not available, the EHS is connected to battery to charge it but it they are available, the EHS is connected to the supercapacitor. Depending on load conditions, there is an option for the supercapacitor or battery to be connected to the load. The flow chart summarizing the operation of the switching network system is presented in Fig. 67.

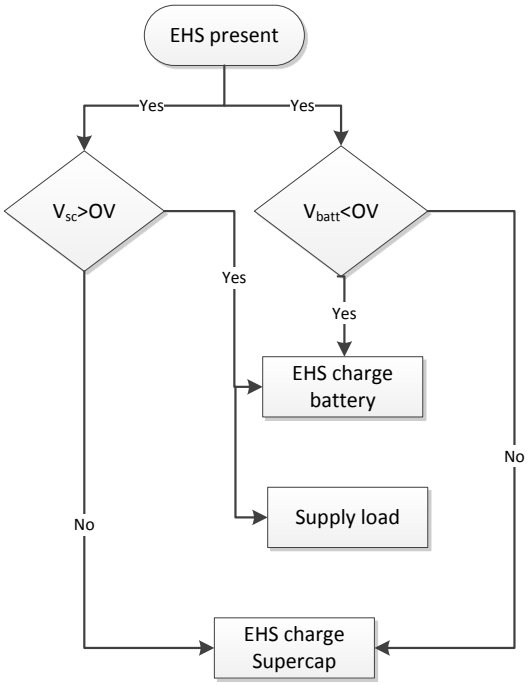

Figure 67 Flow chart showing conceptual idea of switching network system.

The conceptual block diagram of the switching network is presented in Fig. 68. The voltage detector is implemented using a clocked comparator and a series of resistor feedback networks. Depending on battery and supercapacitor voltage conditions, the EHS charges the battery or the supercapacitor.

.

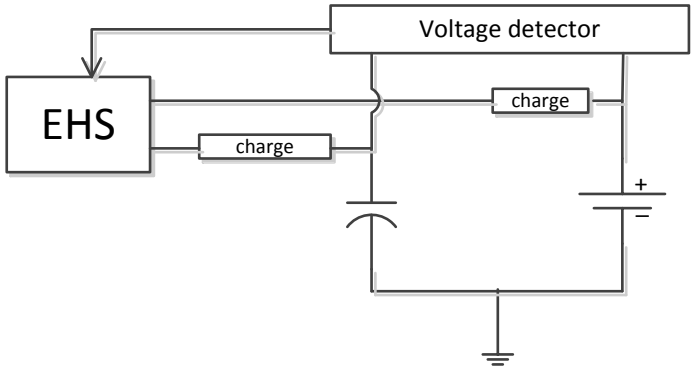

Figure 68 Conceptual block diagram of switching network system.

A clocked comparator, shown in Fig. 69, is used in order to minimize power consumption since the battery serves as its supply voltage. This is to ensure minimal current drain from the battery to the comparator. The comparator is clocked at a frequency of 1MHz.

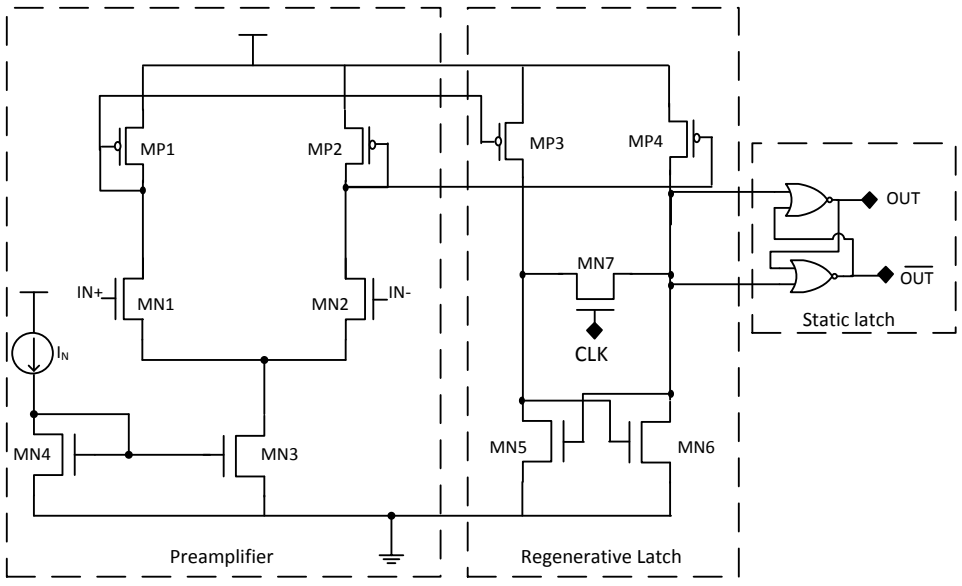

Figure 69 Clocked comparator.

The comparator consists of a preamplifier stage, regenerative latch and a static latch, to serves as a memory to hold the values for a whole clock period. The static latch also serves as an interface to convert the analog signals into digital ones since connecting the analog outputs directly can cause the system to be unstable [82]. The regenerative latch (MN5, MN6, MP3, MP4 and MN7) amplifies the analog signals to full rails while the preamplifier stage (MN1, MN2, MP1 and MP2) amplifies the input signal to improve the sensitivity of the comparator [83].

The differential pair transistors, MN1 and MN2, are sized for minimum noise, mismatch reduction and moderate gain. To reduce parasitics, the transistors sizes used for the regenerative latch are kept minimum. The gain, A_{vp}, for the preamplifier stage and that for the regenerative stage, A_r, are respectively

$$A_{vp} = \frac{g_{MN1}}{g_{MP1}};\ A_r = \frac{g_{MP3}R_{N7}}{2 - g_{MN5}}$$

where g_m is transconductance and R is the output impedance.

To size the pre-amplifier based on low average power consumption, i_f=1 is chosen and an I_{ds} of 500nA. Using equation 6,

$$g_{mN1,N2} = \frac{2 * 0.5\mu A}{26mV * (1 + \sqrt{1 + 1})} = 15.9\mu A/V$$

The dimensions of the transistors can be calculated using equation 7.

$$\left(\frac{W}{L}\right)_{N1,N2} = \frac{g_{mN1,N2}}{\mu C_{ox}\Phi_t(-1 + \sqrt{1 + i_f})} = 29.6$$

The dimensions of the transistors used in the comparator are presented in table 14.

Table 14 Clocked comparator transistor dimensions

Transistor	**W/L(µm)**
MN1	(4/2)*2
MN2	(4/2)*2
MN3	(4/2)*4
MN4	(4/2)*4
MN5	(4/0.4)*1
MN6	(4/0.4)*1
MN7	(4/0.4)*1
MP1	(4/2)*6
MP2	(4/2)*6
MP3	(4/0.4)*1
MP4	(4/0.4)*1

Fig. 70 shows the output of the clocked comparator. As the signal crosses the reference voltage, the output logic switches between one and zero depending on whether the signal is greater or less than the reference voltage.

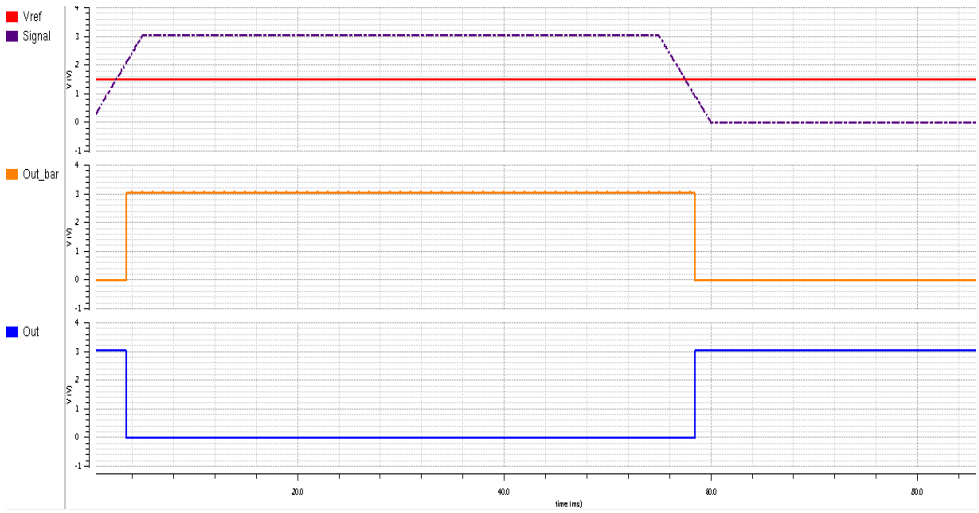

Figure 70 Operation of clocked comparator.

The switching network block enables switching between input charging source and the two storage elements depending on input source availability and load conditions. The transistor level implementation is presented in Fig. 71.

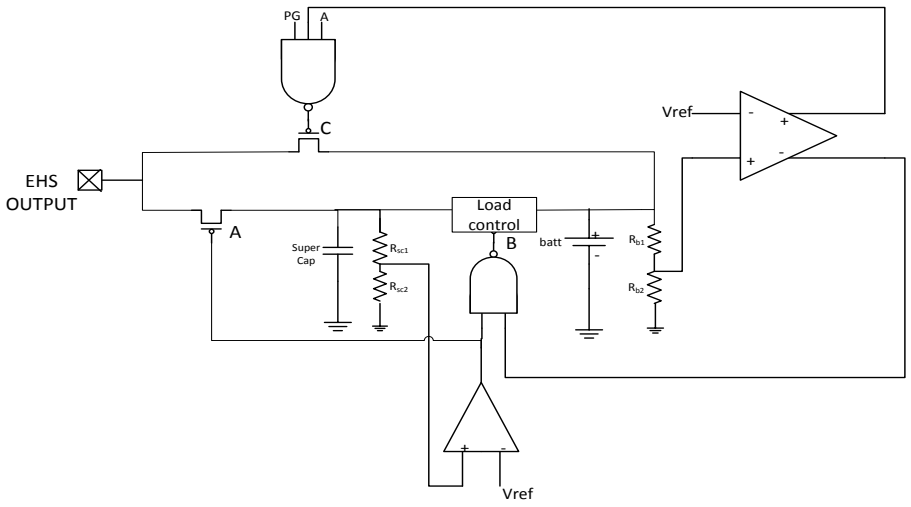

Figure 71 Transistor level implementation of switching network system.

From Fig. 71, switch A is turned on, when the supercapacitor voltage is below a set threshold, e.g. 3V, to allow the supercapacitor to be charged. When the battery is not fully charged, but the supercapacitor is, switch C turns on to allow the battery to be charged from the EHS. This depends on whether the AC/DC input is available or not (PG input), if it is not available, charging from the EHS will proceed or vice versa. Signal B serves to connect the supercapacitor or battery to the load based on which storage element is ideal for the particular application. The comparators are included to

prevent overcharging of the battery and the supercapacitor. Sizing of the switches are based on a small r_{on} by using equation 45.

If $r_{on}<1\Omega$, then $g_{ds} < 1\Omega^{-1}$. Therefore, for a $V_{in}=3.3V$ and $g_{ds}<10\Omega^{-1}$,

$$\left(\frac{W}{L}\right)_1 > 8000$$

To determine the values of the resistors, R_{sc1}, R_{sc2}, R_{b1} and R_{b2}, the following equation is used,

$$V_{batt,sc} = 1.2\left(1 + \frac{R_{s1,b1}}{R_{s2,b2}}\right) \tag{47}$$

If $V_{batt,sc}$ is 3V,

$$R_1 = 1.5R_2$$

It should be noted that the EHS operates independently of the pulse charger as long as AC/DC or USB inputs are available.

Fig. 72 shows the operation of the switching network system when the pulse charger is off. The priority of the EHS is to charge the supercapacitor to 3V. During this period, switch A (SW_A) is on and all other switches are off. When the supercapacitor is fully charged and the system detects that the battery voltage is below the overvoltage threshold, the EHS proceeds to charge the battery, turning on switch C (SW_C). Once the supercapacitor voltage falls below 3V, the EHS goes back to charging it. This is seen by observing the switching action of switch A. The system is designed in such a way that

none of the switches are on at the same time to isolate each power source to provide reverse current protection.

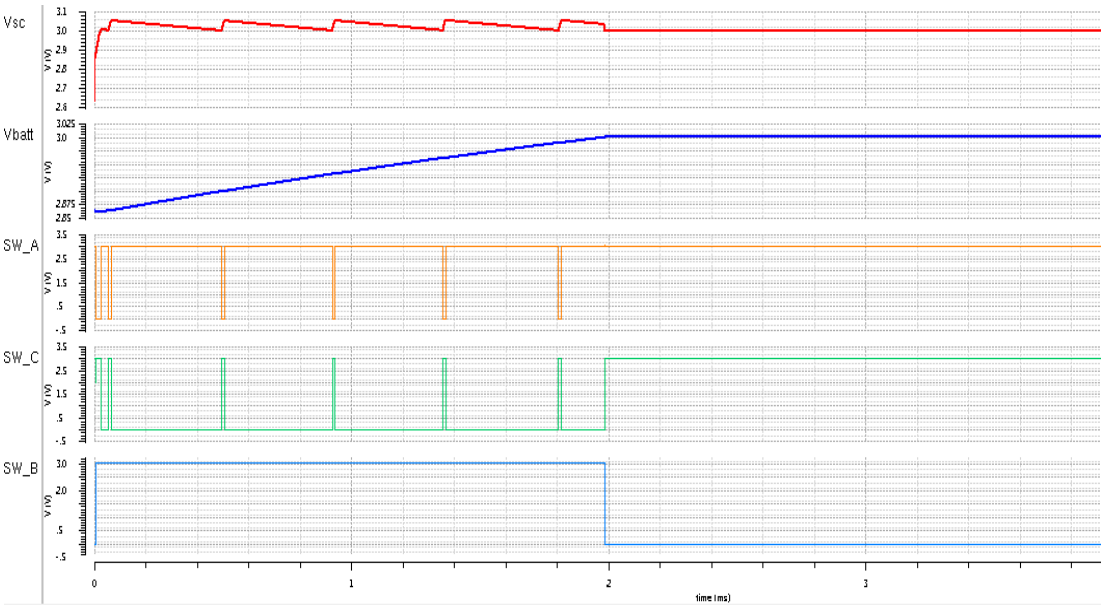

Figure 72 Operation of switching network system.

5. EXPERIMENTAL RESULTS

This section seeks to provide results from the designed IC operating under real life conditions. The IC was designed using the IBM 0.18µm process with the area of the die being 4mm^2. It was packaged using an open cavity 8mm by 8mm Quad Flat No-Lead (QFN). The experimental results of the proposed pulse charger indicating proof of concept, the step down DC-DC converter and the switching network system are presented. Comparison of previous works versus the proposed pulse charger in this thesis is made. A micrograph of the designed chip is shown in Fig. 73.

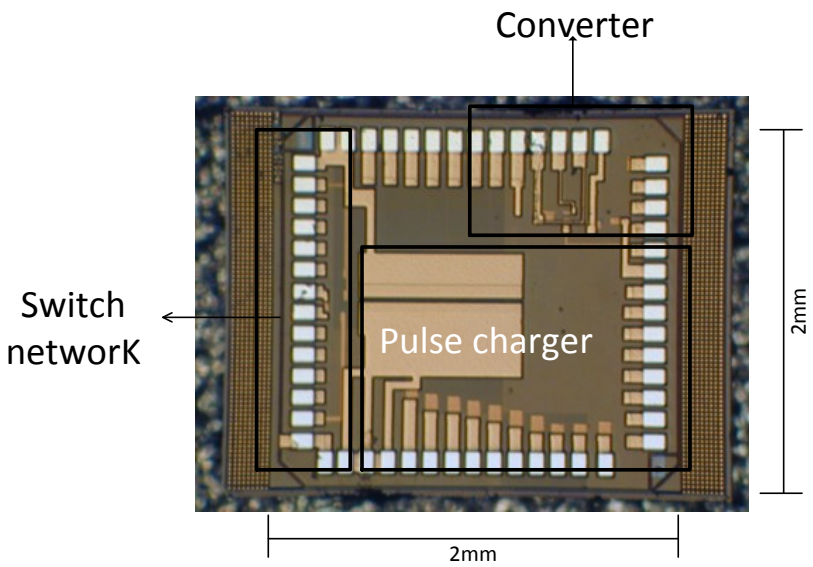

Figure 73 Micrograph of user programmable battery charging system IC.

Fig. 74 shows the instruments used in the testing and measurement of the proposed charging system. It provides a pictorial representation of how the experimental setup looks like.

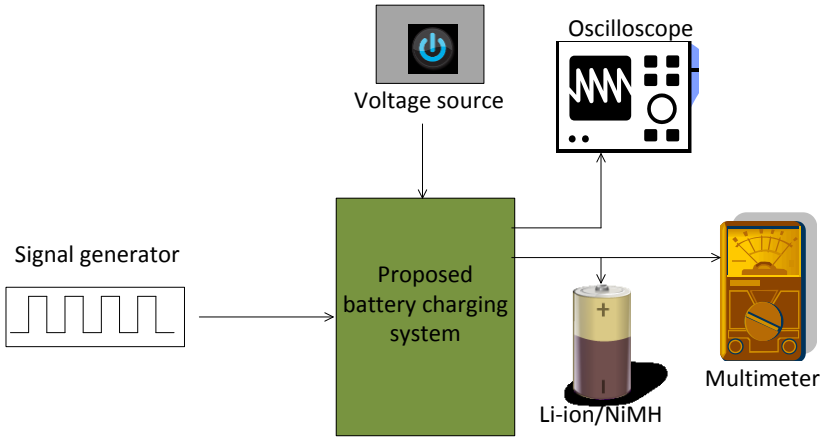

Figure 74 Pictorial representation of experimental setup.

5.1 Proposed pulse charger

Since pulse charging is applicable to NiMH, Li-ion and Lead acid batteries. To prove the proposed pulse charger works in normal mode, it is used to charge a 2500mAh NiMH battery. A current limited input voltage source of 3.3V/300mA is used as the source. A clock signal of 1KHz is used. The schematic of the test bench used to verify the operation of the proposed pulse charger is shown in Fig. 75.

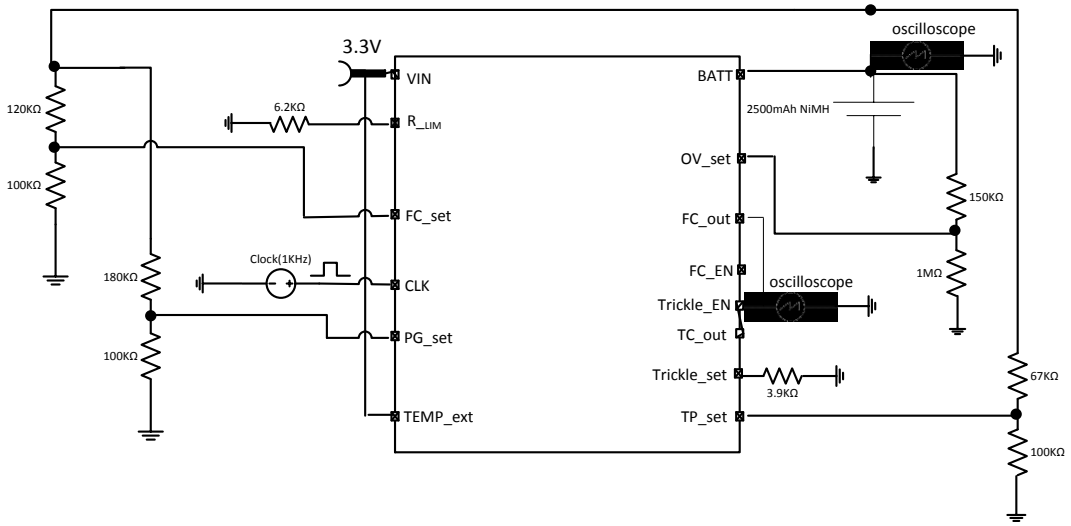

Figure 75 Test bench to verify operation of proposed pulse charger.

Fig. 76 shows the charging of the 2500mAh NiMH battery using the proposed pulse charger with the above setup. It took about 85 minutes to attain a nominal voltage of 2.5V.

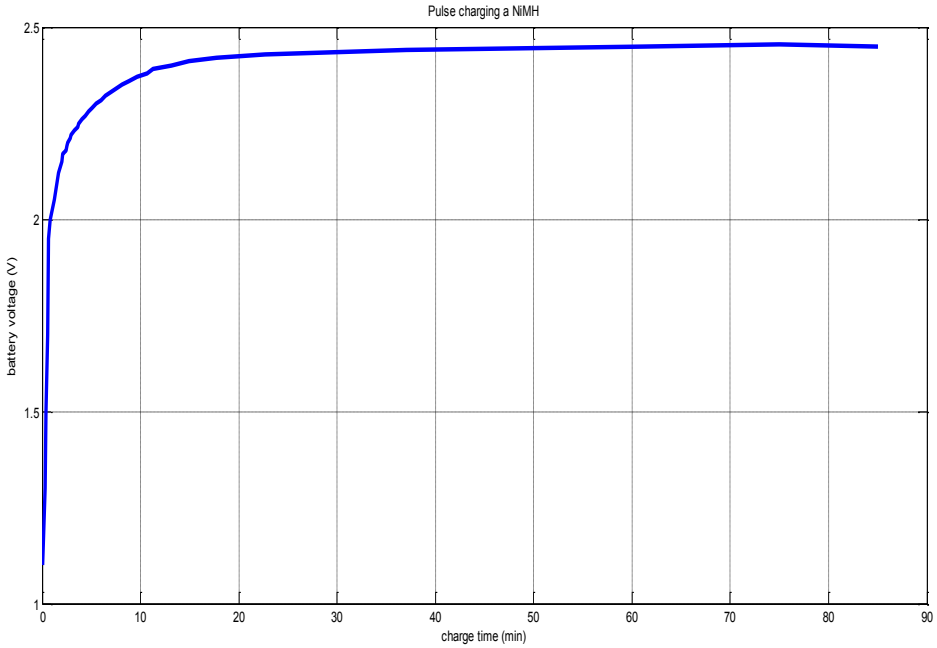

Figure 76 Test result verifying operation of proposed pulse charger in normal mode.

To verify that the pulse charger can be reconfigured to operate as a trickle charger, it was used to charge a 3V Panasonic Li-ion coin cell. It can be observed from Fig. 77 that, operating in trickle charge mode takes a very long time for the battery to attain full capacity. In this case, the Li-ion coin cell took about 400 minutes to attain a maximum voltage of 2.92V. It can therefore be used as an overnight charger.

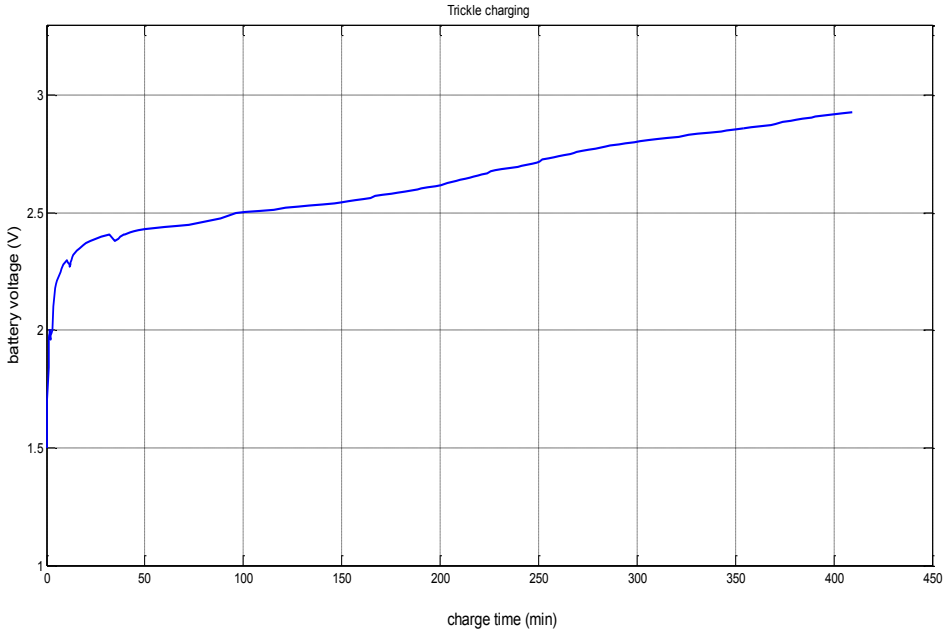

Figure 77 Trickle mode charging of Li-ion cell using reconfigured pulse charger.

The pulse charger is reconfigured to operate as a constant current charger and used to charge a 2000mAh NiMH rechargeable battery to its nominal voltage of 2.5V when the constant current was set to 300mA, which is about 15% of the required full charge current. It is noticed from Fig. 78 that to charge to the nominal voltage of 2.5V, it took about 220 minutes. More current could have been used to charge the NiMH but with maximum constraints on the allowable charge current to prevent damage to the IC, the charge current was limited to 300mA.

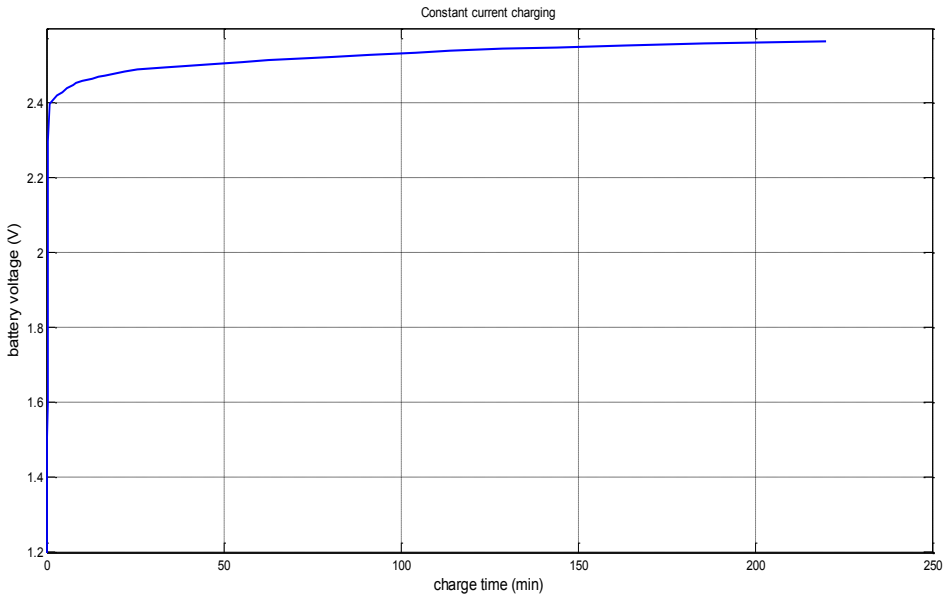

Figure 78 Constant current charging using reconfigured pulse charger.

5.2 Switched capacitor converter

The schematic of the test bench used to verify operation of the switched capacitor converter is shown in Fig. 79. The converter is tested for output variation during input voltage variation and efficiency. The resistors, 50KΩ and 100KΩ, are what sets the output voltage to 1.8V. The values can be changed to obtain a different output. The output and flying capacitors are set to 1μF. A 1MHz clock signal is used.

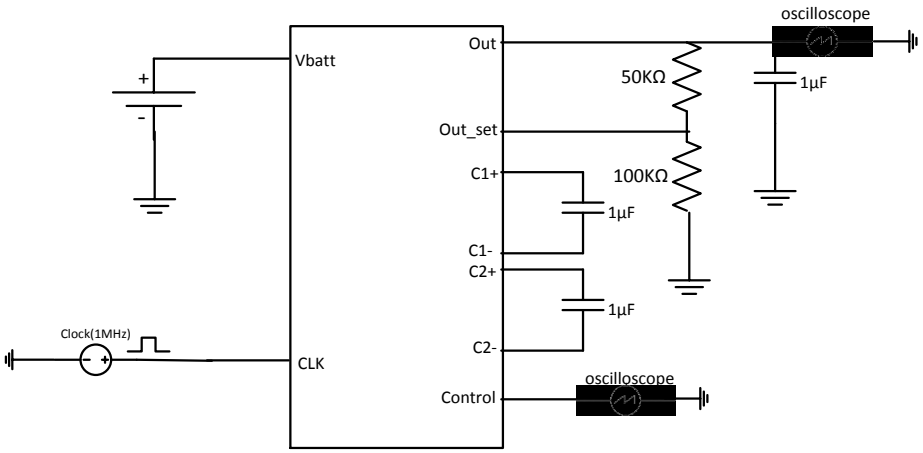

Figure 79 Schematic of switched capacitor test bench.

1µF capacitors are used for the flying capacitors and output capacitors. The smaller the output capacitance, the larger the output voltage ripples, as seen in Fig. 80. Increased output capacitance reduces the ripple significantly as Fig. 81 shows.

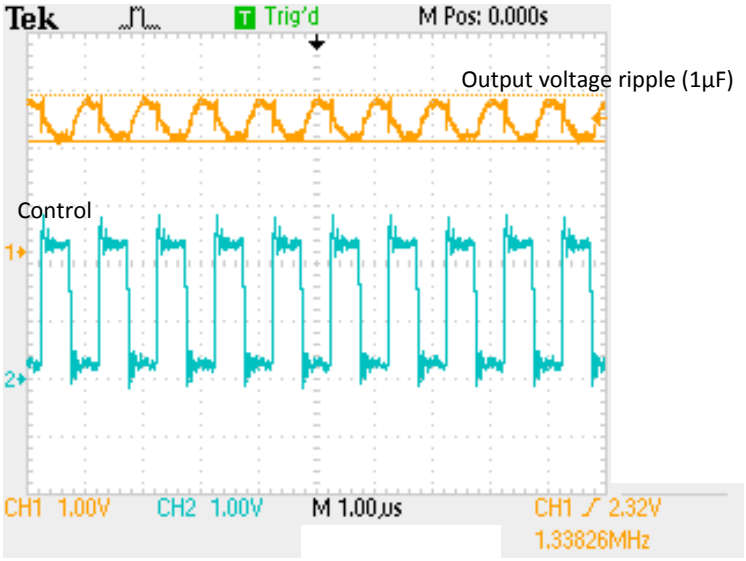

Figure 80 Control signal for clock phases and output voltage ripple of converter.

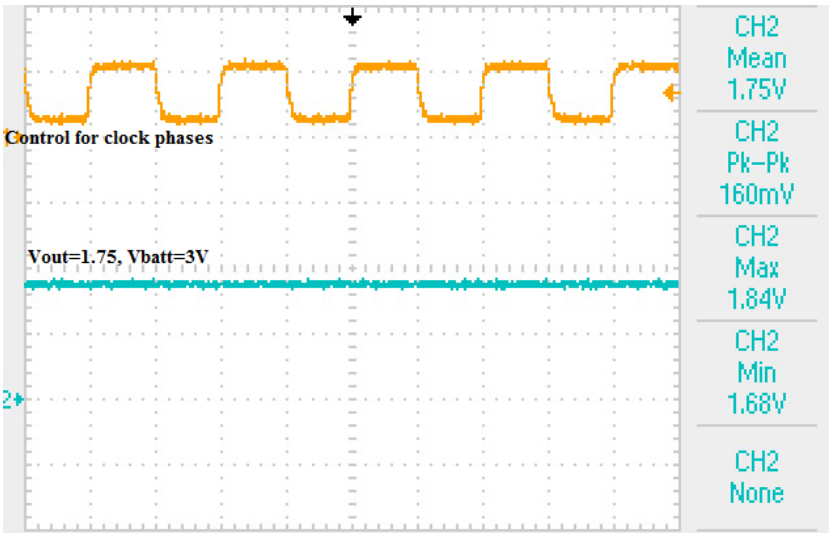

Figure 81 Converter's output with a 3V input and increased output capacitance.

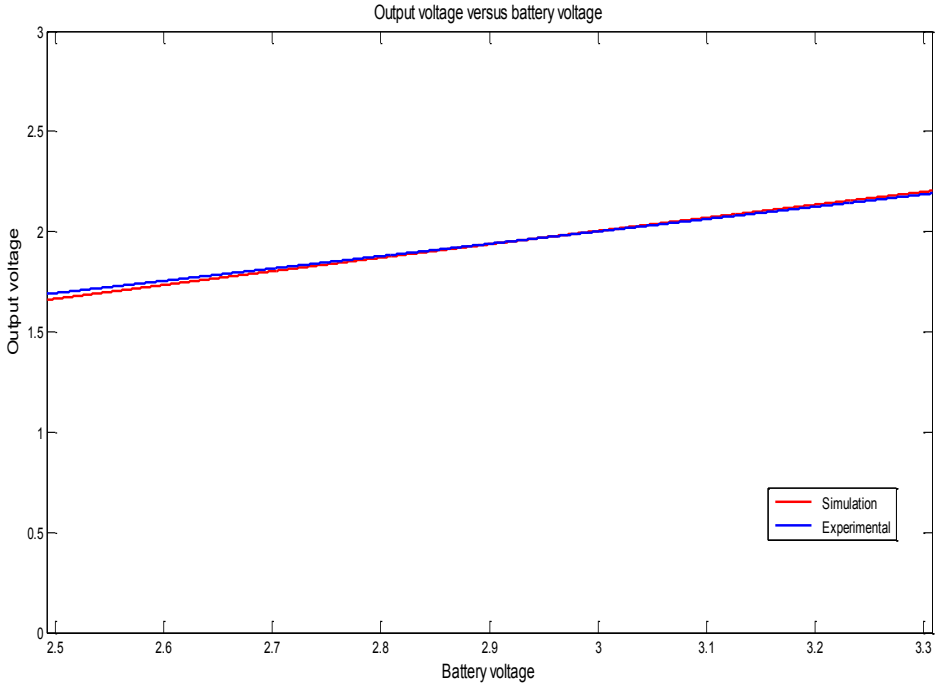

Figure 82 Output voltage variation versus input voltage variation.

Fig. 82 shows the variation of the output voltage as input voltage varies. Experimental results are very similar to simulated results. Fig. 83 shows the efficiency of the converter. As load current increases, the efficiency decreases, but since the converter is for low current application, it operation will be about 90% efficient at an input voltage of 3V.

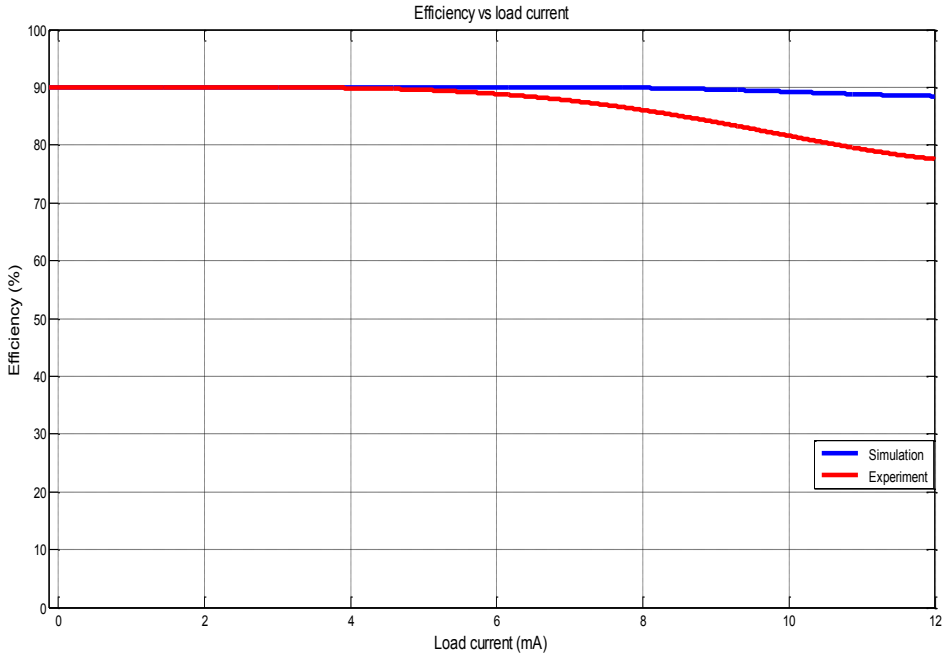

Figure 83 Efficiency of converter.

5.3 Switching network system

To test the operation of the switches in the switch network system, a schematic of the test bench used is shown in Fig. 84. The maximum voltages of the battery and

supercapacitor (SC) are to 3V. This is done by setting the resistances to 150KΩ and 100KΩ. A current limited input voltage source of 3.3V/200µA is used to characterize the EHS. The supercapacitor is set to 10µF while the battery is emulated using a 300µF capacitor. SW_A is the switch between the EHS input and supercapacitor, SW_B is the switch between the supercapacitor and battery, which only turns on when there is a load present, and SW_C is the switch between the EHS input and battery.

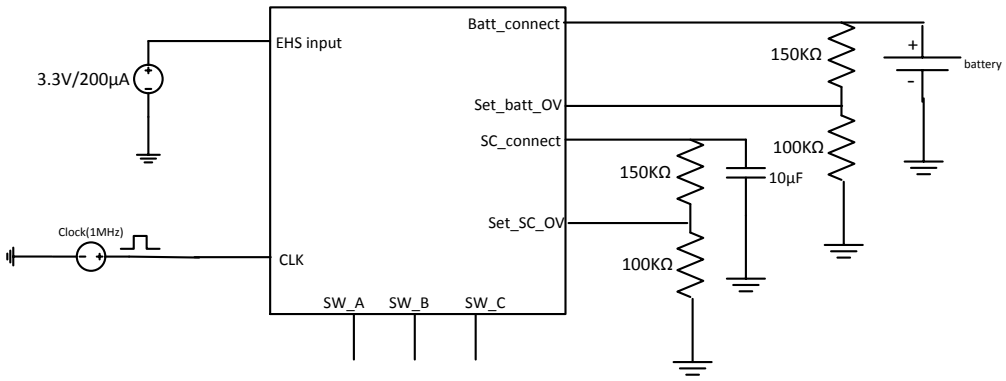

Figure 84 Schematic of switching network system test bench.

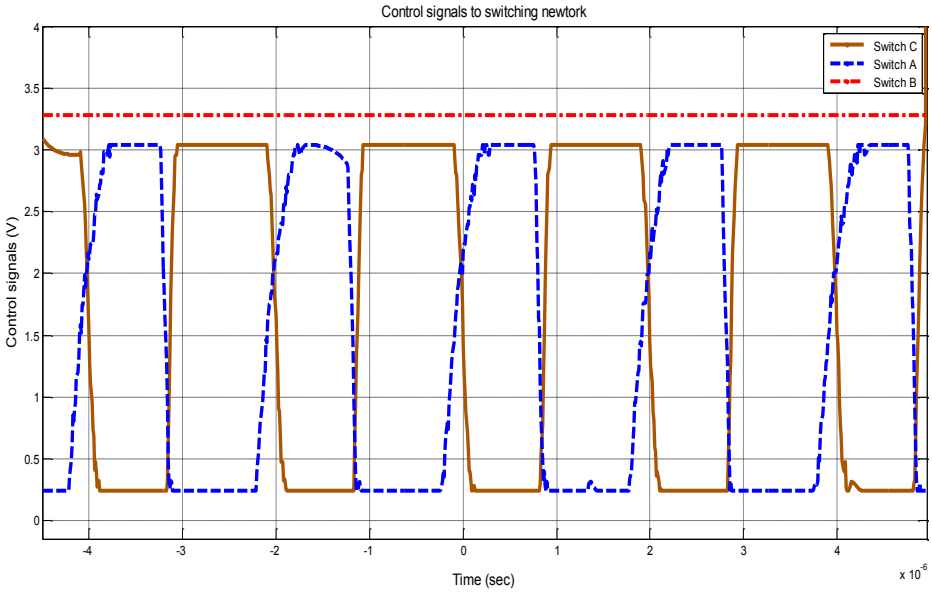

Figure 85 Operation of switching network for supercapacitor and battery < 3V.

Fig. 85 shows the operating signals to the switches during operation of the switching network system. The EHS is charges the supercapacitor intermittently, each time to 3V and switches to charge the battery (SW_C) until it attains a voltage of 3V. After this happens, the EHS is connected constantly to the supercapacitor (SW_A). The signals to the switches are slewed, mainly because of the large input capacitances of the switches. Signal B is high mainly because there is no load attached to the system. Fig. 86 presents the view from an oscilloscope.

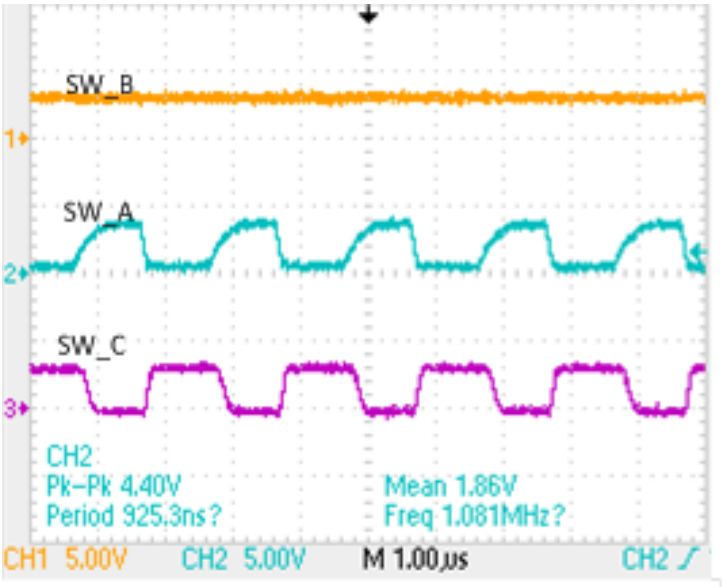

Figure 86 Operating signals of switching network system.

5.4 Comparison with previous works

The proposed charging system in this thesis varies in comparison with previous works [56] - [60]. In [56] - [58] in table 15, a pre-charge phase is not indicated in the design. This is because an assumption was made that the battery will not go into a pre-charge state. [59] - [60] have a pre-charge phase but it is not user programmable. In the proposed charging system designed in this thesis, this phase can be programmed by an external resistor to provide a maximum current of 20mA. Options to charge the battery from a USB network, wall adapter or an EHS provides flexibility, compared to the other previous works which can charge a battery from either a wall adapter or USB.

Table 15 Comparison of proposed charger with previous works

	VFPCS [57]	**DVVPCS[58]**	**PLL based [56]**	**LTC4052 /LTC1730 [59],[60]**	**This work**
Input source	AC/DC	AC/DC	AC/DC	AC/DC	AC/DC or USB or EHS
Battery type	Li-ion	Li-ion	Li-ion	Li-ion	Li-ion & NiMH
Pre-charge phase	-	-	-	Predefined	User set trickle current
Over-voltage protection	-	-	-	Predefined	User set maximum cell voltage
Over temperature	-	-	-	Present	present
Charge current	Average current	Average current	Average current	User defined (wall adapter dependent)	User defined (wall adapter dependent)
Implementation	software	software	discrete	analog	analog
Modulation type	PFM-predefined	PWM-predefined	-	Predefined	PWM-user set
Cell maximum voltage	4.2V	4.2V	4.2V	4.2V	3.3V
User reconfigurable	No	No	No	No	Yes

Also, [56] - [58] were implemented using software or discrete electronic components and pulses voltage into the battery. This work is implemented on silicon and pulses charge current into the battery similar to what is in [59] - [60]. With [56] - [58] charging a 4.2V battery, a supply voltage of 5V was used. In this work, the maximum battery voltage is 3.3V and hence, the input voltage range is limited to a maximum 3.6V to prevent oxide damage. Also, in all the previous works listed above, the modulation types are all predefined and the system designed for a Li-ion battery. The user does not have control over it to change charge profile while in this work, the user has control of all thresholds and the control of the charging algorithm. The system designed in this thesis, as compared to the previous work is completely versatile. It has been verified that it can be reconfigured as a constant current charger to charge a NiMH battery and as a trickle charger to serves as an overnight charger and possible for a battery to be charged via an EHS.

6. CONCLUSIONS

The design of a user programmable battery charging system has been presented in this thesis. The performance of this charging system has been verified through simulation and further proved through experimental results. The concept of the pulse charger operation ensures that it can be reconfigured to be used in different applications. The step down DC-DC converter can provide a stable output voltage for low current applications, at voltages above the nominal battery voltage, with high efficiency values. The switching network system further increases the number of applications in which the charging system can be used, by proving the concept that a battery can be charged via an energy harvesting system.

In summary, this proposed charging system could easily be used in many applications, ensuring low cost and convenience. Not purchasing different types of chargers for different applications can reduce cost and ensure that, at any time and place, a battery could be charged using a wall outlet, USB or an energy harvesting system depending on which one is available. This provides convenience for users. Further research on this charging system should focus on making the pulse charger adaptable to various conditions. Increasing the efficiency of the step down DC-DC converter, by implementing different gain configurations, to match changes in varying battery voltage should also be looked at. More emphasis should be placed on expanding the application of the switching network system to account for battery undervoltage and varying load and input conditions.

REFERENCES

[1] Global Industrial Analysts, "Consumer Batteries: A Global Strategic Business Report," [Online]. Available: http://www.prweb.com/releases/consumer_batteries/primary_secondary/prweb8605940.htm, August 29, 2011.

[2] Stan D'Souza, "Microchip: Transformerless Power Supply," [Online]. Available: http://www.jimfranklin.info/microchipdatasheets/91008b.pdf, February 11, 2011.

[3] John Woodgate, "Line Filter Capacitors," [Online]. Available: http://my.execpc.com/~endlr/line-filter.html, February 11, 2011

[4] Sebastian Anthony, "How USB Charging Works, or How to Avoid Blowing Up Your Smartphone," [Online] Available: http://www.extremetech.com/computing/115251-how-usb-charging-works-or-how-to-avoid-blowing-up-your-smartphone, January 24, 2012.

[5] Engineering Edge, "USB Cables/Interface Overview" [Online]. Available: http://www.engineersedge.com/computer_technology/usb_cables.htm, February 10, 2013.

[6] Universal Serial Bus Technology, "Battery Charging v.1.2 Spec and Adopters Agreement," [Online]. Available: http://www.usb.org/developers/devclass_docs/BCv1.2_011912.zip, February 10, 2013.

[7] Kema Inc., "Market Evaluation for Energy Storage in the United States," [Online]. Available: http://www.copper.org/about/pressreleases/pdfs/kema_report.pdf, January, 2012.

[8] David Connolly, "A Review of Energy Storage Technologies for Integration of Fluctuating Renewable Energy," [Online]. Available: http://dconnolly.net/files/A%20Review%20of%20Energy%20Storage%20Technologies.pdf, October 11, 2010.

[9] Jim Eyer and Garth Corey, "Energy Storage for Electricity Grid: Benefits and Market Potential Assessment Guide," Sandia Report [Online]. Available: http://sgstage.nrel.gov/sites/default/files/resources/energy_storage.pdf, February, 2010.

[10] IEC Market Strategy Board, "Electrical Energy Storage," [Online]. Available: http://www.iec.ch/whitepaper/pdf/iecWP-energystorage-LR-en.pdf, December, 2011.

[11] Electropaedia, "Fuel Cell," [Online]. Available: http://www.mpoweruk.com/fuel_cells.htm, February 11, 2013.

[12] Office of Basic Energy Sciences, DOE, "Basic Research Needs for Electrical Energy Storage," [Online]. Available: http://web.anl.gov/energy-storage-science/publications/EES_rpt.pdf, July 2007.

[13] H.F Gibbard, "Nickel Metal Hydride Battery Applications," *Proceedings of the Ninth Annual Battery Conference on Applications and Advances*, January, 1994.

[14] Electropaedia, “Battery Applications,” [Online]. Available: http://www.mpoweruk.com/applications.htm, February 11, 2013.

[15] Texas Instruments Inc., “Using NiMH and Li-ion Batteries in Portable Applications,” [Online]. Available: http://www.ti.com/lit/an/slua015/slua015.pdf, February 26, 2013.

[16] Interstate Powercare, “Motive Power Batteries,” [Online]. Available: http://interstatepowercare.com/PDF/pc_io_manual_2007.pdf, February 26, 2013.

[17] Grigorii L Soloveichik, “Battery Technologies for Large-Scale Stationary Energy Storage” *Annual Review of Chemical and Biomolecular Engineering*, Vol. 2, no. 5, pp. 503-527,2011.

[18] H. Oman, “Aerospace and Military Battery Applications,” *IEEE Aerospace and Electronic Systems Magazine*, Vol.17, no. 10, October 2002.

[19] The Boston Consulting Group, “Batteries for Electric Car, Challenges, Opportunities and Outlook to 2020,” [Online]. Available: http://www.electricdrive.org/index.php?ht=a/GetDocumentAction/id/27906, January, 2010.

[20] Dan Leistikow, “An Update on Advanced Battery Manufacturing,” [Online]. Available: http://energy.gov/articles/update-advanced-battery-manufacturing, October 16, 2012.

[21] East Penn Manufacturing Co. Inc.,“Battery Applications,” [Online]. Available: http://www.dekabatteries.com/assets/base/0149.pdf, January 31, 2007.

[22] West Marine, “Selecting a Marine Storage Battery,” [Online]. Available: http://www.westmarine.com/webapp/wcs/stores/servlet/WestAdvisorView?langId=-1&storeId=11151&page=Selecting-a-Marine-Storage-Battery#.URlMm2cbBSQ, February 11, 2013.

[23] Department of Defense, “Unmanned Systems Integrated Roadmap: FY2011-2036,” [Online]. Available: http://www.defenseinnovationmarketplace.mil/resources/UnmannedSystemsIntegratedRoadmapFY2011.pdf, February 11, 2013.

[24] Energizer, “Battery Internal Resistance,” [Online]. Available: http://data.energizer.com/PDFs/BatteryIR.pdf, December, 2005.

[25] Learning about Electronics, “Battery Internal Resistance,” [Online]. Available: http://www.learningaboutelectronics.com/Articles/Battery-internal-resistance, February 11, 2013.

[26] Energizer, “Energizer L91,” Energizer [Online]. Available: http://data.energizer.com/PDFs/l91.pdf, February 11, 2013.

[27] Jaycar Electronics,“Battery Terms and What They Mean.” [Online]. Available: http://www1.jaycar.com.au/images_uploaded/battglos.pdf, September 11, 2012.

[28] Green Batteries, “Glossary of Battery Terms.” [Online]. Available: http://www.greenbatteries.com/batteryterms.html, September 11, 2012

[29] Corrosion Doctors, “Self-Discharge of Batteries,” [Online]. Available: http://corrosion-doctors.org/Batteries/self-compare.htm, February 12, 2013

[30] Battery University, “Global Battery Markets.” [Online]. Available: http://batteryuniversity.com/learn/article/global_battery_markets, February 25, 2013

[31] Davide Andrea, “Battery Management Systems for Large Lithium-Ion Battery Packs,” *1st ed. Artech House Inc.*, 2011

[32] Infiniti Research Limited, “Global Lithium Battery Market 2011-2015,” [Online]. Available: http://www.reportlinker.com/p0962689-summary/Global-Lithium-Battery-Market.html, August, 2012.

[33] Pike Research, “Revenue for Lithium Ion Battery Market Set to Grow by 700% by 2017,” [Online]. Available: http://www.prnewswire.com/news-releases/revenue-for-lithium-ion-battery-market-set-to-grow-by-700-by-2017-142516205.html, March 13, 2012.

[34] Electropaedia, “Battery Chargers and Charging Methods,” [Online]. Available: http://www.mpoweruk.com/chargers.htm, October 6, 2012.

[35] Yuh-Shyan Hwang, Shu-Chen Wang, Fong-Cheng Yang and Jiann-Jong Chen, “New Compact CMOS Li-ion Battery Charger Using Charge-Pump Technique for Portable Applications,” *IEEE Transactions on Circuits and Systems*, Vol. 54, no. 4, pp. 705-712, April 2007.

[36] Rhino-Charge Engineering, “Pulse Technology,” [Online]. Available: http://www.tstonramp.com/~rhinocharge/pulsetech_faq.html, February 23, 2007.

[37] Scott Dearborn, “Charging Lithium-Ion Batteries: Not all Charging Systems Are Created Equal,” [Online]. Available:

http://www.microchip.com/stellent/groups/designcenter_sg/documents/market_communication/en028061.pdf, September 12, 2006.

[38] J. A. Paradiso and T. Starner, "Energy Scavenging for Mobile and Wireless Electronics," *IEEE Pervasive Computing*, Vol. 4, no. 1, pp. 18-27, January, 2005.

[39] S. Chalasani and J.M. Conrad, "A Survey of Energy Harvesting Sources for Embedded Systems," *IEEE Southeastcon*, pp. 442 – 447, April, 2008.

[40] Murugavel Raju, "Energy Harvesting," [Online]. Available: http://www.ti.com/corp/docs/landing/cc430/graphics/slyy018_20081031.pdf, November 10, 2008.

[41] M.R. Mhetre, N.S. Nagdeo and H.K. Abhyankar, "Micro Energy Harvesting for Biomedical Applications: A Review," *3rd International Conference on Electronics Computer Technology (ICECT)*, Vol. 3, pp. 1-5, April 2011.

[42] Vytautas Bielinskas, "Efficiency of Solar Energy Harvesting," [Online]. Available: http://construction21.eu/articles/h/efficiency-of-solar-energy-harvesting.html, October 3, 2012.

[43] National Instruments, "Using Energy Harvesting Devices with National Instruments Wireless Sensor Networks (WSN)," [Online]. Available: http://www.ni.com/white-paper/12128/en#toc2, September 28, 2012.

[44] Pai H. Chou and Sehwan Kim, 'Techniques for Maximizing Efficiency of Solar Energy Harvesting Systems," [Online]. Available: http://www.ece.uci.edu/~chou/icmu10.pdf, February 17, 2010.

[45] Jeff Gruetter ,“Solar Energy Harvesting,” [Online]. Available: http://cds.linear.com/docs/en/article/SolarEnergyHarvesting.pdf, October 19, 2010.

[46] Voltaic, “Amp Solar Charger,” [Online]. Available: http://www.voltaicsystems.com/amp.shtml, October 11, 2012.

[47] Simone Dalola, Marco Ferrari, Vittorio Ferrari, Michele Guizzetti, Daniele Marioli and Andrea Taroni, “Characterization of Thermoelectric Modules for Powering Autonomous Sensors,” *IEEE Transactions on Instrumentation and Measurement*, Vol. 58, no. 1, pp. 99-107, January 2009.

[48] Nicholas S. Hudak and Glenn G. Amatucci, “Small-scale Energy Harvesting through Thermoelectric, Vibration, and Radio Frequency Power Conversion,” *Journal of Applied Physics*, vol. 103, no. 10, February. 2008.

[49] M. Kishi, H. Nemoto, T. Hamao, M. Yamamoto, S. Sudou, M. Mandai, and S. Yamamoto, “Micro-thermoelectric Modules and their Application to Wristwatches as an Energy Source,” *Proceedings 18th International Conference on Thermoelectrics*, pp. 301–307, August 1999.

[50] Gumballtech, “Energy Harvesting: Charge your Wearable Technology with Heat, Sun, and Vibration,” [Online]. Available: http://www.gumballtech.com/2012/02/21/energy-harvesting-charge-your-wearable-technology-with-heat-sun-and-vibration/, February 21, 2012.

[51] T.A. Smith, J.P. Mars and G.A. Turner, "Using Supercapacitors to Improve Battery Performance," *Power Electronics Specialists Conference*, Vol. 1, pp. 124-128, 2002.

[52] A. Burke, "Ultracapacitors: Why, How, and Where is the Technology", *Journal of Power Sources*, Vol. 91, no. 1, pp. 37-50, November 2000,

[53] Marin S. Halper and James C. Ellenbogen, "Supercapacitors: A Brief Overview," [Online]. Available: http://wwwsrv1.mitre.org/work/tech_papers/tech_papers_06/06_0667/06_0667.pdf, March 5, 2008.

[54] Illinois Capacitor, Inc., "Supercapacitors," [Online]. Available: http://www.illinoiscapacitor.com/pdf/papers/supercapacitors.pdf, January 13, 2012.

[55] Jun Li, Edward Murphy, Jack Winnick and Paul A. Kohl, "The Effects of Pulse Charging on Cycling characteristics of Commercial Lithium-ion Batteries," *Journal of Power Sources*, Vol. 102, no. 1-2, pp. 302-309, December 2001.

[56] L. R. Chen, " PLL-Based Battery Charge Circuit Topology," *IEEE Transactions on Industrial Electronics*, Vol. 51, no. 6, pp. 1344–1346, December 2004.

[57] L. R. Chen, "A Design of an Optimal Pulse Charge System by Frequency Varied Technique," *IEEE Transactions on Industrial Electronics*, Vol. 54, no. 1, pp. 398–405, February 2007.

[58] L. R. Chen, "Design of Duty-Varied Voltage Pulse Charger for Improving Li-ion Battery Charging Response," *IEEE Transactions on Industrial Electronics*, vol. 56, no. 2, pp. 480–487, February 2009.

[59] Linear Technology, "LTC4052-4.2-Lithium-ion Battery Pulse Charger with Overcurrent Protection," [Online]. Available: http://www.linear.com/product/LTC4052-4.2, January 1, 2008.

[60] Linear Technology, "LTC1730- Lithium-ion Battery Pulse Chargers with Overcurrent protection," [Online]. Available: http://www.linear.com/product/LTC1730, January 1, 2008.

[61] Maxim Integrated, "MAX1879-Simple, Efficient, 1-Cell Li+ Pulse Charger." [Online]. Available: http://www.maximintegrated.com/datasheet/index.mvp/id/2544, May 30, 2001.

[62] International Warehouse, "A123-3.3VB Lithium Ion 2300mAh Single Cell Battery," [Online]. Available: http://www.hobbyking.com/hobbyking/store/__16575__A123_3_3VB_Lithium_Ion_2300mAh_Single_Cell_Battery.html, January 11, 2013

[63] Fairchild Semiconductor, "CMOS Schmitt Trigger-A Uniquely Versatile Design Component," *Fairchild Semiconductor Application note*, no. 140, June 1975.

[64] I. Chang, A.A. Abidi, and C.R. Viswanathan, "Flicker Noise in CMOS Transistors from Subthreshold to Strong Inversion at Various Temperatures," *IEEE Transactions on Electronic Devices*, Vol. 41, no. 11, pp. 1965-1971, November, 1994.

[65] Yuan Taur and Tak H. Ning, "Fundamentals of Modern VLSI Devices," *1st. ed., Cambridge University Press*, ch. 3, pp. 120-128, October1998.

[66] E.A. Vittoz, "The Design of High-Performance Analog Circuits on Digital CMOS Chips," *IEEE Journal of Solid-State Circuits*, Vol. 20, no. 3, pp. 657-665, June 1985.

[67] M. Filanovsky and H. Baltes "CMOS Schmitt Trigger design", *IEEE Transactions on Circuits and Systems*, Vol. 41, no. 1, pp. 46-49, January 1994.

[68] Munish Kumar, Parminder Kaur and Sheenu Thapar, "Design of CMOS Schmitt Trigger," *International Journal of Engineering and Innovative Technology (IJEIT)*, Vol. 2, no. 1, July 2012.

[69] F. B. Diniz, L. E. P. Borges and B. de. B. Neto, "A Comparative Study Of Pulsed Current Formation for Positive Plates of Automotive Lead Acid Batteries," *Journal of Power Sources*, Vol. 109, no. 1, pp. 184–188, June 2002.

[70] Technical Document Center, "Recharging the Unchargeable," [Online]. Available: http://techdoc.kvindesland.no/radio/psu/20061103160627551.pdf, November 3, 2006.

[71] Marian Stofka, "Rectangular-waveform generator produces 25 and 75% duty cycle." *EDN Design Ideas*, no. 5, pp. 74-75, May 2010.

[72] Anico, "Charging at High and Low Temperatures," [Online]. Available: http://www.anico.hu/anico.php?o=tudod-e/toltes%20kulonb%20homersekleteken_angol, February 26, 2013.

[73] Vadim V. Ivanov and Igor M. Filanovsky, "Operational Amplifier Speed and Accuracy Improvement: Analog Circuit Design with Structural Methodology," *1st ed., Springer*, ch. 6, pp. 114–115, March, 2004.

[74] Lonne Mays, "Advanced ICs Facilitate Application-Specific Configuration of Li-ion Battery Chargers," *Electronics world*, Vol. 115, pp. 16-18, July 2009.

[75] Yoshiyasu Saito, Kiyonami Takano and Akira Negishi, "Thermal Behaviors of Lithium-ion Cells during Overcharge," *Journal of Power sources*, Vol. 97-98, pp. 693-696, July 2001.

[76] Takahisa Ohsaki, Takashi Kishi, Takashi Kukobi, Norio Takami, Nao Shimura *et al*, " Overcharge Reaction of Lithium-ion Batteries", *Journal of Power Sources*, Vol. 146, no. 1-2, pp. 97-100, August 2005.

[77] I. Doms, P. Merken, R. Mertens, and C. Van Hoof, "Integrated Capacitive Power-Management Circuit for Thermal Harvesters with Output Power 10 to1000μW," *IEEE International Solid State Circuits Conference- Digest of Technical Papers*, pp. 300–301, February, 2009.

[78] Mengzhe Ma, "Design of High Efficiency Step-Down Switched Capacitor DC/DC Converter," M.Sc. thesis, Oregon State University, May, 2003.

[79] Linear Technology, "LTC3250 - High Efficiency, Low Noise, Inductorless Step-Down DC/DC Converter," Linear Technology [Online]. Available: http://www.linear.com/product/LTC3250, September 19, 2009.

[80] Linear Technology, "LTC1503 - High Efficiency Inductorless Step-Down DC/DC Converter," Linear Technology [Online]. Available: http://www.linear.com/product/LTC1503, January 30, 2010.

[81] Walt Kester, Brian Erisman and Gurjit Thandi, "Switched Capacitor Voltage Converters," [Online]. Available: http://www.analog.com/static/imported-files/tutorials/ptmsect4.pdf, March 26, 2009.

[82] Ahmad Shar, "Design of a High-Speed CMOS Comparator," M.Sc. thesis, Linköping Institute of Technology, November, 2011.

[83] Shubhara Yewale and Radheshyam Gamad, "Design of Low Power and High Speed CMOS Comparator for A/D Converter Application," *Wireless Engineering and Technology*, Vol. 3, pp. 90-95, April, 2012.